Analysis of Optimal Dispatch of Energy Systems, Market Rules, and Market Power in Wholesale Electricity Markets

A DISSERTATION
SUBMITTED TO THE FACULTY OF THE
UNIVERSITY OF MINNESOTA
BY

Nathan Roswell Paine

IN PARTIAL FULFILLMENT OF THE REQUIREMENTS
FOR THE DEGREE OF
DOCTOR OF PHILOSOPHY

Dr. Frances R. Homans, Adviser

August 2021

Acknowledgements

There are several people I want to express thanks to for their support and helping me to develop academically and professionally. First and foremost, I want to thank my adviser Frances Homans for her motivation, patience, and guidance. She was always willing to give her time to help me be successful in my academic work. Throughout my time in the program, she has always believed in me and demonstrated all the best qualities of a great adviser and teacher.

I am also very thankful to Dr. Elizabeth Wilson and Dr. Steven Taff for their support and funding of my research. They both helped me immensely in my research and professional development. It was a great opportunity for me to be part of multi-disciplinary research teams during my time in the program and work with so many talented people. This dissertation would also not be possible without their support and mentorship. More specifically, I want to thank the following faculty and research team members for their valuable comments and feedback on my dissertation. I am thankful to Dr. Frances Homans, Dr. Elizabeth Wilson, and my research team members Melissa Pollak and Dr. Jeffrey Bielicki for their comments and feedback on Chapter 2 – *Why Market Rules Matter: Optimizing Pumped Hydroelectric Storage When Compensation Rules Differ*. Their contributions were especially helpful during the journal review and publication process, which resulted in the article being published in the November 2014, Volume 46 edition of the journal Energy Economics (pages 10-19). I am also thankful for the helpful comments and guidance from Dr. Steven Taff, Dr. Thomas Kuehn, and research team member Andy Mevissen on Chapter 3 - *The production and use of chilled-water to increase efficiency of a geothermal power system under different temperature and price conditions*. Finally, I want to thank my committee members Dr. Stephen Polasky and Dr. Jeffrey Apland, as well as Dr. Marc Bellemare, for providing thoughtful feedback on this dissertation.

Last, I want to thank the Department of Applied Economics for so many great experiences in the classroom and research settings. I can honestly say that I had nothing but the best experiences with the faculty, who are great teachers, motivators, and very generous with their time in support of their students. My time in the program helped me immensely in furthering my interests in energy economics and policy and developing professionally.

Abstract

The focus of this dissertation is on the operation of electric power systems, specifically on wholesale electricity markets and the potential for exercising market power in wholesale markets for electricity. Restructuring of the electric utility industry has encouraged Independent Power Producers (IPPs) to enter the industry and sell power in the wholesale electricity markets. However, as the United States continues the transition to restructured electricity markets, there are concerns about the market power that producers may exert. This dissertation is composed of three essays exploring these topics using dynamic optimization methods and empirical analysis.

The first essay uses a framework to measure production costs and the component of price that is above marginal cost. I incorporate the start-up costs of generators. Using data from January 2016 to December 2018, I find evidence that market power was exercised, particularly in months having unseasonably cold temperatures and fuel price spikes as well as during the winter peak season. The results also suggest that the degree of market power increases during the peak hours of the day.

The second essay utilizes a dynamic optimization model to illustrate how a low-temperature geothermal power plant can be flexibly dispatched to offer multiple different services in addition to base-load power to a utility customer. The utility industry still thinks of geothermal as a base-load resource, but I show that low temperature resource geothermal power plants offer more flexibility than other renewable energy technologies and thus can be operated as a variable energy resource to accommodate intermittent resources and alleviate transmission congestion.

The third essay examines the interaction of policies, markets, and technologies that creates the modern electrical system. Integrating large amounts of electricity generated by variable renewable resources, such as from wind and solar, into electricity systems may require energy storage technologies to synchronize electricity production with electricity demand. Electricity markets compensate the performance of these energy storage technologies for the services they provide, and these markets are often operated by regional Independent System Operators (ISOs) that specify the market rules for this compensation. To examine how different ISO rules can affect the operation and profitability an energy storage technology, I develop a dynamic programming model of pumped hydroelectric storage (PHES) facility operation under the market rules from the Midcontinent ISO and ISO-New England. I show how differences in rules between these ISOs produce different operational strategies and profits and may not incentivize energy storage projects where they are most needed.

Table of Contents

List of Tables

List of Figures

Notation

COP=Coefficient of Performance

C_p=Specific Heat, kJ/kg C

LWT=Temperature that the Water Leaves the Chiller, °C

M_{water}=Mass of Water, kg

$\dot{p}$=Rate of Power Production, kW

$\dot{q}$=Rate of Energy Transfer, kW

t=Time Step, s

ΔT=Change in Temperature, °C

T_{amb}=Ambient Temperature, °C

T_H=absolute temperature of the geothermal resource

T_A=absolute ambient air temperature

List of Abbreviations

ACE	Area Control Error
AGC	Automatic Generation Control
DA	Day-Ahead
LMP	Locational Marginal Price
IPP	Independent Power Producer
ISO-NE	Independent System Operator-New England
MISO	Midwest Independent System Operator
PHES	Pumped Hydroelectric Energy Storage
RT	Real-Time

1. Introduction

The electricity industry has undergone significant changes since the mid-1990s in the transition from investor-owned utilities, where generation, transmission, and distribution are bundled, to a structure where generation, transmission, and distribution are unbundled. This transition was enabled by changes in federal regulation, starting with the Federal Energy Regulatory Commission (FERC) Order 888, which allowed for the creation of wholesale electricity markets and required non-discriminatory access to transmission. Subsequently, FERC Order 2000 was issued, which provided the regulatory framework for the creation of Regional Transmission Operators (RTOs). RTOs administer the wholesale electricity markets, operate the electric power grid, and coordinate long-term planning around the adequacy of resources. The transition from vertically integrated investor-owned utilities to a structure where generation, transmission, and distribution are unbundled has not occurred evenly across the United States. In part, this is due to significant opposition to restructuring since the 2000-01 energy crisis in California. According to the Energy Information Association (EIA) (n.d.), there are six RTOs and one Independent Service Operator (ISO):

- PJM Interconnection (PJM)
- Midcontinent ISO (MISO)
- California ISO (CAISO)
- Southwest Power Pool (SPP)
- New York ISO (NYISO)
- New England ISO (ISO-NE)
- Electric Reliability Council of Texas (ERCOT)

These seven RTOs/ISOs serve approximately two-thirds of consumers in the United States (Boyd and Hanis, 2020).

The goal of restructuring the electric utility industry has been to improve the efficiency of the electric utility industry. Many positives have been associated with restructuring of the electric utility industry, such as greater opportunities for IPPs and greater penetration of renewable energies. However, Wolak (2000) makes the point that the transition to competitive wholesale electricity markets has brought with it new policy challenges. Since the energy crisis in California, the issue receiving the most attention is the opportunity to exercise market power. Chapter 1 of this dissertation considers the exercise of market power in the PJM region. Market power is defined as the ability of a power producer to manipulate the market clearing price of electricity above the competitive price level. Under traditional cost-of-service regulation, regulators determine prices and thus utilities are unable to exercise market power through the

manipulation of prices. RTOs and ISOs have adopted different market rules to mitigate the potential for exercising market power on the part of producers. Yet, there may still be opportunities to extract monopoly rents. In chapter 1, I investigate the exercise of market power in the PJM region, which offers an interesting comparison to most studies of market power which focus on the CAISO territory, since CAISO and PJM have different market structures and market rules.

The restructuring of the electricity industry has led to large growth in the share of electricity generated by independent power producers (IPPs) with more than 40 percent of U.S. power production being supplied by IPPs as of 2017 according to Gifford et al. (2017). However, they note that independent power producers have had financial struggles because their revenues generally do not cover fixed and variable production costs. Nevertheless, the movement to greater competition in the generation market has opened many opportunities for IPPs. There is also a greater imperative for IPPs to develop operating strategies for mitigating risk and increasing the probability of being profitable. Chapters 2 and 3 of this dissertation consider the operating strategies and economic viability of different energy storage systems. Chapter 2 of this dissertation uses a dynamic programming model to investigate an operating strategy from the perspective of a single low-temperature geothermal power plant seeking to maximize profit from the sale of electricity. Conditions are discussed under which the low-temperature geothermal power plant with chilled-water cooling system is economically viable. Chapter 3 of this dissertation considers the economic viability of pumped hydroelectric storage (PHES). In this chapter I develop a dynamic programming model of pumped hydroelectric storage (PHES) facility operation under the market rules from the Midcontinent ISO and ISO-New England. I show how differences in rules between these ISOs produce different operational strategies and profits, which in turn impact the economic viability of energy storage projects. The results highlight how policies and institutions designed to promote competition have major implications for the development of the electric utility industry and the opportunities that exist for different players to profit from increased competition.

1.1 Dissertation Objectives

In Chapter 1, I investigate concerns about the exercise of market power. Competitive benchmark models are constructed with and without the incorporation of start-up costs. The competitive benchmark price is determined by the intersection of residual demand with the aggregate marginal curve. I infer the exercise of market based on the difference between the system-wide energy price and the competitive benchmark price.

Chapter 2 describes a low-temperature geothermal plant with a chilled-water cooling system. Using a dynamic programming model, I analyze the relationship between the ambient temperature and the existence of arbitrage opportunities in such a system.

In Chapter 3, I use a dynamic programming model to investigate the profit-maximizing behavior of a PHES facility and estimate revenue streams from selling both electricity and grid reliability services into different competitive wholesale electricity markets with different compensation mechanisms. The solution to the model determines optimal market bidding strategies for electricity and reliability services that operate under both the MISO and ISO-NE market rules. By comparing the value of PHES systems and the impacts of these different rules on revenue streams, a better understanding of the value of different policies and how they monetize the benefits provided by PHES is achieved.

2. Chapter 1 - Measuring Market Power in the PJM Region

2.1 Introduction

The transition to deregulated wholesale electricity markets in the late 1990s and the 2000-2001 California electricity crisis fueled concerns about the potential for the exercise of market power by market participants. Across the United States, restructuring of the electricity industry has taken on different forms with some regions being further along in making market-based reforms. Many experts have noted that restructuring is based on the concept that market-based reforms would result in greater efficiency from fostering competition in the marketplace that would ultimately result in lower costs to retail customers (Borenstein and Bushnell, 2015). However, there have been negative experiences with restructuring, most notably the 2000-2001 California electricity crisis in which the state experienced rolling blackouts as a result of market manipulation in which producers withheld capacity during certain times to increase electricity prices in the wholesale market. The California electricity crisis, in particular, slowed and/or stalled efforts to implement market-based reforms in the industry in some parts of the United States. The electricity crisis in California and negative experiences elsewhere increased concern and awareness about possibilities for electricity suppliers to exercise market power in the wholesale electricity markets by acting strategically, such as by withholding capacity, in order to manipulate electricity prices.

Several studies have been conducted on the California electricity market showing potential for the exercise of market power by producers (Harvey and Hogan, 2001; Borenstein, Bushnell, and Wolak, 2002; Joskow and Kahn, 2002). California has experienced many periods of high electricity prices and these studies show that prices have exceeded the competitive benchmark price. Concerns about the abuse of market power leading to excessively high prices prompted development of market power mitigation processes. Market mitigation generally falls into one of two distinct approaches: structural approaches that analyze whether the market structure is likely to lead to market power abuses, and direct approaches that assess whether supply bids exceed a competitive benchmark. One of the most well-known structural tests is the Herfindahl-Hirschman Index (HHI) test. Most of the literature before and shortly after the 2000-2001 California electricity crisis makes the point that the HHI test, which is a measure of market power based on market share, is not ideal for measuring the possibility for exercising market power in wholesale electricity markets (see for example Borenstein and Bushnell 2000). Blumsack (2002) called for the use of the pivotal supplier concept in assessing the potential for exercising market power. A power plant is generally considered to be a pivotal supplier if its

generation capacity is required for satisfying the demand for electricity. Blumsack argues that there is greater potential for pivotal suppliers to manipulate market prices since they are required to be dispatched to satisfy demand for electricity. The pivotal supplier concept has been adopted by the RTOs, whose purpose it is to administer the wholesale electricity markets and operate the transmission grid, in the tests they use to monitor the electricity markets for the potential manipulation of electricity prices. Pivotal supplier tests, which are tests of market structure, are generally favored by RTOs over direct approaches that seek to compare market prices to a cost-based offer because costs are not observable and cannot always be determined with sufficient accuracy for purposes of setting thresholds to determine excessive pricing. Since the competitive benchmark price is not observable and cannot always be measured directly, the RTOs have increasingly looked to the use of pivotal supplier tests for assessing the possibility of market power abuses.

This paper analyzes the exercise of market power in the PJM electricity market because this region offers an interesting comparison to some of the prior research focusing on the exercise of market power in California's electricity market. First, PJM was established in 1997 and its market mitigation rules, which utilize the pivotal supplier test, have had time to mature. Therefore, the results in this paper could support a market power mitigation approach based on the pivotal supplier concept. If the prevailing system-wide electricity prices are at the competitive level, this could be interpreted as demonstrating the effectiveness of the pivotal supplier structural test for market monitoring and mitigation as used in PJM. Second, PJM differs significantly from California in terms of its generation and transmission assets. Blumsack (2002) points out that the PJM power system network is more spatially dense than systems in other regions of the United States. Additionally, it has many interconnections with other systems that also enhance its capability to import/export power. The PJM market is in a region where the amount of generation and transmission assets and configuration of the electricity grid should favor competitive market prices. Given these favorable conditions, we can observe whether system-wide electricity prices are competitive.

Two models of competitive benchmark prices are utilized to evaluate the degree of market power in the PJM region. The first model is based on the competitive benchmark model developed in Borenstein, Bushnell, and Wolak (2002). The second model represents an extension to the first model because it takes into account the start-up costs of fossil fuel power plants. The results from the competitive benchmark price models show that differences in model construction can lead to differences in conclusions about the competitive effects of restructuring the electricity

industry. Taking start-up costs into account tends to result in the measurement of competitive benchmark prices that are closer to the mean level of system-wide electricity prices.

This paper is organized into the following sections. Section 2 provides background information to support the construction of the competitive benchmark models. Section 3 describes the assumptions about the operation of power plants and prices within the PJM region. This section also describes some features of the model and the mechanics of the marginal cost calculation. Section 4 discusses electricity prices and demand for power in the PJM Region. Section 5 describes the methodology for estimating the marginal cost of generation. Section 6 contains a discussion of the results. Section 7 provides conclusions and offers avenues for future research.

2.2 Background

Borenstein and Bushnell (2015) provide a comprehensive and up-to-date account of the history of restructuring in the electricity industry in the United States. Beginning in the 1990s, there was a transition from a system of vertically integrated monopolies in which the utilities owned and operated the transmission grid, power plants, and distribution network to the current structure in which these assets are unbundled. Currently, the retail level of the electric utility industry is still subject to cost-of-service regulation in most areas of the United States. However, operational control of the transmission grid has been removed from utilities and given to RTOs. There are currently seven RTOs in the United States charged with operating the transmission grid and administering the wholesale electricity market. A core function of the RTOs is to ensure that all power suppliers have free access to the transmission grid. Restructuring of the electricity industry has thus led to a proliferation of Independent Power Producers (IPPs) that either receive a market-based price for the power they supply in the wholesale markets or enter into bilateral contracts with buyers for the sale of power.

Several papers were published after the 2000-2001 California electricity crisis analyzing the degree of market power in wholesale electricity markets (Borenstein, 2000; Harvey and Hogan, 2001; Joskow and Kahn, 2002; Borenstein, Bushnell, and Wolak, 2002; Wolak, 2003; Borenstein, 2005; Borenstein and Holland, 2005; Bushnell, Mansur, and Saravia, 2008; Wolak, 2010). The essential feature of the models in these papers is an aggregate marginal cost function constructed from the marginal cost of each power plant. Marginal cost is determined by incorporating detailed information at the power plant level on the efficiency of each power plant, fuel costs, and variable operations and maintenance costs. The competitive benchmark price is determined as the marginal cost of production where the aggregate marginal cost curve intersects

with level of electricity consumed during a particular time period. These studies vary in terms of the incorporation of additional variables and components of marginal cost, including scheduled and unplanned outages, net imports of power, and technical characteristics of the transmission grid and/or generation power plants.

In these models, power plants are assumed to produce power at maximum capacity if their position along the aggregate marginal cost curve falls on or below the point of intersection between the aggregate marginal cost curve and residual demand Generators are assumed to shut down operations if their position along the aggregate marginal cost curve falls above the point of intersection. Some authors claim that these models produce results that underestimate the competitive benchmark price and overestimate market power abuses because they ignore start-up costs. It should be noted, however, that this simplifying assumption may have done a reasonably good job of approximating the power plant costs prior to the introduction of high levels of renewable energy sources. With higher levels of renewable generation, more fossil fuel plants are operated as load-following and have more frequent start-ups. Therefore, it becomes more important to account for start-up costs in the estimation of a competitive benchmark price. Staffell and Green (2016) present a simple model to account for start-up costs. First, they use a heuristic method for estimating the number of start-ups per year. Fossil fuel plants are assumed to be in one of only two possible states, either on or off. Then the number of start-ups per year for each power plant is estimated based on the number of times the system-wide load crosses over a certain quantity from below. Next, they multiply the estimated number of startups by the cost per startup to arrive at their estimate of start-up costs. This approach has the advantage of using a method that is straightforward to incorporate start-up costs in the estimation of the competitive price level.

2.3 Model Assumptions

I utilize data on prices, demand, power production, and generators within the PJM region to estimate the hourly competitive price level over three years from the beginning of 2016 to the end of 2018. Estimated competitive prices are derived following methods outlined in Borenstein, Bushnell, and Wolak (2002). Hourly aggregate marginal cost of generation curves are constructed, and the competitive price levels are determined based on their intersections with observed hourly electricity loads. The estimated competitive price level is compared to the system-wide electricity price for each time period to determine the degree of market power. Bigger deviations between the system-wide market price and the estimated competitive price level represent more evidence that power plants exercise market power.

Power plants are assumed to always be in one of two states: (1) actively producing power at maximum capacity, or (2) shut down. Several assumptions are made with respect to the price-taking power plants, treatment of hydroelectric power, and treatment of net imports in order to derive an hourly residual demand that would be satisfied with fossil fuel generation in a competitive market environment. The focus is on fossil fuel plants for assessing the degree of market power abuses because nuclear, wind, solar, and other renewables are treated as must-run power plants with an effective zero marginal cost of generation. Therefore, the observed levels of generation from these power plants are subtracted from the actual load to obtain a residual demand quantity that is satisfied with fossil fuel generation. Aggregate marginal cost of fossil fuel generation curves are constructed for each hour. The hourly residual demand level and aggregate marginal cost of generation curve are used to derive the competitive price level for each hour. The essential mechanics of the model use output, measured by metered load, and aggregate marginal cost to determine the hourly competitive electricity price. The deviation between the estimated competitive price and the observed system-wide market price is then used to assess the degree of market power.

2.3.1 Start-up Costs

The costs of starting up a fossil fuel plant, as well as other constraints such as the speed a fossil fuel plant can be ramped up or down, affect the operation of fossil fuel plants. With higher levels of renewable energy, it is expected that the residual demand served by fossil fuel plants will fluctuate more as we move through the diurnal cycle and transition between peak and off-peak periods. This pattern results in more frequent start-ups and shutdowns of fossil fuel plants that are load-following leading to considerable impacts on the cost of operating these plants (Graeter and Schwartz, 2020).

Start-up costs are not included in the marginal cost formula because they are incurred when a power plant transitions from an inactive state to an active state and thus are not paid when already in an active state. The incorporation of start-up costs in the estimation of the competitive price level is based on the notion that power plants will only start up if electricity prices are expected to be high enough to recover the start-up costs. Therefore, the basic approach I use for incorporating start-up costs is to compute the average start-up cost for the amount of time that the power plant is in full operation and add this component to the marginal operating cost in each time period. Since power plant data on start-ups and shutdowns are not available, I estimate this based on residual demand and the cost structure of individual power plants using the approach presented in Staffell and Green (2016). A simple illustration of this approach is contained in

Figure 1 (below), which shows the hourly residual demand satisfied by fossil fuels from January 1, 2016 to January 31, 2016. The intra-day variation in residual demand in the PJM region creates a need for short-term operation of load-following fossil fuel power plants to serve peak demand. The horizontal lines represent different levels of residual demand. Generators are started up (shut down) when the residual demand level exceeds (falls short of) the generator's hourly demand point on the aggregate marginal cost curve.[1]

Figure 2-1: Residual Demand with Load Points

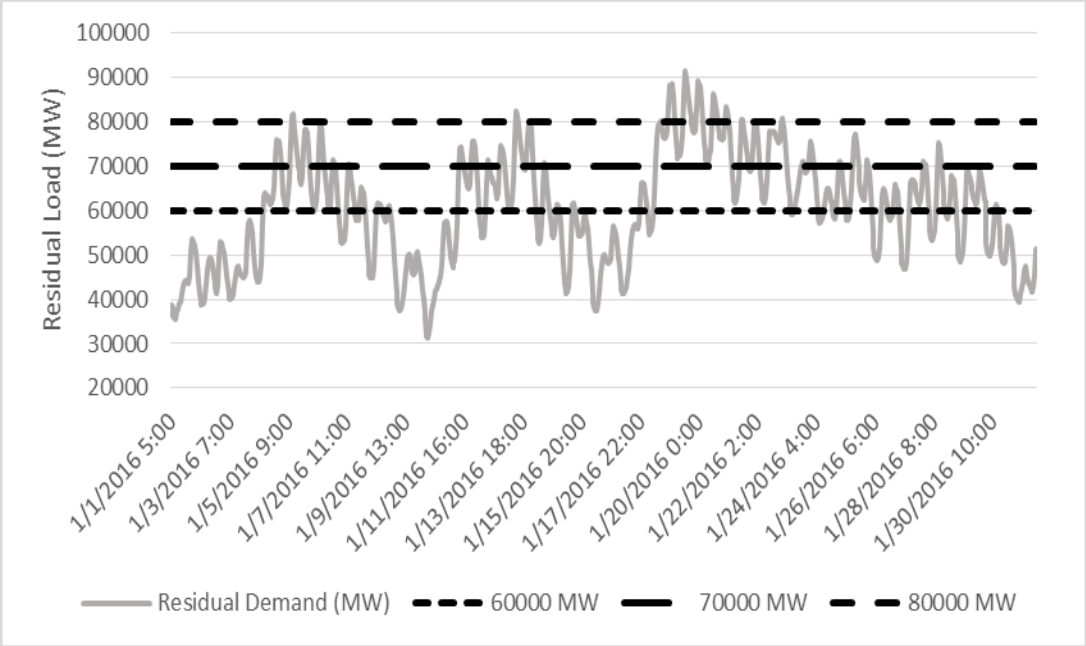

More specifically, the number of start-ups from January 2016 to December 2018 is estimated by calculating each power plant's hourly residual demand point $Q_{n,t}$. The value $Q_{n,t}$ is determined by ordering the fossil fuel plants (must-run plants are excluded) from lowest to highest marginal cost and calculating the cumulative sum of capacity. Then, if the observed hourly level of residual demand Q_t, which is the demand level served by fossil fuel generation after accounting for all of the must-run generation, exceeds the quantity $Q_{n,t}$, the *n*th power plant will start up. Likewise, if Q_t falls below $Q_{n,t}$ then the *n*th power plant will shut down. The

[1] This model assumes that the lower marginal cost power plants are started up before those with higher marginal costs. However, it may be optimal from an average cost perspective to dispatch a lower start-up cost/higher marginal cost power plant instead of a higher start-up cost/lower marginal cost power plant (Joskow and Kahn, 2002; Mansur, 2008). This leads to a possible overestimation of start-up costs (and, thus, marginal costs). The number of start-ups is also over-estimated since there is no allowance for fossil fuel plants to operate at a minimum load level. These shortcomings may result in a higher estimated competitive market price and thus may miss detecting market if it exists.

horizontal lines in Figure 1 (above) represent three different residual demand points: 60,000 MW, 70,000 MW, and 80,000 MW and are used for the purpose of illustration. When observed hourly residual demand crosses over the 70,000 MW residual demand point from below to above, any generators with hourly residual demand points <=70,000 MW will be turned on. When the actual hourly residual demand level crosses over the 70,000 MW residual demand point from above to below, any generator with an hourly residual point equal to or greater than 70,000 MW will stop producing power. The estimated number of start-ups is multiplied by the start-up cost (in $/MW of capacity) to obtain a total start-up cost. Estimated start-up costs for coal and natural gas generators were obtained from a study by the National Renewable Energy Laboratory (NREL) (Kumar, Besuner, Lefton, Agan, and Hilleman, 2012). The total start-up cost is divided by the total power production (in MWh) over the period of continuous operation from starting up to shutting down in order to obtain a start-up cost per MWh of power production.

2.3.2 Power plant Assumptions

Following the methodology of Borenstein, Bushnell, and Wolak (2002), the estimation of the marginal cost of power production was simplified by segmenting generators based on fuel type into two groups: (1) generators that are price takers (must-run power plants), and (2) generators that influence the system-wide electricity price. Hydroelectric, nuclear, wind, solar, and other renewable fuel types are considered price takers in the wholesale electricity market. These power plants represented approximately 22 percent of the total installed capacity in the PJM region in 2016 (see the appendix). Coal, natural gas, oil, and biomass power plants are considered to have an influence on price. Collectively, these fuel types represented the other 78 percent of installed capacity in the PJM region in 2016.

The hourly observed generation of the price taking power plants is used to obtain a residual level of demand that is served by fossil-fuel and other power plants. Nuclear, wind, and solar are considered to be must-run generation having zero marginal costs. I also assume that hydroelectric power plants are price takers and would follow the same observed generation schedule in a perfectly competitive market. Fossil fuel and other generators are combined in a second group. The marginal cost of generation for power plants in the second group is estimated based on heat rates (the amount of energy required to generate one MWh of electricity) obtained from 2016 eGRID data, the price of fossil fuels, and data on variable operations and maintenance costs. The heat rate is given as mmBTU/MWh. Prices for fossil fuels are the delivered price to U.S. power plants quoted in terms of $/mmBTU. The The fuel price and heat rate are used to calculate the cost of fuel per MWh.

2.3.3 PJM Transmission

PJM has many transmission ties between its territory and neighboring areas and, most of the time, the PJM region is a net importer of power. The large amount of transmission capacity in the PJM region and neighboring territories helps to facilitate the least-cost dispatch of generation among neighboring areas and promotes market efficiencies within the PJM region. Given the large number of interconnections, it is reasonable to assume that there are no transmission constraints between areas. It follows from this simplifying assumption that the marginal plant exporting power to PJM has a marginal cost equal to the day-ahead system-wide price in the PJM region, assuming that power plants outside the PJM region behave in a perfectly competitive manner. The assumption of no congestion between the PJM region and neighboring territories is also consistent with our approach to abstract away from transmission congestion within the PJM region to make it possible to compare the estimated competitive benchmark price to the system-wide market price, which is the energy price without transmission congestion and transmission losses. Section 2.3.4 (below) discusses the comparison to the system-wide energy price, which is determined with no transmission congestion and losses, to determine the degree market power is exercised in the PJM region. I follow Borenstein, Bushnell and Wollak (2002) and make a second simplifying assumption that power plants exporting power to the PJM region are price takers. That is, power plants outside the PJM region do not behave strategically to alter the system-wide market price in the PJM region by withholding capacity.[2]

2.3.4 Marginal Cost Calculation

The marginal cost of fossil fuel power plants and other generation, such as biomass, is a function of average heat rates, variable operations and maintenance costs, and fuel costs. The aggregate marginal cost curve is then constructed using the capacities and calculated marginal cost of each power plant. For the calculating marginal cost, the heat rate gives the efficiency with which the power plant converts thermal energy to output energy. More precisely, the heat rate is the ratio of thermal energy required to output energy. A heat rate of 3.412 mmBTU/MWh is perfect efficiency since one KWh of electricity has the same amount of energy as 3,412 BTU. I

[2] Borenstein, Bushnell, and Wolak (2002) provide the following logic to demonstrate the conservativeness of this assumption. They reason that if the converse was true, then the level of observed net imports would be lower than the quantity of net imports assuming power plants exporting to PJM behave in a perfectly competitive manner. Therefore, if this simplifying assumption fails, the estimated competitive benchmark price will be biased upward and measurement of the degree of market power will biased downward.

use the 2016 eGRID data[3] to obtain heat rates in terms of mmBTU/MWh for every fossil-fuel power plant within the PJM balancing authority. The prices for fossil fuels and other fuel types were obtained from the EIA in terms of $/mmBTU. Variable operations and maintenance costs were also obtained from the EIA for different fossil fuel types. The eGRID data include heat rates for each power plant. Therefore, the available data allow for heterogeneous heat rates. The data on variable operations and maintenance costs vary by fuel type, so variable operations and maintenance costs are homogenous across power plants of the same fuel type. The following equation gives the marginal cost of generation:

$$MC = HR * F + VOM \quad (1)$$

where

HR is the heat rate in mmBTU/MWh,

F is the fuel cost in $/mmBTU,

and *VOM* is the variable operations & maintenance cost per MWh.

Fuel prices were obtained from the EIA's Monthly Energy Review (2020). The cost of distillate fuel is used for Oil generation. The fuel prices are given in terms of the cost of delivery of the fuel at electric generating plants (in $/mmBTU, including taxes).

2.4 Electricity Prices and Loads

PJM operates two different electricity markets: a day-ahead market and real-time market. The real-time market determines the spot price of electricity at five-minute intervals based on the actual state of the transmission grid. The day-ahead market for electricity determines hourly prices for the next day. Both the day-ahead and real-time markets for electricity use locational marginal pricing. Settlement of the day-ahead market is based on lowest cost and optimal conditions in the transmission grid, and almost all generation is offered through the day-ahead market. Normal real-time operating conditions in the transmission grid will produce real-time prices that are similar to the day-ahead prices, and virtual bids drive convergence in the day-ahead and real-time prices. However, if unexpected shocks such as outages occur, the spread between real-time and day-ahead prices will widen. Therefore, real-time prices exhibit more volatility compared to day-ahead prices. Since almost all generation is committed through the day-ahead market, I use the day-ahead system energy price. Day-ahead system energy prices are obtained from the PJM public database (PJM Data Miner 2, 2019). The system-wide market price is defined as the market-clearing price without any congestion costs or transmission losses. Using locational marginal pricing, the price at each node can be decomposed into three

[3]Data on heat rates for power plants with the PJM balancing authority were downloaded from https://www.epa.gov/energy/emissions-generation-power plant-integrated-database-egrid.

components: the system-wide energy price, cost of transmission loss, and a transmission congestion cost. The system-wide energy price is computed by netting out the costs of transmission loss and congestion which create price differentials between different locations.

Because the system-wide energy price is the price without costs of congestion and transmission losses, it is comparable to the modeled competitive benchmark price level which also does not account for transmission congestion. Even though power plants are actually dispatched out of least cost order due to transmission congestion, the locational marginal prices are not comparable to the modeled competitive benchmark price since the competitive benchmark price is determined from a least cost dispatch assuming optimal conditions with no transmission congestion. In addition, I use the day-ahead system-wide energy price instead of the real-time system-wide energy price because the modeled competitive benchmark price assumes optimal conditions in the transmission grid. The real-time system energy price can diverge from the day-ahead system energy price if there is an unexpected major outage, for example, that would result in the re-dispatch of power plants out of merit order, which is the ordering of power plants from lowest to highest marginal costs.

Appendix D shows the average electricity prices by hour of day and for dates by month and year from Jan 2016 to December 2018. Peak hours are usually considered to be from 7am to 10pm. The electricity prices are the highest between 6am and 9pm which corresponds closely to the usual peak period definition. Electricity prices in the PJM region are generally highest during the summer and winter months. There was a spike in prices in January 2018 attributed to a shortage in the supply of natural gas due to unseasonably cold temperatures. Temperatures were also lower than normal during March/April 2018. Figures 2-2 and 2-3 below show the level of residual demand served by fossil fuels. Residual demand levels are generally the highest during the summer and winter months.

Figure 2-2: Residual Demand Box and Whisker Plot (Jan 2016 - Dec 2018)

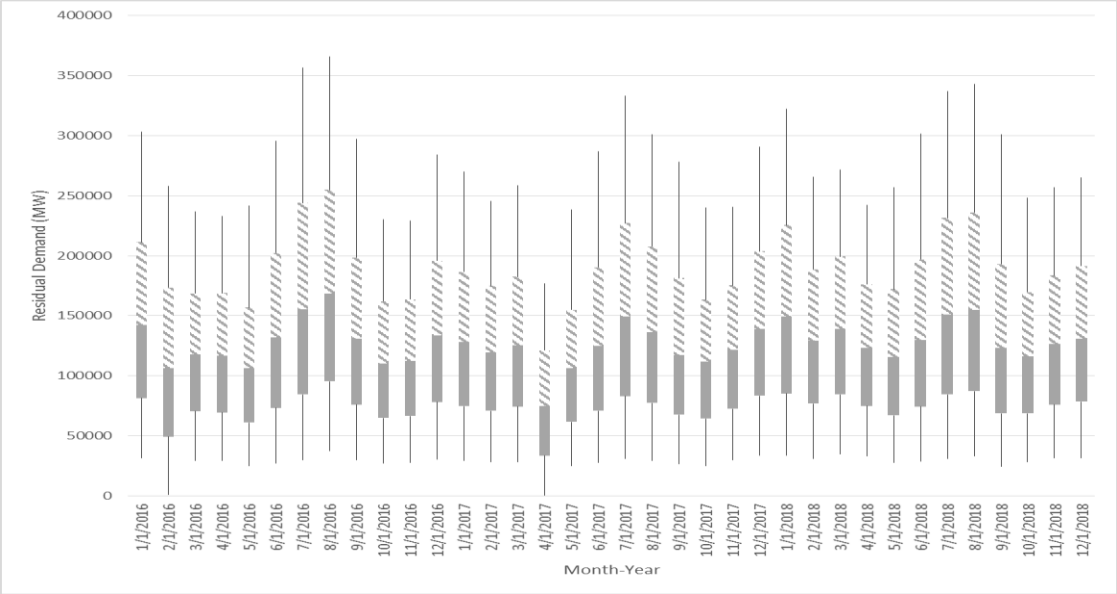

Notes: The data are sourced from PJM Data Miner 2 (2019). The boxes show the interquartile range for each month and the whiskers show the max and min values for residual demand.

Figure 2-3: Residual Demand (Jan 2016 - Dec 2018)

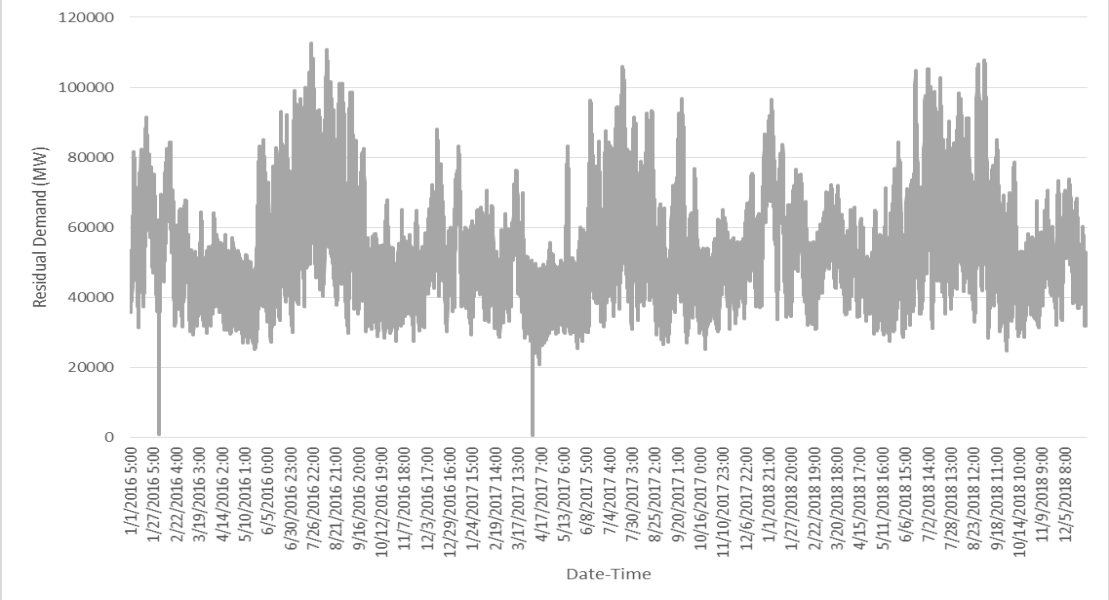

Notes: Data sourced from PJM Data Miner 2.

2.5 Marginal Cost of Generation

The hourly marginal cost of generation is determined by the intersection of the aggregate marginal cost curve with the residual metered load. The residual metered load is calculated for each hour of each day by first subtracting the observed generation from hydroelectric, nuclear,

storage, solar, wind, and other renewables from the metered load. PJM provides data on the observed generation by fuel type for each hour of each day. Using these data, I calculate the residual quantity of metered load that is satisfied with fossil fuel generation. The amount of capacity that is allocated for regulation reserve is added to the residual quantity of the metered load. However, it should be noted that the amount of capacity that clears the PJM Regulation Market is a small percentage of the residual metered load, so it is not material to the marginal cost calculation. Nonetheless, this capacity is not available for satisfying the metered load, and therefore it needs to be added in to improve the accuracy of the marginal cost calculation (see PJM Manual 11).

Additionally, the aggregate marginal cost curve is adjusted by accounting for the effects of forced outages. A forced outage means the power plant has no capacity available for energy production. This can be due to scheduled maintenance or an unexpected breakdown, for example. Unexpected forced outages will have an immediate effect on the real-time market, but an outage will also impact the day-ahead system energy price for the duration of the outage period. The competitive benchmark price will increase when lower marginal cost plants experience forced outages because these are taken out of the aggregate marginal cost calculation. If forced outages are not incorporated into the model, there will be a tendency to underestimate the competitive price and thus overestimate the degree of market power. Forced outages are applied to the power plant capacities in each hour of each day using a simulation method presented in Kumar, Shivani, Deepika, and Aman (2013) and Borenstein, Bushnell, and Wolak (2002). As in their models, forced outages are treated as a stochastic component of the model. Power plants are assumed to be in one of two possible states. They either have 100 percent of capacity available for power production or zero percent available due to a forced outage. The forced outages are assumed to last for a one-month period of time. PJM provides monthly data on the Equivalent Demand Forced Outage Rate by generation type and nameplate capacity. PJM Manual 22 defines the Equivalent Demand Forced Outage Rate as the proportion of time a power plant is unavailable due to a forced outage. The probability of the two possible states can be described as follows:

$$P(S = s) = \begin{cases} 1-p \\ p \end{cases} \quad (2)$$

where p is the probability of an outage. The probability p is determined for each power plant for each month from the PJM data on Equivalent Demand Forced Outage Rates. Simulations of

forced outages are run for each month to determine the sensitivity of the marginal cost of generation to forced outages.[4]

After the forced outages are determined, the fossil fuel power plants are ordered by their constant marginal cost in ascending order. Section 2.3.4 (above) describes the methodology for determining each power plant's monthly constant marginal cost. The marginal cost of fossil fuel generation is determined for each hour of each day by the marginal power plant required to satisfy the residual metered load. Figure 2-4 (below) shows the aggregate marginal cost curves for January 2016, January 2017, and January 2018. Tables 2-1 and 2-2 (below) compare the capacity-weighted marginal cost of coal and natural gas generation. Natural gas power plants have a higher capacity-weighted marginal cost compared to coal power plants in every month of 2018. In the warmer months of 2016, the capacity-weighted marginal cost of natural gas power plants dropped below that of coal because the price of natural gas was relatively low. The capacity-weighted marginal cost of natural gas power plants increased during months when the price of natural gas increased due to unseasonably cold temperatures.

Figure 2-4: Aggregate Marginal Cost Curves

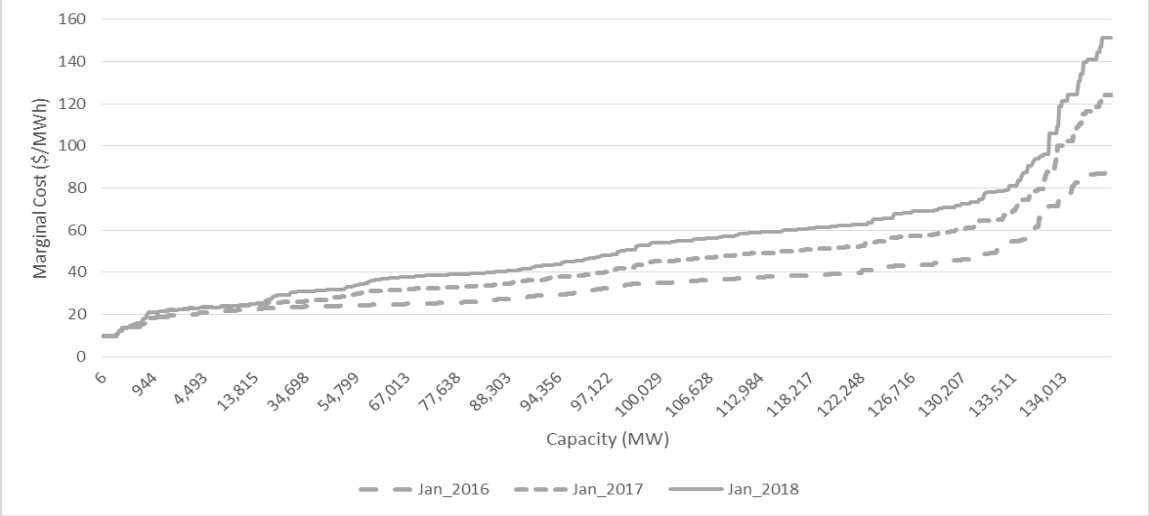

[4] The simulations are implemented in Microsoft Excel with the BINOM.INV function. The number of trials is set to 1, the probability of an outage is determined by the Equivalent Demand Forced Outage Rate, and the RAND function is used to get the criterion value. According to Microsoft Excel documentation, the RAND function can be used to generate a random number from a uniform distribution with a support less than or equal to 1 and greater than or equal to 0. The BINOM.INV function produces the smallest value for which the Bernoulli CDF is greater than or equal to the criterion value. For example, if the criterion value is 0.7 and probability of a forced outage is 0.2, then the BINOM.INV will return a value of 0. In each simulation, the RAND function is used to generate a sequence of random numbers for each power plant for each month. The sequence of random numbers and Equivalent Demand Forced Outage Rates are used to determine which state each power plant is in for each month. I ran 100 simulations to determine the sensitivity of the marginal cost of generation to forced outages.

Table 2-1: Capacity-weighted Average Marginal Cost of Coal Generation

Month	Year 2016	Year 2018
Jan	34.0	33.3
Feb	33.9	33.3
Mar	34.8	32.8
Apr	34.6	33.3
May	34.6	33.0
Jun	33.7	33.0
Jul	33.9	33.1
Aug	33.9	33.1
Sep	34.0	33.0
Oct	33.3	33.0
Nov	33.4	33.1
Dec	34.4	32.0

Notes: The capacity-weighted average marginal cost is the average marginal cost of power plants weighted by the capacity of each power plant. Since the inputs into the marginal cost calculation are monthly fuel prices, heat rates, and variable operations and maintenance costs, the marginal cost of a power plant will change on a monthly basis. Therefore, we calculate the capacity-weighted average marginal cost on a monthly basis averaging over all of the power plants.

Table 2-2: Capacity-weighted Average Marginal Cost of Gas Generation, 2016 and 2018

Month	Year 2016	Year 2018
Jan	34.3	54.6
Feb	31.0	40.3
Mar	26.3	35.9
Apr	28.2	35.4
May	27.9	34.5
Jun	30.7	35.2
Jul	33.8	37.0
Aug	33.6	36.8
Sep	34.8	35.2
Oct	35.4	38.0
Nov	34.3	45.9
Dec	42.3	48.1

2.6 Discussion and Results

Discussion and results are presented in the following sections, first without start-up costs and then with start-up costs included.

2.6.1 Estimation of the Competitive Price Level without Start-up Costs

The results below compare the competitive benchmark price to the day-ahead system energy price. The difference between the competitive benchmark price and the day-ahead system energy price as a percent of the competitive benchmark price is used as a measure of market power. Figure 2-5 (below) shows that the day-ahead system energy price is typically higher than the competitive benchmark price, more so during peak periods. The results also show that the competitive benchmark price tends to be higher compared to the day-ahead system energy price during nighttime, which is the off-peak period. These results are consistent with the expectation that more opportunities exist to exercise market power during peak periods. During peak periods, there is a greater likelihood for power plants to be a pivotal supplier due to transmission congestion.[5] These power plants may anticipate that they will have a very strong strategic position because low-cost competition may be unable to respond due to transmission congestion. Market participants are expected to have more opportunities to exercise market power under these market conditions, and, therefore, we expect to see that the day-ahead system energy price is higher than the competitive benchmark price. The consistency of the results with the expectations provides additional confidence in the general approach to modeling the competitive benchmark price.

The deviance between the system-wide electricity price and the estimated competitive benchmark price suggests that market power mitigation in the PJM Region could be more effective at preventing the exercise of market power. I believe this is largely due to how PJM applies the pivotal supplier test, which looks only at single transmission constraints and focuses on whether a single power plant is a pivotal supplier. First, the pivotal supplier test may fail to detect the exercise of market power since it only looks at a single transmission constraint and does not consider the possibility that another constraint would prevent other power plants from supplying additional power. In other words, the relevant market for determining a pivotal supplier

[5] Market power is exercised when power plants withhold power so that their marginal cost is less than the market clearing price but equal to marginal revenue. When power is withheld, more expensive power plants become the marginal plant. The system-wide energy price will reflect the clearing of more expensive power when less expensive power plants exercise monopoly power through withholding capacity (Wolak and Patrick, 2001). Capacity is typically withheld during peak periods when there is more transmission congestion, since firms are unlikely to possess sufficient market power in the absence of transmission congestion (Borenstein, Bushnell, and Stoft, 2000).

is all of the power plants that could relieve the single constraint (constraint A). However, it is possible that other constraints would prevent these power plants from relieving constraint A. Second, under this application of the pivotal supplier test, it is possible for the exercise of market power to go undetected if no one power plant can manipulate electricity prices by itself, but power plants acting in concert are able to manipulate electricity prices. For example, a power plant may expect other power plants to engage in anti-competitive behavior, and therefore find it profitable to withhold capacity and/or submit an offer price that exceeds the competitive benchmark price.

The results also show that the system-wide market price deviates the most from the competitive market price during the colder months. February 2017 was unseasonably warm which produced a decrease in natural gas prices and metered load. March 2016 and February 2018 also produced warmer than average temperatures across the PJM region. The average difference between the estimated competitive price the system-wide market price in the months of March 2016, February 2017, and February 2018 is smaller compared to most of the other winter months from January 2016 to December 2018. The weather in March/April 2018 was unseasonably cold which produced higher natural gas prices in March/April/May 2018 because natural gas is also used for heating. The deviation between the system-wide market price and the competitive price widened over these three months. We also observe larger average deviations between the estimated competitive price and the system-wide electricity price during March/April 2017 when the weather across the Mid-Atlantic was colder than normal. Even after accounting for the spike in natural gas prices, I find that the system-wide market price in January 2018 departed significantly from the competitive level. This month corresponds to a shortage in natural gas due to temperatures that were colder than normal and a spike up in the metered load. My results suggest that that there were more opportunities for market participants to exercise market power when the metered load spiked up in January 2018, even after accounting for the spike in the system-wide market price stemming from the spike in demand.

Figure 2-5: Day-ahead System Energy Price and Competitive Benchmark

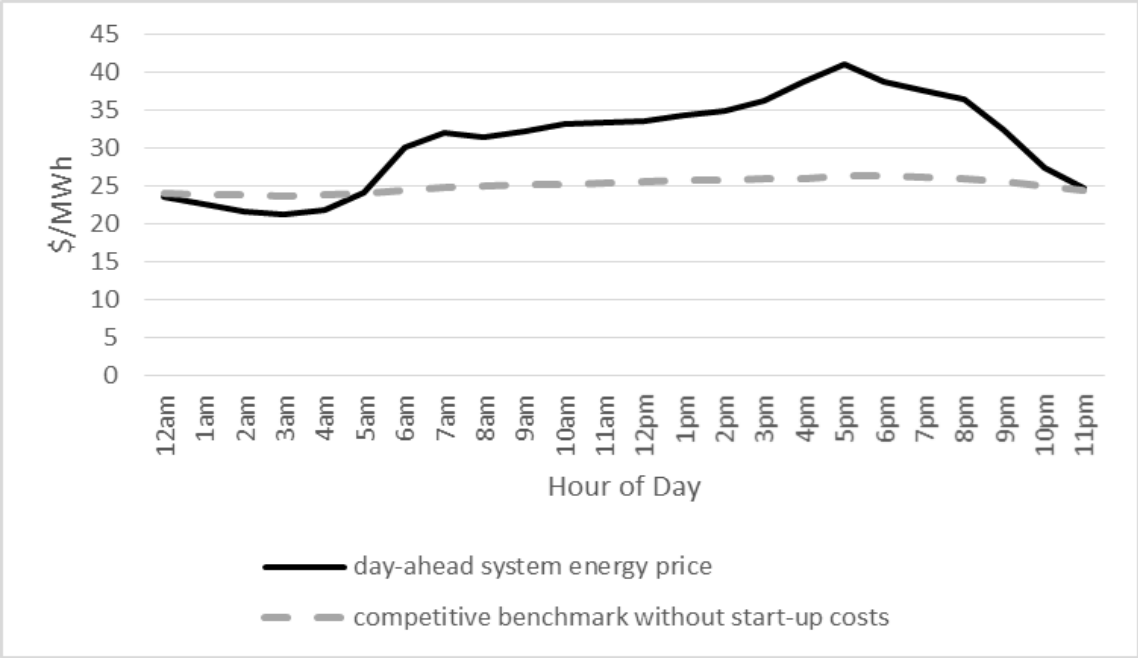

Notes: Hourly prices are averaged over the 1,095 days in the years 2016 to 2018.

Table 2-3: Summary Statistics for Deviations from Competitive Benchmark, 2016

$$100 \cdot \frac{1}{n} \sum_{i=1}^{n} \frac{P_i - MC_i}{MC_i}$$

Month	Min	First Quartile	Median	Third Quartile	Max	Average
Jan	-90.4%	-3.9%	12.1%	35.4%	198.2%	20.4%
Feb	-57.5%	-9.9%	4.9%	28.8%	196.3%	13.1%
Mar	-56.9%	-12.1%	0.6%	14.9%	94.7%	2.6%
Apr	-32.8%	-3.5%	12.3%	35.7%	115.1%	18.7%
May	-64.6%	-18.7%	2.5%	16.4%	148.0%	0.7%
Jun	-81.9%	-19.5%	4.1%	28.9%	129.8%	5.9%
Jul	-73.6%	-11.7%	4.7%	29.8%	191.0%	12.2%
Aug	-57.6%	-11.1%	9.1%	41.5%	221.8%	16.8%
Sep	-90.4%	-14.7%	2.8%	33.7%	251.6%	14.0%
Oct	-38.0%	-6.9%	14.5%	35.1%	181.6%	17.7%
Nov	-29.7%	-7.7%	3.0%	22.3%	91.8%	8.5%
Dec	-21.2%	2.9%	13.6%	30.6%	169.7%	20.0%

Notes: The summary statistics are calculated from hourly data on the deviation between the system-wide energy price and the competitive benchmark price as a percentage of the competitive benchmark price.

Table 2-4: Summary Statistics for Deviations from Competitive Benchmark, 2017

$$100 \cdot \frac{1}{n} \sum_{i=1}^{n} \frac{P_i - MC_i}{MC_i}$$

Month	Min	First Quartile	Median	Third Quartile	Max	Average
Jan	-19.5%	2.0%	11.5%	29.2%	177.4%	17.7%
Feb	-26.7%	-3.6%	4.9%	16.6%	95.1%	8.5%
Mar	-26.7%	1.1%	17.0%	41.0%	254.3%	25.9%
Apr	-28.0%	-2.8%	21.0%	43.2%	149.9%	22.3%
May	-40.7%	-5.4%	15.4%	34.6%	328.7%	18.8%
Jun	-57.6%	-16.4%	1.2%	24.3%	99.4%	4.8%
Jul	-60.1%	-14.8%	4.0%	33.5%	194.4%	11.8%
Aug	-57.5%	-15.4%	0.1%	24.7%	119.2%	6.4%
Sep	-58.1%	-15.1%	3.0%	35.6%	558.8%	18.1%
Oct	-42.6%	-5.8%	17.8%	38.3%	128.9%	20.5%
Nov	-31.9%	-2.7%	12.7%	37.6%	162.7%	20.3%
Dec	-21.4%	1.1%	14.0%	40.0%	354.4%	35.8%

Table 2-5: Summary Statistics for Deviations from Competitive Benchmark, 2018

$$100 \cdot \frac{1}{n} \sum_{i=1}^{n} \frac{P_i - MC_i}{MC_i}$$

Month	Min	First Quartile	Median	Third Quartile	Max	Average
Jan	-17.2%	13.3%	51.3%	160.8%	497.5%	99.1%
Feb	-30.2%	-12.6%	-2.4%	10.0%	189.0%	2.8%
Mar	-23.0%	7.5%	18.8%	39.6%	229.7%	28.1%
Apr	-18.2%	13.2%	38.5%	59.6%	166.0%	39.6%
May	-35.9%	-7.5%	31.9%	61.8%	280.7%	36.1%
Jun	-33.1%	-16.2%	7.7%	35.5%	256.3%	14.4%
Jul	-45.5%	-13.5%	8.7%	37.5%	227.3%	16.1%
Aug	-23.9%	-10.0%	11.4%	40.4%	132.9%	17.8%
Sep	-29.4%	-6.6%	20.9%	48.4%	256.4%	26.9%
Oct	-24.1%	8.3%	32.2%	59.0%	270.9%	39.9%
Nov	-37.1%	29.7%	44.1%	64.1%	157.8%	45.9%
Dec	-20.9%	7.4%	22.3%	33.8%	110.5%	22.0%

Simulations of forced outages were run using the methodology described in Section 2.5. Tables 6, 7, and 8 (below) show summary statistics for the difference between the competitive benchmark price and the day-ahead system energy price as a percent of the competitive benchmark price. The results show some variation in the degree of market power across the simulations. This is consistent with expectations based on how the simulations were implemented. Since the probability of a forced outage in the simulations does not depend on time of day, the simulated outages should be considered unexpected. Unplanned outages can have a noticeable effect on wholesale electricity prices. In practice, most outages are planned to occur during off-peak periods to allow for maintenance to be performed with minimal impact on market operations. Therefore, the computed competitive benchmark price is higher than it should be, reducing the likelihood we will conclude that there is market power.

Table 2-6: Summary Statistics Monte Carlo Simulations, 2016

$$100 \cdot \frac{1}{n} \sum_{i=1}^{n} \frac{P_i - MC_i}{MC_i}$$

Month	Min	First Quartile	Median	Third Quartile	Max
Jan	18.4%	20.1%	20.3%	20.9%	21.2%
Feb	11.3%	12.9%	13.2%	13.5%	13.8%
Mar	1.4%	2.4%	2.7%	2.8%	3.6%
Apr	17.5%	18.5%	18.8%	19.0%	19.5%
May	-0.9%	0.4%	0.6%	1.1%	1.6%
Jun	4.7%	5.1%	6.0%	6.5%	7.1%
Jul	7.2%	10.4%	12.3%	14.4%	15.9%
Aug	14.3%	15.3%	16.7%	17.7%	21.8%
Sep	11.6%	13.5%	14.1%	14.8%	15.3%
Oct	17.1%	17.4%	17.7%	18.0%	18.4%
Nov	8.1%	8.3%	8.5%	8.7%	8.7%
Dec	18.1%	19.1%	20.2%	20.9%	21.6%

Notes: For each simulation, the average deviation between the system-wide energy price and the competitive benchmark price as a percentage of the competitive benchmark price was calculated for each month. Summary statistics were calculated to show the distribution of the average percentage deviation between the system-wide energy price and the competitive benchmark price.

Table 2-7: Summary Statistics Monte Carlo Simulations, 2017

$$100 \cdot \frac{1}{n} \sum_{i=1}^{n} \frac{P_i - MC_i}{MC_i}$$

Month	Min	First Quartile	Median	Third Quartile	Max
Jan	15.6%	17.0%	17.7%	18.3%	20.3%
Feb	6.2%	7.6%	8.7%	9.6%	9.9%
Mar	23.7%	25.1%	26.0%	26.6%	27.3%
Apr	21.1%	21.9%	22.5%	22.7%	23.3%
May	17.2%	18.3%	18.8%	19.6%	20.2%
Jun	3.0%	4.3%	4.8%	5.3%	6.3%
Jul	10.1%	10.6%	11.7%	12.8%	14.1%
Aug	3.0%	5.5%	6.6%	7.6%	8.2%
Sep	16.8%	17.5%	18.2%	18.6%	19.5%
Oct	19.8%	20.1%	20.4%	20.9%	21.4%
Nov	18.2%	19.9%	20.5%	20.9%	22.0%
Dec	32.3%	35.0%	36.3%	37.0%	37.6%

Table 2-8: Summary Statistics Monte Carlo Simulations, 2018

$$100 \cdot \frac{1}{n} \sum_{i=1}^{n} \frac{P_i - MC_i}{MC_i}$$

Month	Min	First Quartile	Median	Third Quartile	Max
Jan	92.4%	97.7%	98.8%	100.1%	106.8%
Feb	-0.5%	2.1%	3.0%	3.6%	5.1%
Mar	26.5%	27.5%	28.1%	28.7%	29.6%
Apr	38.3%	39.3%	39.5%	39.8%	41.1%
May	33.8%	35.0%	36.7%	37.2%	37.9%
Jun	12.6%	13.6%	14.4%	15.1%	16.3%
Jul	10.6%	15.2%	16.5%	17.7%	18.3%
Aug	12.1%	16.8%	17.6%	19.3%	21.5%
Sep	24.1%	26.2%	26.7%	27.9%	28.6%
Oct	38.9%	39.5%	39.8%	40.3%	41.0%
Nov	43.7%	45.0%	46.1%	46.6%	48.0%
Dec	20.3%	21.4%	22.0%	22.6%	23.7%

2.6.1.1 Sensitivity of Competitive Benchmark to the Quantity of Net Imports

Data show that PJM is often a net importer of power. We note the following relationship between the competitive benchmark price and the level of net imports. If the competitive price level is lower (higher) than the system-wide market price, then the level of net imports would decrease (increase) from the observed level in the PJM data. If the decrease in the level of net imports is not accounted for in the model, then my measurement of the degree market power is exercised will be biased upward. PJM does not provide data that would enable me to construct supply curves for imports and exports. Therefore, instead of making the quantity of net imports a function of price in the model, I use sensitivity testing to test the robustness of the results to different levels of net imports. Table 2-9 shows that net imports are a small percentage of the total metered load. Therefore, I do not expect significant variation in the results of the model across the scenarios in the sensitivity testing. The results of the sensitivity testing presented below confirm this expectation.

Table 2-9: Net imports as a Percentage of Total Metered Load

	Net imports as a percentage of total metered load		
Month	**Year 2016**	**Year 2017**	**Year 2018**
Jan	3.00%	1.50%	1.70%
Feb	2.90%	2.10%	2.20%
Mar	3.00%	2.60%	0.80%
Apr	2.20%	4.30%	0.90%
May	1.60%	3.80%	1.90%
Jun	4.00%	3.60%	3.00%
Jul	3.60%	3.40%	3.00%
Aug	3.10%	3.30%	3.50%
Sep	4.30%	4.00%	4.00%
Oct	4.40%	3.00%	4.10%
Nov	2.20%	2.10%	2.20%
Dec	2.80%	2.90%	3.80%

I tested the sensitivity of different levels of net imports by shocking the level of imported (exported) generation downward (upward) compared to the observed level of net imports. For each shock scenario, I calculate the residual demand that is satisfied with fossil fuel generation. The quantity of imported (exported) generation was shocked downward (upward) by 15%, 25%, 50%, and 60% of the observed level to account for the potential bias upward in the estimated degree of market power discussed above. The results presented in Tables 2-10, 2-11, and 2-12 (below) confirm this expectation and show the degree of market power has minor variation across the shocks applied to net imports. These results indicate the model outputs based on the observed level of net imports are robust to different levels of net imports and comparable to results that would be obtained with the competitive level of net imports.

Table 2-10: Average Deviation from Competitive Benchmark by Level of Net Imports, 2016

$$100 \cdot \frac{1}{n} \sum_{i=1}^{n} \frac{P_i - MC_i}{MC_i}$$

Month	-15% net imports	-25% net imports	-50% net imports	-60% net imports	Observed net imports
Jan	20.3%	20.1%	19.8%	19.7%	20.4%
Feb	12.9%	12.9%	12.6%	12.5%	13.1%
Mar	2.4%	2.4%	2.1%	2.1%	2.6%
Apr	18.6%	18.5%	18.4%	18.3%	18.7%
May	0.7%	0.6%	0.5%	0.4%	0.7%
Jun	5.8%	5.7%	5.5%	5.4%	5.9%
Jul	11.8%	11.5%	10.8%	10.5%	12.2%
Aug	16.5%	16.3%	15.7%	15.5%	16.8%
Sep	13.8%	13.7%	13.4%	13.3%	14.0%
Oct	17.6%	17.5%	17.2%	17.1%	17.7%
Nov	8.5%	8.5%	8.4%	8.4%	8.5%
Dec	19.4%	19.2%	18.4%	18.2%	20.0%

Table 2-11: Average Deviation from Competitive Benchmark by Level of Net Imports, 2017

$$100 \cdot \frac{1}{n} \sum_{i=1}^{n} \frac{P_i - MC_i}{MC_i}$$

Month	-15% net imports	-25% net imports	-50% net imports	-60% net imports	Observed net imports
Jan	17.6%	17.4%	17.1%	17.0%	17.7%
Feb	8.3%	8.3%	8.0%	7.9%	8.5%
Mar	25.7%	25.7%	25.4%	25.4%	25.9%
Apr	22.2%	22.1%	22.0%	21.9%	22.3%
May	18.8%	18.7%	18.6%	18.5%	18.8%
Jun	4.7%	4.6%	4.4%	4.3%	4.8%
Jul	11.4%	11.1%	10.4%	10.1%	11.8%
Aug	6.1%	5.9%	5.3%	5.1%	6.4%
Sep	17.9%	17.8%	17.5%	17.4%	18.1%
Oct	20.4%	20.3%	20.0%	19.9%	20.5%
Nov	20.3%	20.3%	20.2%	20.2%	20.3%
Dec	35.2%	35.0%	34.2%	34.0%	35.8%

Table 2-12: Average Deviation from Competitive Benchmark by Level of Net Imports, 2018

$$100 \cdot \frac{1}{n} \sum_{i=1}^{n} \frac{P_i - MC_i}{MC_i}$$

Month	-15% net imports	-25% net imports	-50% net imports	-60% net imports	Observed net imports
Jan	99.0%	98.8%	98.5%	98.4%	99.1%
Feb	2.6%	2.6%	2.3%	2.2%	2.8%
Mar	27.9%	27.9%	27.6%	27.6%	28.1%
Apr	39.5%	39.4%	39.3%	39.2%	39.6%
May	36.1%	36.0%	35.9%	35.8%	36.1%
Jun	14.3%	14.2%	14.0%	13.9%	14.4%
Jul	15.7%	15.4%	14.7%	14.4%	16.1%
Aug	17.5%	17.3%	16.7%	16.5%	17.8%
Sep	26.7%	26.6%	26.3%	26.2%	26.9%
Oct	39.8%	39.7%	39.4%	39.3%	39.9%
Nov	45.9%	45.9%	45.8%	45.8%	45.9%
Dec	21.4%	21.2%	20.4%	20.2%	22.0%

2.6.2 Estimation of the Competitive Price Level with Start-up Costs

The results presented in the previous sections indicate that not all of the components of operating cost that determine the competitive price level have been captured because we would expect see consecutive months with smaller deviations from the system-wide electricity price during time periods when demand is low and/or fuel prices are lower. The fact that the results indicate higher levels of market power in every month of every year in my sample period suggests I am missing an important component of operating cost. In this section, I discuss the inclusion of start-up costs and competitive benchmark prices with and without start-up costs. The results presented below suggest that start-up costs are an important component of the system-wide electricity price.

The figures below plot the estimated number of start-ups and estimated number of operating hours for all of the coal and natural gas power plants in the PJM region using the methodology presented in Staffell and Green (2016). More than 70 percent of installed capacity in the PJM region is coal and natural Gas. Tables 2-1 and 2-2 (above) show the capacity-weighted average marginal cost of natural gas power plants is below the capacity-weighted average marginal cost of coal power plants from March 2016 to June 2016 when the price of natural gas

was low compared to prices in 2017 and 2018. From September 2018 to December 2018, the price of natural gas was relatively high, and the capacity-weighted average marginal cost of the natural gas power plants is above that of coal power plants. Figure 2-6 below shows that most of the natural Gas capacity is estimated to be operated as peaking power plant. That is, most of the natural Gas capacity is estimated to have fewer start-up events and a smaller number of operating hours compared to coal power plants, which were operated as baseload and mid-merit power from September 2018 to December 2018. Figure 2-6 below shows that most of the coal power plants are providing baseload power (high number of operating hours/low number of start-up events) or mid-merit power (high number of operating hours/high number of start-up events) when the price of coal is lower than natural gas.

During the period from March 2016 to June 2016, natural gas power plants had a lower capacity-weighted MC compared to coal power plants. Figure 2-7 below shows that most of the natural gas capacity is estimated to be operated as a baseload power plant or mid-merit power plant. Most of the coal capacity is operated as a mid-merit power plant. Since coal was relatively more expensive, the coal power plants operated during a fewer number of hours compared to the period from September 2018 to December 2018. Natural gas power plants typically have a higher number of operating hours compared to the period from September 2018 to December 2018 when generating electricity from natural gas power plants is comparatively more expensive.

The results also show fewer start-ups during the period from March 2016 to June 2016 compared to the period from September 2018 to December 2018. This is consistent with expectations because the metered load is lower from March 2016 to June 2016 compared to the period from September 2018 to December 2018, so the electricity prices have smaller peaks. The prices in the appendix also show that electricity prices typically peak twice per day during colder months, once during the morning ramp-up and once in the evening. This pattern of demand also results in more frequent start-up and shutdown events for peaking and mid-merit power plants.

Figure 2-6: Estimated Number of Start-ups and Operating Hours (Sep 2018 – Dec 2018)

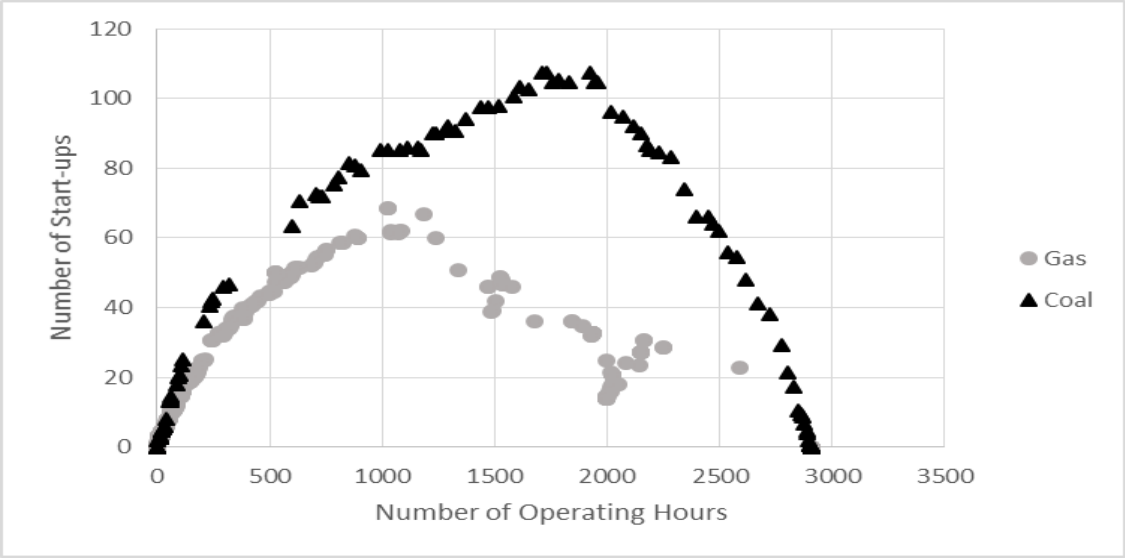

Figure 2-7: Estimated Number of Start-ups and Operating Hours (Mar 2016 – Jun 2016)

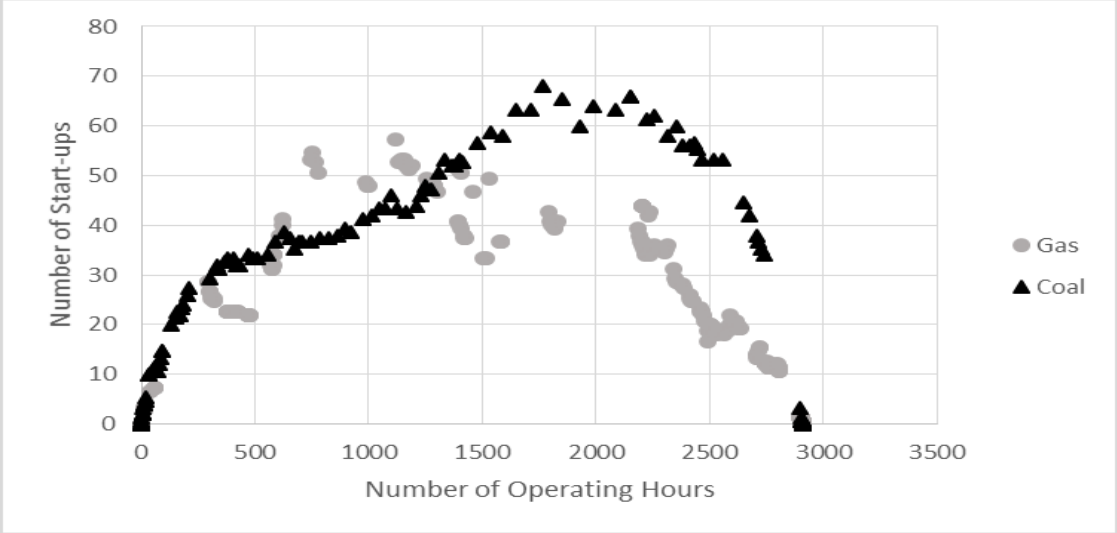

Figure 2-8 shows the estimated average hourly competitive prices with and without start-up costs compared to the average system-wide electricity price over the time period from January 2016 to December 2018. The results with start-up costs follow a little more closely the pattern of system-wide electricity prices. However, the similar trend in estimated competitive prices indicates that this simplistic approach to estimating the number of start-ups may not adequately capture the inter-temporal tradeoffs in production decisions. Nonetheless, this approach will tend to overestimate the competitive benchmark price because it does not allow for the possibility of power plants running at minimum load, thus reducing the possibility of concluding that there is market power even if it does exist. The competitive benchmark price without start-up costs does have a little less variation. The level of competitive benchmark prices with start-up costs is also closer to the mean level of system-wide electricity prices. This provides some evidence that the

market-based supply bids incorporate start-up costs. There is still evidence of market power during peak hours when the system-wide electricity price exceeds the estimated competitive price. However, the results also show the estimated competitive price exceeds the system-wide electricity price during off-peak hours by a similar margin. My model assumes the hourly supply bids incorporate the pro-rata share of start-up costs. However, these results suggest that power plants may only incorporate start-up costs in their supply bids during peak hours when the expected price of electricity exceeds their marginal cost.

Figure 2-8: Competitive prices with and without Start-up Costs

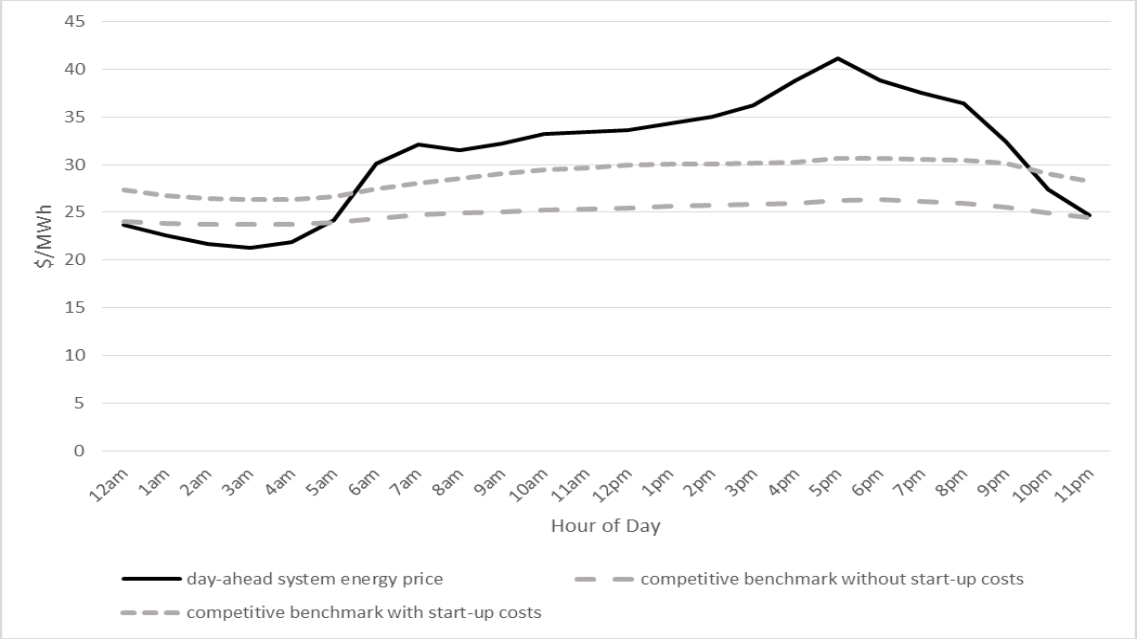

Notes: Hourly prices are averaged over the 1,095 days in the years 2016 to 2018. Competitive benchmark prices are presented for models with and without start-up costs.

The results in table 2-9 below show less evidence of market power compared to the case without start-up costs. The system-wide electricity price exceeds the average estimated competitive price during the winter peak period when temperatures were colder (Nov/Dec 2016 were unseasonably warm). These results should be interpreted as conservative because this approach used to incorporate start-up costs does not allow generators to produce power at levels between maximum and minimum output. Since power plants can only be in one of two states, either on or off, start-up costs are also overestimated because all start-ups are assumed to be "cold" start-ups (defined as starting up from shutdown) as opposed to ramping up from a minimum level of production which is less costly. Cold start-ups are significantly more costly than ramping up from a minimum level of power production. The approach also does not allow for the possibility that it may be more cost effective to dispatch a power plant with low start-up

costs and high marginal costs instead of dispatching a power plant with high start-up costs and a low marginal cost. In my model, power plants are dispatched according to their position along the aggregate marginal cost curve. Therefore, the power plant with a lower marginal cost and higher start-up costs would be dispatched. The overestimation of start-up costs may result in the underestimation of market power during the summer peak period when the estimated number of start-up and shutdown events for peaking and mid-merit power plants is the highest. However, the percentage deviation with and without start-up costs tends to be lower during the summer peak period compared to the winter peak period, suggesting other factors are also contributing to this result. I note that the price of natural gas deliveries to power plants is lower during the summer peak period compared to the winter peak period. As a result, the aggregate marginal cost curves during the winter peak months tend to be steeper with bigger jumps compared to the summer peak months (see the figure below, for example). This creates additional opportunities for power plants to profitably withhold power during the peak winter months in order to drive up the system-wide energy price, which may result in a higher degree of market power being exercised during the winter peak period. The consistency of these results gives confidence that I have captured all of the most important determinants of the competitive price level.

Figure 2-9: Aggregate Marginal Cost Curves of Fossil Fuel Generation

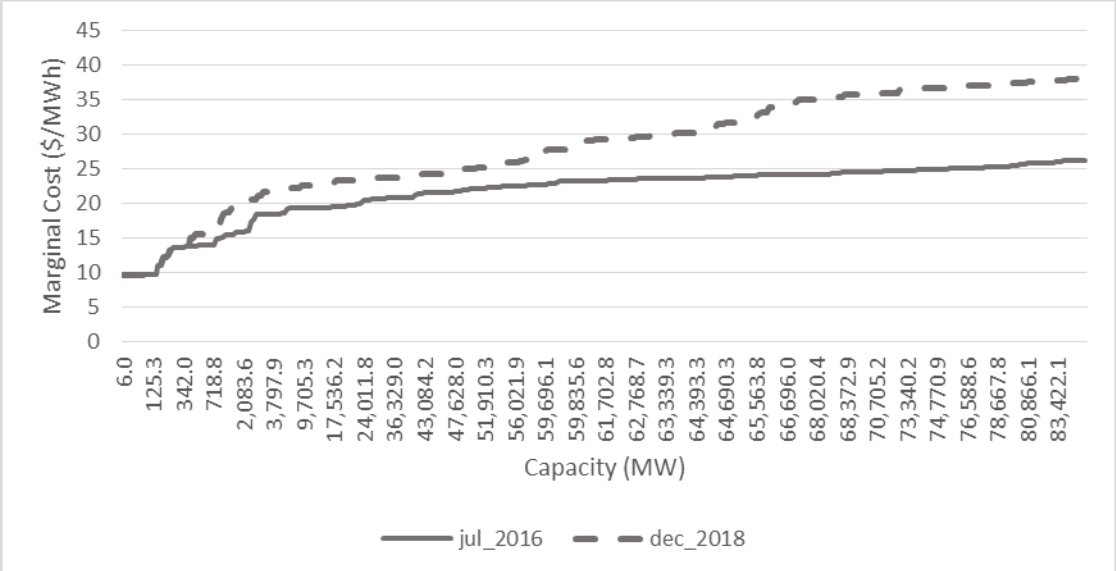

Notes: The aggregate marginal cost curves were constructed by ordering power plants by their monthly constant marginal cost in ascending order.

Table 2-13: Average deviation from Competitive Benchmark with Start-up Costs

		$100 \cdot \frac{1}{n}\sum_{i=1}^{n} \frac{P_i - MC_i}{MC_i}$	
Month	**Year 2016**	**Year 2017**	**Year 2018**
Jan	15.5%	7.3%	73.8%
Feb	7.6%	-0.5%	-5.1%
Mar	1.9%	6.7%	11.2%
Apr	18.0%	22.4%	23.7%
May	-1.5%	8.8%	16.7%
Jun	-8.7%	-10.7%	1.5%
Jul	-5.7%	-9.9%	-3.1%
Aug	-6.1%	-15.0%	-3.3%
Sep	-11.8%	-3.9%	0.9%
Oct	0.2%	5.1%	23.3%
Nov	-14.8%	17.6%	26.2%
Dec	-0.3%	33.6%	18.2%

A comparison to the results in Borenstein, Bushnell, and Wolak (2002) shows that the PJM region exhibited a smaller degree of market power, as measured by the deviation between the system energy price and competitive benchmark price, compared to California during the electricity crisis in 2000. The degree of market power in the PJM region from October 2018 to December 2018 when the price of natural gas spiked upward is comparable to that in California during the summer of 1998 before the energy crisis. We observe lower levels of market power in PJM during unseasonably cold months (e.g., Mar/Apr/May 2017 and Mar/Apr/May 2018) compared to peak periods in California. There are several reasons these results suggesting lower levels of market power in PJM compared to California are consistent with expectations. First, as mentioned above, PJM has more interconnections and a higher concentration of transmission, demand centers, and power plants. These differences should lead to less congestion and fewer pivotal suppliers, resulting in fewer opportunities to exercise market power. Additionally, I am comparing to a study of market power in California's electricity market that was conducted in 2002 when the wholesale electricity market was fairly immature. In contrast, PJM was established in 1997 and is market rules have matured. Therefore, I expect market monitoring and mitigation to be more effective at limiting the degree of market power compared to the California electricity market in 2000. Finally, I have captured start-ups, whereas Borenstein, Bushnell, and

Wolak (2002) do not account for start-ups, leading them to perhaps overestimate the degree of market power in California. This comparison of results also gives added credibility to the results produced in my study because I estimate smaller deviations between the system-wide price and estimated competitive price (with the exception of the Jan 2018 spike in electricity prices in PJM) over periods of multiple months compared to the 3-month period of time in 2000 from June 2000 to July 2000 when California's electricity industry was in crisis.

2.7 Conclusion

This paper analyzed the degree of market power in the PJM region from 2016 to 2018. The results presented in this paper show some evidence that market power was exercised, particularly in months having unseasonably cold temperatures and fuel price spikes as well as during the winter peak season. The results also show the degree of market power increases during the peak hours of the day. These results are consistent with expectations because there are more opportunities to exercise market power during peak hours. Transmission congestion during peak hours will lead to the presence of more pivotal suppliers. Additionally, output during peak hours is on a steeper part of the aggregate marginal cost curve (output during peak hours is higher). This creates opportunities for power plants that anticipate a strategic advantage to manipulate market prices by withholding supply to boost prices. PJM's market mitigation aims to curb such abuses of market power *ex ante* by using a structural test for market power. If market power is detected supply offers are mitigated to a cost-based level. However, as discussed above, the application of the pivotal supplier test may result in failures to detect the exercise of market power. These results are also consistent with studies of market power in the California electricity market showing market power is typically exercised when temperatures increase during the warm summer months. My results show there are generally more opportunities to exercise market power in the PJM region during the cold winter months. There is also evidence of market power when start-up costs are incorporated.

A future area of research would use dynamic programming to study the inter-temporal tradeoffs in production decisions. Power plants could be modeled as operating between max and min output levels, which would allow for a more accurate simulation of start-ups and shut downs and estimation of costs associated with ramping up and ramping down production. In reality, coal plants with higher start-up costs would reduce power output so they do not have to undergo a cold start-up (defined as starting up from a complete shutdown). My model assumes power plants are in one of two states, either producing power at full capacity or shut down. Since the costs associated with a cold start-up are higher than costs with ramping down and ramping up or

undergoing a hot start-up, my results with start-up costs should be a conservative estimate of the degree of market power, but the simplistic approach does not capture the production decisions in a realistic manner. That said, the model with start-up costs provides a more realistic representation of the power system in the PJM region than the model without, thereby allowing for a direct analysis of the exercise of market power within the PJM region. The results of the model are shown to be conservative and robust.

3. Chapter 2 - The Production and Use of Chilled-Water to Increase Efficiency of a Geothermal Power System under Different Temperature and Price Conditions

3.1 Introduction

The electricity industry continues to transition from traditional cost-of-service regulation to a restructured industry based on markets for electricity at the wholesale level and open-access to transmission. The transition to a competitive marketplace is being facilitated by several factors, including technological change, government policy, and institutional change in the electric utility industry. As the electricity industry moves towards greater competition, the generation, distribution, and transmission facilities are being unbundled to facilitate competition by increasing access to the market for power generation. The Energy Policy Act of 1992 established open access to the transmission system. In 1996, FERC Orders 888 and 889 "the open access rule" removed impediments to wholesale competition and encouraged the creation of market exchanges. FERC Order 2000 established the regional transmission organizations with authority to operate the transmission system and administer wholesale power markets. The Midwest ISO (MISO) was the nation's first RTO and opened the MISO energy markets in 2005. There are currently many different wholesale power markets operating throughout the United States and covering roughly 60 percent of the territory of the United States.

New institutions continue to be designed to reduce potential for market power by encouraging more independent power producers to enter the generation market. The movement to greater competition in the generation market has opened many opportunities for power marketers and independent power producers. There is also a greater imperative for utility companies to develop operating strategies for mitigating risk and increasing the probability of the individual units being profitable.

The policies and institutions designed to promote competition have major implications for development of the electric utility industry and the opportunities that exist for different players to profit from increased competition. This paper investigates an operating strategy from the perspective of a single low-temperature geothermal power plant seeking to maximize profit from the sale of electricity. This paper makes an important contribution by illustrating how a low-temperature geothermal power plant can be flexibly dispatched to offer multiple different services in addition to base-load power to a utility customer. The utility industry still thinks of geothermal as a base-load resource, but low temperature resource geothermal power plants offer more flexibility than other renewable energy technologies and can be operated as variable energy resources. Geothermal is capable of offering firmly flexible generation because it can achieve

high ramp speeds. For example, geothermal is capable of ramping up and down as wind generation varies. Opportunities exist today for locating low temperature resource geothermal in many areas and dispatch it flexibly to accommodate intermittent resources and alleviate transmission congestion. However, boosting power output during periods with high ambient air temperatures and high electricity prices would greatly expand these opportunities in warmer climates.

It is widely known that low-temperature geothermal resources are abundant in the United States. According to the U.S. Geological Survey, more than 120,000 MW of these resources (125 – 175 degrees Celsius) have yet to be put to use (Williams et al., 2008). This abundance allows for considerable flexibility in decisions about siting low-temperature geothermal power plants. Other energy technologies, such as PHES plants and compressed air energy systems (CAES), are more constrained by geologic conditions and surface topologies. The disadvantage of air-cooled low-temperature geothermal is that power output is constrained by the difference between the temperature of the geothermal resource and the ambient air temperature. Since power production from low-temperature geothermal resources has a low thermodynamic efficiency, it is important to find economical ways to boost overall efficiency.

In this paper I investigate the use of a closed-loop, chilled-water cooling and thermal energy storage system to boost power output during periods with high ambient air temperatures and high electricity prices. The chilled-water cooling system is an add-on to an air-cooled low-temperature geothermal power plant. The system is used to exploit temporal mismatches between periods of higher power output and periods of high prices. Chilled water is produced during periods with low electricity prices and low ambient air temperatures (higher power output). Then the stored chilled water is used to boost power output during periods with high electricity prices and typically lower power output.

The chilled-water cooling system is effectively a price arbitrage system. The concept presented runs counter to the common misunderstanding that geothermal should only be operated as base-load generation. Unlike coal-fired and nuclear generation, geothermal is flexible generation with high ramp rates in both the up and down directions. Therefore, geothermal is ideal for providing many different market and transmission services such as ancillary services. Although the geothermal power plant in our system operates much like base load power in that it does not ramp output up or down, our system does seek to increase the value of geothermal generation by energy arbitrage. In fact, the chilled-water cooling system is very similar to utilizing a power plant to provide generation during high demand periods and ramping down a power plant to accommodate excess intermittent generation during low demand periods. Our

geothermal plant does not supply generation to the power system during low demand periods. Instead, it uses power output to produce chilled water.

Previous research on boosting power output of low-temperature air-cooled geothermal plants during higher ambient air temperature conditions has been motivated by the need for water conservation (Sohel et al, 2009; Ashwood and Bharathan, 2011). Water-augmented cooling methods, which could be employed during hot summer peak demand times, were evaluated for their economic value by estimating incremental increases in power production and revenue and computing payback periods. These "hybrid-cooling" options could be used if the geothermal plant is in a location with inadequate cold-water resources for cooling the power plant.

In this paper, similar results are reported in terms of incremental power gains and revenue increases for a chilled-water cooling/storage system. Furthermore, since the chilled-water cooling system is closed-loop and is an add-on to an air-cooled system, this type of dual cooling system also lowers water consumption compared to evaporative cooling systems. However, unlike in Sohel et al. (2009) and Ashwood and Bharathan (2011), the primary motivation for installing the closed-loop chilled-water cooling system is not to reduce water consumption.

Instead, the primary interest is in using this system to capture arbitrage value by storing low-cost energy in the form of chilled water and then using this to increase energy delivery into the market during summer peak demand periods. These arbitrage opportunities exist when periods of high power output (at low ambient air temperatures) coincide with periods of low electricity prices and periods of low power output (at high ambient air temperatures) coincide with periods of high electricity prices. The closed-loop chilled-water cooling system is a thermal energy storage system. The thermal reservoir is the chilled water, which is maintained at a temperature below the ambient air temperature. Thermal energy taken from the geothermal resource is used to produce chilled water, which is stored in insulated tanks for later use as a coolant.

Our thermal energy storage system is similar to other energy storage technologies because it stores energy in the form of chilled water and the chilled water is used to boost electrical power production. Therefore, our system has similarities to others that store and discharge electricity directly. Other thermal storage systems, such as those using electrical power to produce chilled water during off peak periods and then using the stored chilled water to cool a large building during times of peak demand, are functionally similar. Ellis (2012) describes the use of thermal energy storage in a chilled water production system for the Texas Medical Center in Houston. Thermal energy storage is used to meet peak demand for chilled water, and is found to yield several economic benefits that favor its use over increasing chilled water production

capacity. First, the installation of the system was determined to be cost effective compared to building new production capacity. Second, the thermal energy storage system consumes less energy. This is because it chills water at night when temperatures are lower so that, even after accounting for heat gain in the storage tank and the losses associated with pumping water into and out of the tank, total energy consumption is lower. Third, the thermal energy storage system levels the demand for energy and takes advantage of using lower-cost energy to chill water. Oldak (2012) describes the role and benefits of thermal energy storage in demand-side management schemes in detail. The benefits of leveling demand for energy are well known.

The traditional chilled water energy storage scheme is similar to the one described here in some respects. Both schemes derive economic benefits from taking advantage of the diurnal pattern in prices. Both schemes also benefit from the energy savings associated with producing chilled water at night when the ambient air temperatures are lower. However, there are critical differences between using thermal energy storage in demand-side management programs versus our system, which is used for boosting power production and overall efficiency of a power plant. First, on the demand side there is increasing demand for chilled water to cool large buildings as the ambient temperature increases, which is taken as given and must be satisfied. The alternatives are to increase production capacity and/or install storage technology. In our system, the production of chilled water depends on whether the benefits of boosting power production outweigh the costs of consuming energy to produce the chilled water. Although both systems take advantage of the diurnal price pattern, our system is intended for exploiting arbitrage opportunities whereas the thermal energy storage system described above shifts production of chilled water, which must take place, to lower-cost periods.

In Section 3.2, I describe the low-temperature geothermal plant with chilled-water cooling system. This also discusses the relationship between the ambient temperature and the existence of arbitrage opportunities that could be taken advantage of by such a system. Section 3.2 also presents the dynamic programming model and solution method to obtain the state path and optimal policy function. Section 3.3 presents the results of the optimal dispatch model. Section 3.4 contains a discussion of the results.

3.2 Methods

3.2.1 System Studied

The specific technology modeled is a low-temperature resource geothermal power plant using CO_2 as the working fluid. Carbon dioxide has certain advantages over water for extracting

low-temperature heat (Randolph and Saar, 2011). It should be noted, however, that the results could be generalized to any low-temperature geothermal plant with an air-type cooling system.

Figure 3.1 illustrates the direct CO_2 Plume Geothermal (CPG) power production system discussed in this paper. The CO_2 is sequestered underground in a warm, porous rock structure reservoir underneath an impervious cap rock. The hot CO_2 rises by natural convection in the reservoir to the bottom of the production well, state (1). As it rises up the production well, the pressure decreases due to flow friction and the change in elevation. At the surface, state (2), the warm high pressure, low density CO_2 passes through the turbine, state (3), which drives a generator to produce electric power. The CO_2 then proceeds through a condenser, state (4), where it exits as a lower pressure, high-density liquid. The liquid then travels down the injection well back to the bottom of the reservoir, state (5), where it is heated as it travels toward the bottom of the production well and the cycle starts again. Though natural convection (e.g., a thermosiphon) is sufficient to drive the CO_2, a pump was used to optimize the flow rate.

Figure 3-1: Schematic of Direct CPG System

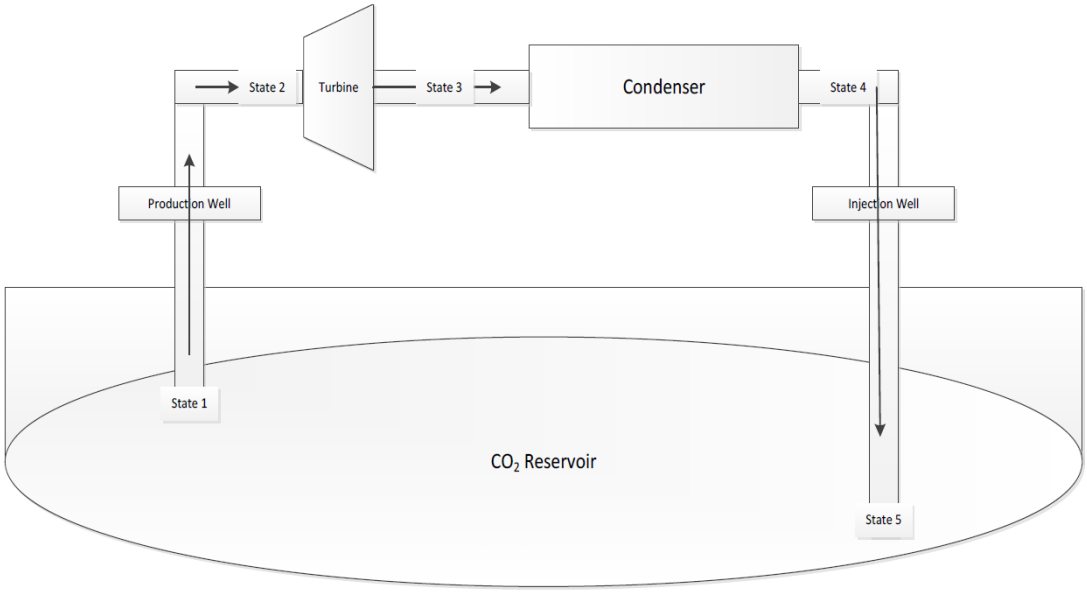

Notes: This is a direct system where the CPG power plant combines electrical generation with CO_2 sequestration. The CO_2 is the geothermal fluid and the CPG power plant uses a CO_2-based, direct-turbine for power generation. Supercritical CO_2 is injected into geologic reservoirs and a heated CO_2 is piped back to the surface for direct use and then re-injected into the geologic reservoir (Saar and Randolph, 2011). The water tank would be insulated to minimize heat loss. I estimate that we would need two 1924 KW chillers to use all the power output from the CPG plant to chill water during time increments when chilling water is determined to be the optimal use of the power output. I set the storage capacity to 9,000 m^3 so that there are six hours of thermal energy storage (1,500 m^3 of chilled water is needed to cool the power plant over one hour). Six hours of thermal energy storage is desirable for taking full advantage of daily arbitrage

opportunities because high electricity prices occur generally over a peak period of demand that stretched from the mid-to-late afternoon into the evening.

The turbine inlet, state (2), is fixed assuming a constant CO_2 mass flow rate and reservoir conditions. The amount of power that can be extracted from the CO_2 turbine is limited by the exhaust pressure, which is governed by the condensing temperature of the CO_2 that follows the ambient dry bulb air temperature. The power output from the turbine is converted to electricity in a generator. It can either be sold to the grid or used to operate the two 1924 kW chillers. The water is chilled from 15.6°C to 10°C as this is a typical operating condition for commercially available air-cooled chillers. After the water has been cooled it is stored in one of the four 2,250 m^3 water tanks. When it is financially advantageous to do so, the stored chilled water is used to condense the CO_2 instead of water that has been cooled in the cooling tower. When the stored chilled water temperature is less than the temperature of the water leaving the cooling tower, the condensing pressure and temperature of the CO_2 can be reduced by switching from the cooling tower water to the stored chilled water. This increases the power output of the turbine and generates more electricity. This situation often occurs during peak summer demand. The figure below shows a layout of the entire above ground system, including the CO2 power components and the chilled water production and storage components. I note that this chilled-water cooling system is very similar to one presented in Ellis (2012), which found that heat loss from the stratified chilled water storage tank was minimal and parasitic power losses associated with pumping water into and out of the chilled water storage tanks are minimal.

Figure 3-2: Surface Layout of the Geothermal Power Plant with Chilled-Water Cooling System

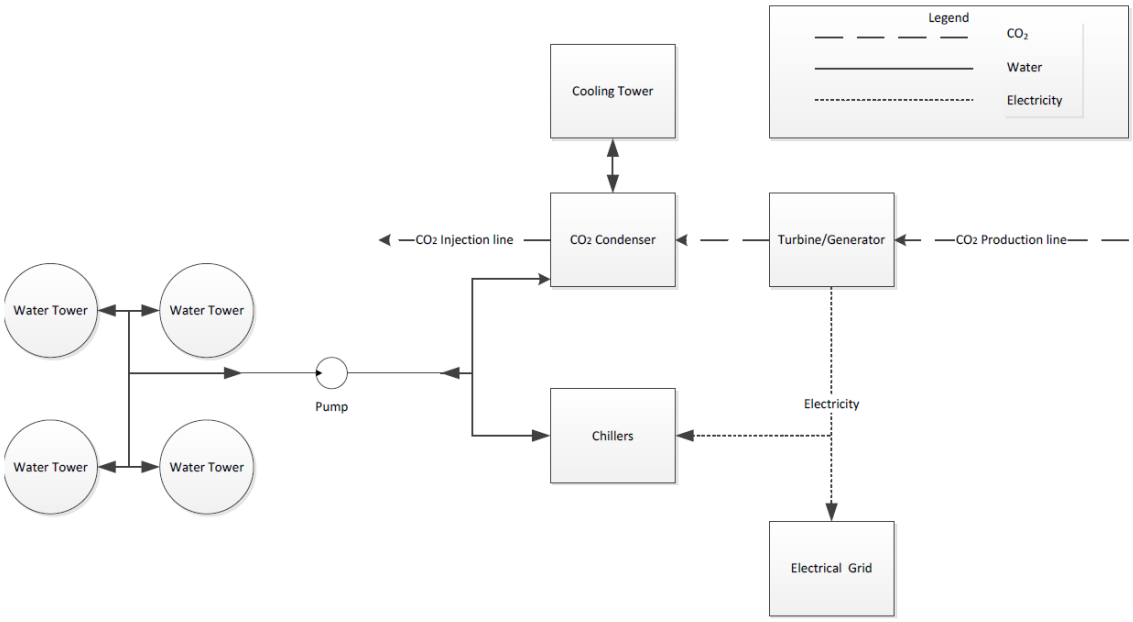

Assuming enough chiller capacity is available to use all of the power that is produced by the geothermal power plant, the amount of water chilled can be calculated using Equation 1 where $\dot{q}$ is the cooling capacity of the chiller.

$$M_{water} = \dot{q}t/C_p\Delta T \quad (1)$$

The change in water temperature, ΔT, is assumed to be 5.6°C. The rate of energy removal from the water is determined using Equation 2 where $\dot{p}$ is the power supplied to the chiller.

$$\dot{q} = \dot{p} * COP \quad (2)$$

I estimated the chiller COP as a function of the ambient air temperature for various LWTs, which is the temperature that the water leaves the chiller in degrees Celsius. The relationship between the COP and the ambient air temperature for a LWT of 10°C is estimated to be:

$$COP = 5.6091 - 0.0756 \cdot T_{amb} \quad (3)$$

This is representative of commercial air-cooled chiller products.[6]

I assume the water stored in the water tanks is stratified independent of the amount of time the water has been stored in the tanks. Thus, 10°C can be used for all chilled water calculations and 15.6°C for all warm water calculations.

[6] This equation is based on performance data for air-cooled chillers from Daikin McQuay, a commercial HVAC company (Daikin McQuay, 2009). A linear association between the COP and ambient air temperature was estimated.

Table 3-1: Summary of the Chilled Water Cooling and Thermal Energy Storage System

Parameter	Value
Discharge time	6 hours
Maximum volume of chilled water	9000 m^3
Chilled water discharge rate	25 $m^{3/min}$
Chiller cooling capacity	1924 kW
Electrical input	628 – 835 kW
Number of chillers	2
Total capital cost	$4.25 million
Annual revenue requirement	$466,067

Notes: The overnight capital cost of the chilled water system in Ellis (2012) is $13 million. I estimated the capital cost of our chilled-water cooling system based on quotes for two 550-ton chillers and scaling linearly the capital cost of the chilled water system in Ellis (2012), with the storage tank and system to pump water into and out of the tank. Our system's discharge is 24.5 percent of the discharge rate in Ellis (2012) and our maximum storage volume of chilled water is 27 percent of the maximum volume in Ellis (2012). Therefore, I assume that our capital costs for the storage tanks and the system to move water into and out of the tanks is approximately 25 percent of the capital cost in Ellis (2012). The annual revenue requirement is based on a 7 percent weighted average cost of capital and a 20-year operating lifetime.

3.2.2 Ambient Air Temperature and Power Production

The maximum power production from air-cooled low-resource temperature geothermal power plants depends on the difference between the temperature of the geothermal reservoir and the ambient air temperature:

$$\eta = 1 - T_A/T_H \quad (4)$$

where T_H is the absolute temperature of the geothermal resource and T_A is the absolute ambient air temperature. A higher reservoir temperature relative to the ambient air temperature leads to a higher efficiency. Lowering the ambient air temperature by one degree has a more significant effect on overall efficiency than increasing the temperature of the geothermal resource by one degree. This suggests that hybrid-cooling methods for boosting the power production during periods with high ambient temperatures should be investigated for their technical and economic feasibility.

$$\partial\eta/\partial T_A = -1/T_H \quad (5)$$

$$\partial\eta/\partial T_H = T_A/{T_H}^2 \quad (6)$$

$$\partial\eta/\partial T_H = (-\partial\eta/\partial T_A)(T_A/T_H)\,, \quad T_A/T_H < 1 \Rightarrow \partial\eta/\partial T_H < -\partial\eta/\partial T_A \quad (7)$$

Figure 3-3 below shows the relationship between the net power production of the CPG power plant and the ambient air temperature. Two sets of parameters were modeled. Both sets fix the injection and production well diameters at 0.41 m and 0.28 m respectively. The well depth is also fixed at 2.5 km. The two sets of parameters adjust the temperature gradient from the surface to the geothermal reservoir and the reservoir permeability. The first set of parameters fixes the temperature gradient at 35 degrees Celsius per km and the permeability at 5e-14 m^2. The second set of parameters fixes the temperature gradient at 20 degrees Celsius per km and the permeability at 1e-13 m^2.

Figure 3-3: Relationship between Ambient Air Temperature and Net Power

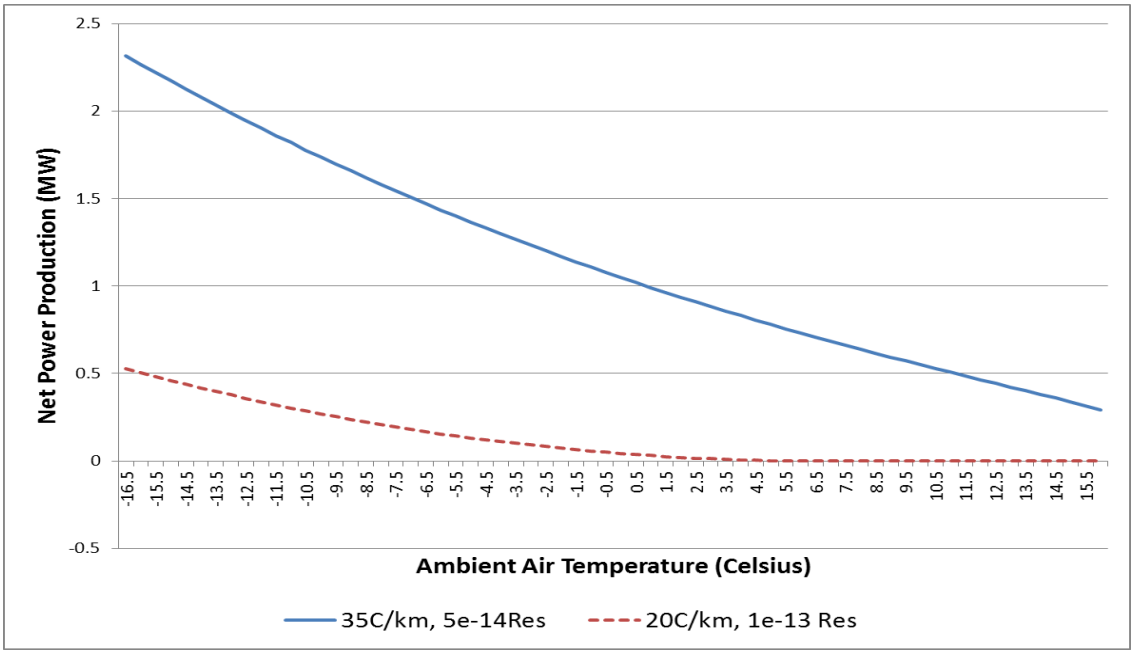

Notes: Net power production generated by the CPG plant is estimated using Engineering Equation Solver (EES) for the system outlined in the schematic of the power plant in subsection 3.2.1.

The two sets of parameters allow me to investigate the impact of the temperature gradient and the permeability of the heat resource on the operations of a CPG power plant with a chilled-water cooling system added on. It is not clear *a priori* whether the chiller will be used more often and contribute more to operational revenue under either scenario. With a lower quality heat resource, the chilled-water cooling system would give more of a boost in net power production when the ambient air temperature is higher because the percentage change in the difference between the heat resource temperature and the cooling temperature is higher compared to the higher quality heat resource. However, a higher quality heat resource provides more power to chill water down to the LWT when electricity prices are low. Therefore, the higher quality heat

resource allows more water to be chilled down to the LWT during periods when prices are low compared to the lower quality heat resource. This suggests that the impact of the heat resource on the use of a chiller is uncertain, and the competing effects may cancel out. I investigated this by running our optimal scheduling model over both sets of parameters.

3.2.3 Ambient Air Temperature and Electricity Prices

I downloaded the hourly ambient air temperatures of three different locations (Shreveport, LA, Carlsbad, NM, and Mitchell, SD) from the National Weather Service. These locations were chosen because they were thought initially to offer interesting comparisons based on their different ambient air temperature profiles. The hourly ambient air temperatures are for the year 2010. The hourly day-ahead prices for electricity near Mitchell, SD and spot prices[7] for electricity near Carlsbad, NM and Shreveport, LA were obtained from the archived data provided by the Midwest ISO and the Southwest Power Pool.

The ambient air temperature is lowest at night and typically reaches a maximum in midafternoon. I expected initially that the price of electricity would be the highest when the ambient air temperature is highest and the CPG power production is the lowest. The loss of power production occurs when the ambient air temperature is high because of the relationship shown in equation 4. The data show a positive relationship between electricity prices and ambient air temperature during the hot summer months. However, there are temporal mismatches between time periods with the highest electricity prices and time periods with the highest ambient air temperatures since use also depends on time of day. For example, the daily maximum air temperature at the three locations frequently occurs outside the period of high electricity prices traditionally defined as 4:00 pm to 7:00 pm when people are coming home from work and adjusting the thermostat, turning on TVs, etc. This suggests that fewer arbitrage opportunities exist from producing chilled water when the ambient temperature is low and using the stored chilled water to cool the plant when ambient air temperature is high.

3.2.4 Description of Mixed Discrete-Continuous Model Framework

I use historical hourly electricity prices and historical hourly temperature data to evaluate decisions about the use of the chilled-water cooling system. The decisions concern when to produce chilled water and when to use it to cool the geothermal plant to increase power

[7] Carlsbad, NM and Shreveport, LA are located in the Southwest Power Pool, which only administers a spot market for electricity.

production. I also evaluate the incremental operating revenue from adding on the chilled-water cooling system and the payback period for the system.

I use a discrete time, continuous state dynamic programming model to describe the economic problem facing the operator of the low-resource temperature geothermal power plant with a chiller. The state space is mixed and includes the discrete state variables, which are the market prices for electricity and the hourly ambient air temperatures, and a continuous state variable, which is the quantity of chilled water. The state space is mixed with discrete and continuous state variables

$$S = \{Q, P, C\} \tag{8}$$

where Q represents the quantity of chilled water in storage tanks on a continuous interval from zero to 9000 cubic meters, $P = \{1 \dots 8760\}$ represents the hourly electricity prices for the year 2010, and $C = \{1 \dots 8760\}$ represents the hourly ambient air temperatures for the year 2010. The full state space can be described as the product $Q \times \{C_t, P_t\}, t = 1 \dots T$. I refer to a specific state in the state space as (q, c, p).

The action space is represented by X and it includes all the actions that may be taken by the operator of the power plant. Specifically, the operator may 1) produce chilled water, 2) consume chilled water to cool the power plant while producing electricity for sale, or 3) produce electricity for sale into the market using the ambient air to cool the power plant.

$$X = \{x_{prod}, x_{use}, x_{air}\} \tag{9}$$

The actions are constrained so that the quantity of chilled water does not exceed the 9000 cubic meters capacity of the storage tanks and the operator does not use more chilled water than is in storage. The continuous state variable is a controlled Markov process so that the quantity of chilled water in time period $t + 1$ depends on the quantity of chilled water in time period t and the action taken in time period t:

$$q_{t+1} = g(q_t, c_t, p_t | x_t) \tag{10}$$

where g is the equation of motion, which says that reaching q_{t+1} is a function of the action x_t taken in state (q_t, c_t, p_t). In the model, the discrete states are exogenous parameters and transition independently of the action x_t taken by the operator.

The reward functions are defined for each action and pair of discrete states as

$$R_{x_{prod}}^{c,p} = 0 \tag{11}$$

$$R_{x_{use}}^{c,p} = (\alpha_i + \beta_i LWT)p \tag{12}$$

where α_i is the intercept, β_i is the slope $(i = 1, 2)$, LWT is the leaving water temperature, and i

indexes the quality of the heat resource.[8] The reward for producing with ambient air is:

$$R_{x_{air}}^{c,p} = (\alpha_i + \beta_i c_i)p \tag{13}$$

where c_i is the ambient air temperature in degrees Celsius at time *t*. I set the temperature of the chilled water leaving the storage tanks to 10 degrees Celsius and the temperature of the chilled water returning to the storage tanks after passing through the power plant condenser to 15.6 degrees Celsius. I also require that the temperature of the chilled water that enters the chiller is 15.6 degrees Celsius and that it is supplied to the storage tanks at 10 degrees Celsius.

The Bellman equation is:

$$V_t(q,c,p) = \max_{x \in X(q,c,p)} \{R_x^{c,p}(q) + V_{t+1}(g(q,c,p,x))\}, q,c,p \in S, t = 1,2,\dots T \tag{14}$$

Where $V_t(q,c,p)$ represents the maximum attainable sum of current and expected future rewards given that the economic process is in state *s* in time period *t*. The Bellman equation captures the economic problem facing the plant operator. The plant operator balances the immediate reward $R_x^{c,p}(q)$ against the future rewards $V_{t+1}(g(q,c,p,x))$.

The model is a finite time horizon model. The operator faces decisions in time periods $1 \dots T$ and $V_{T+1}(q_{T+1}, c_{T+1}, p_{T+1})$ is set equal to zero because there are no rewards beyond the terminal decision period.

3.2.5 Model Solution

Equation (11) gives the mechanism for using backward recursion to solve the optimization problem. The terminal point is free, so I use a backward recursive process to solve beginning at the terminal point plus one additional time period.

$$V_T^*(q_T, c_T, p_T) = \max_{x_T \in X(q_T, c_T, p_T)} \{R_x^{c,p}(q_T) + V_{T+1}(g(q_{T+1}, c_{T+1}, p_{T+1}, x_{T+1}))\} \tag{15}$$

The optimal policy π_T and $V_T^*(q_T, c_T, p_T)$ are obtained. Then I compute $V_{T-1}^*(q_{T-1}, c_{T-1}, p_{T-1})$ from

$$V_{T-1}^*(q_{T-1}, c_{T-1}, p_{T-1}) = \max_{x_{T-1} \in X(q_{T-1}, c_{T-1}, p_{T-1})} \{R_x^{c,p}(q_{T-1}) + V_T(g(q_T, c_T, p_T, x_T))\} \tag{16}$$

This process is continued until I have solved recursively backward for $V_{T-1}^*(q_{T-1}, c_{T-1}, p_{T-1})$ for $i = 0 \dots T$.

I begin by constructing a discrete space on the continuous state space using Chebychev

[8] The intercept and slope coefficients for the 35C/km, 5e-14Res and 20C/km, 1e-13Res heat resources are estimated by fitting a linear relationship to data showing the association between power generated (MW) and the ambient air temperature. The data were generated using the EES to estimate net power production for the system outlined in the schematic of the power plant in subsection 3.2.1.

nodes. Let $\bar{Q}$ represent the discrete space. The optimal value and optimal action are evaluated at the Chebychev nodes during each iteration in $\bar{Q} \times \{C_t, P_t\}$. Then I set up interpolation functions to cover all the points in the state space $\bar{Q} \times \{C_t, P_t\}, t = 1 \ldots T$.

The following algorithm describes the iterative process used to interpolate over the state space.

Set optimal value in time period $T + 1$ equal to zero at each Chebychev node

Compute the basis functions and the coefficient matrix for time period $T + 1$

with the constraint $\Phi(c) = 0$ where ϕ is a row vector of basis functions in the matrix Φ and is evaluated at a Chebychev node *s* and *c* is the coefficient vector

For each Chebychev node

Evaluate the current rewards in time period *T* for each action

Compute the state transitions for each action

Compute the basis functions for the next state reached in time period *T+1* for each action

$\Phi(c)$ where ϕ is evaluated at the next state is the expected future value in time period $T + 1$

Sum the current reward and the expected future value for each action

Select the optimal action, which maximizes the sum of current and expected future rewards

Set the maximum sum equal to the optimal value of being at the Chebychev node in time period *T* and selecting the optimal action

Repeat the process by evaluating the basis functions at each Chebychev node and computing the coefficient vector with the constraint that $\Phi(c) = V$ where V is the vector of optimal values in time period *T* at each Chebychev node

Continue the process until a coefficient vector is computed for each time period $t = 1 \ldots T + 1$.

After I have computed coefficient vectors for each time period $t = 1 \ldots T + 1$, I run simulations of the state path and optimal policy. The following algorithm describes the simulation process.

Set the initial state in time period 1

Compute the current reward for each action

Compute the state transitions for each action

Evaluate Φ at the next state in time period 2 for each action

Compute $\Phi(c)$ for each action

$\Phi(c)$ evaluated at the next state is the expected future reward of being in the next state in time period 2

Sum the current and expected future rewards for each action

Select the maximum sum – this corresponds to the optimal action given the initial state

Find the next state – this is the state in time period 2

Repeat the process for time periods $t = 1 \ldots T$

Output a vector of states and a vector of optimal actions for each time period

Periods $t = 1 \ldots T$

3.3 Results

3.3.1 Forecasting in the model

I estimated the annual value of chilled-water cooling system attached to a low-resource temperature geothermal power plant at three different locations: (1) Mitchell, SD, (2) Carlsbad, NM, and (3) Shreveport, LA. Carlsbad and Shreveport are located in the Southwest Power Pool. The operation of the chilled-water cooling system was optimized to maximize expected operating profits over a one-year time horizon. The optimization was conducted assuming perfect foresight of future hourly electricity prices and ambient air temperatures during the year 2010. I also assume that the operator is a price-taker. Sioshansi et al. (2009) find that the assumption of perfect foresight of electricity prices is convenient and produces qualitatively similar results compared to a naïve forecast. This assumption puts an upper bound on the operating revenue attainable from using a chilled-water cooling system. Sioshansi et al. (2009) estimated a naïve approach to forecasting, where next week's hourly electricity prices were forecasted to be the same as last week's hourly electricity prices, and found that it captures 85 percent of the upper bound on operating revenue.

3.3.2 Efficiency gains

The simulated power gains from use of the chilled water are negative during the winter months and parts of the spring and fall when the ambient air temperature is below the temperature of the chilled water. Power gains increase during the summer months and are the highest during the hottest months of the year. The maximum gain in power at all three locations is about 1.65 MW. The linear relationship between power output (MW) and the ambient air temperature is truncated at zero power output. In all three locations, hourly ambient air temperatures exceeded the temperature corresponding to zero power production.

3.3.3 Production of Chilled Water under Different Price and Temperature Conditions

The model runs used hourly temperatures and electricity prices for the year 2010, which represents perfect forecasts of ambient air temperatures and electricity prices as previously mentioned. Therefore, the results of the model runs represent an upper bound. In the base case, the chiller is never used during the year at all three locations for both the higher and lower quality resources. This result was unexpected, and therefore led me to investigate the conditions needed for making the use of the chiller economical. The results below are generated using the higher quality heat resource at the Mitchell, SD location. I fit electricity prices from July 1, 2010 to July 7, 2010 at Mitchell, SD to a Fourier series model with two cosine and two sine terms. Then I adjusted the cyclical amplitude by factors of two, three, four, five, six, and seven, and ran the model each time with the adjusted prices. The figure below shows that the production of chilled water by factors of upward adjustment in the cyclical amplitude of electricity prices. Our results also suggest that the system approaches a limit on the use and production of chilled water as I continue to increase the cyclical amplitude. This is due to the economics of these operational decisions being also dependent on changes in the ambient air temperature.

Figure 3-4: Production of Chilled Water with Upward Adjustments in the Cyclical Amplitude of Electricity Prices

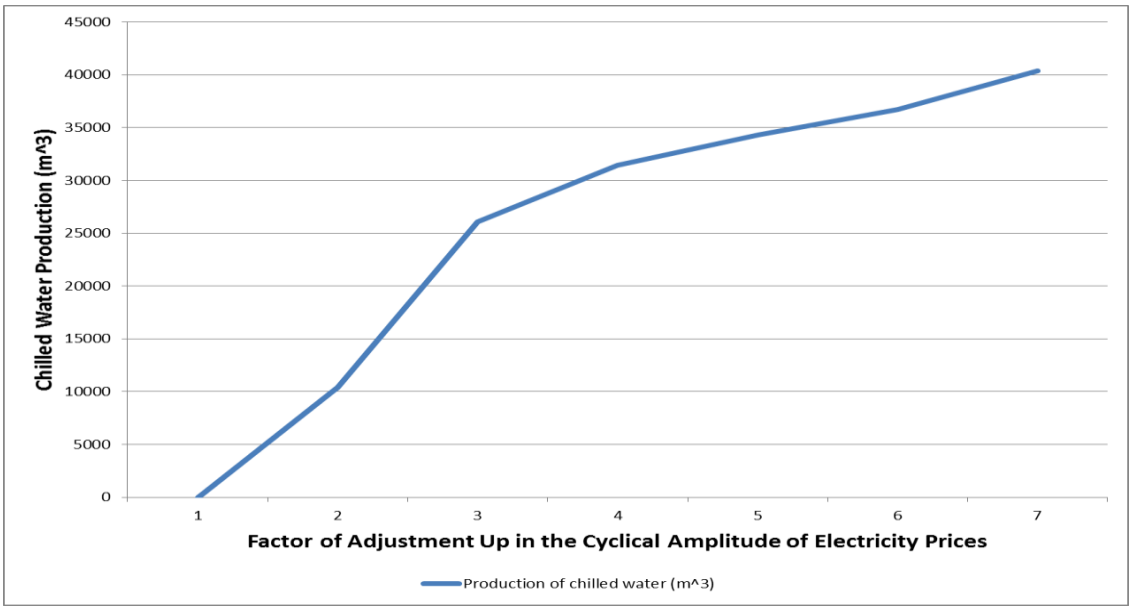

Notes: The cyclical amplitude of prices was adjusted up by factors of one to seven for the period from July 1, 2010 to July 7, 2020. For each factor, the algorithm was run to optimize the production and use of chilled water and total production of chilled water (m^3) was calculated.

A similar analysis was conducted to investigate the impact of changes in the ambient air temperature on the operation of the chilled-water cooling system. A Fourier Series model with two cosine terms and two sine terms was fit to one-week intervals in the electricity price and ambient air temperature and phase differences were calculated for each day in units of time. I calculated phase differences up to seven hours. However, for most of the days the phase difference was found to be in the range of two to four hours. Therefore, I introduced phase difference of zero, one, two, and three hours between the ambient air temperature and the electricity prices, holding the phase difference constant over the same one-week period described above. I ran the model for each level of phase difference and calculated the production of chilled water over the one-week period. For each level of phase difference, the model was run over the seven different cyclical amplitudes in electricity prices described above. Figure 3-5 below shows the results of this analysis. The phase difference has a significant impact on the production of chilled water. A three-hour difference in phase results in about a 20-45 percent decrease in the production of chilled water depending on the cyclical amplitude in electricity prices. As I mentioned previously, a phase difference of three hours is not unlikely given that the peak electricity price is around 6 pm and the ambient air temperature often peaks in the mid-afternoon.

Figure 3-5: Impact of a Phase Difference between Electricity Prices and Ambient Air Temperature

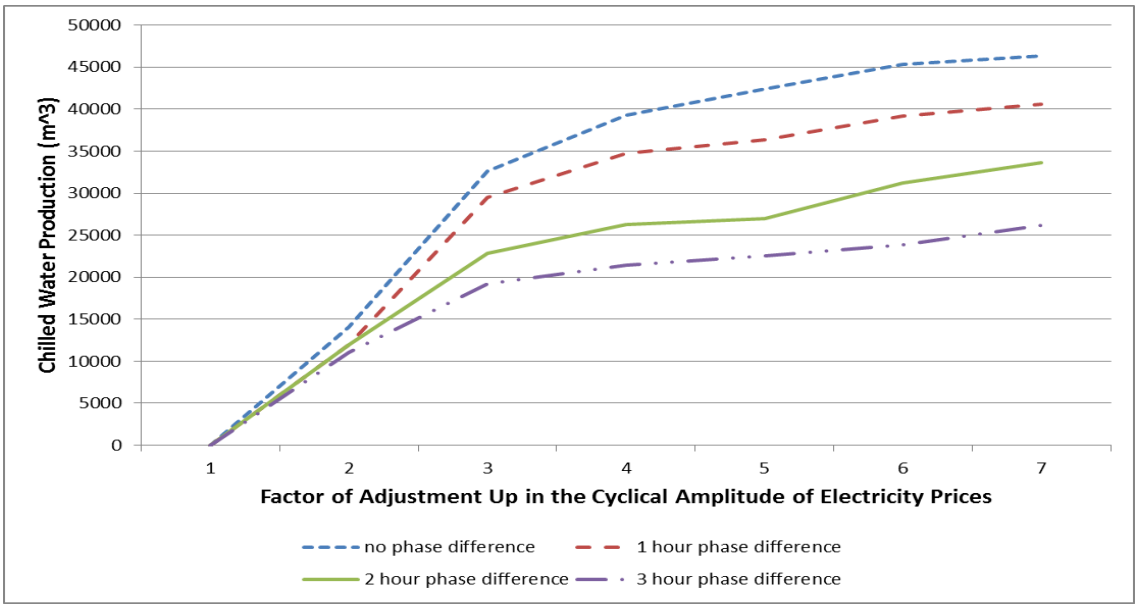

Notes: This figure shows the impact of the interaction between the phase lag and price spread on the production of chilled water for a one-week period. There are seven different price spreads and four different phase lags. The production of chilled water for a one-week period was computed for each combination of phase lag and price spread.

It should also be noted that even if there is no phase difference between electricity prices and the ambient air temperature, the chiller-water cooling system is not used unless I adjust upward the cyclical amplitude in electricity prices. This suggests that the price spreads are not high enough to make using the chilled-water cooling system economical even when there is no difference in phase between prices and ambient air temperatures.

A second analysis was conducted by varying the cyclical amplitude of changes in ambient air temperature. Increasing the cyclical amplitude of changes in ambient air temperature had no effect on operations. There was no production of chilled water even when the cyclical amplitude was adjusted up by a factor of 15. This result is not surprising considering that increasing the spread increases opportunity costs and as well as arbitrage opportunities. That is, more power output can be achieved when the ambient air temperature is low. Therefore, the opportunity cost of not selling the power increases. However, more chilled water can be produced and a larger percentage increase in power output can be achieved when the ambient air temperature is higher. Both effects seem to cancel each other out.

3.4. Discussion

3.4.1 Conditions for the use of the chilled-water cooling system

I have simulated the operation of a low-temperature resource geothermal power plant with a chilled-water cooling and storage system. Previous research has explored the use of water augmented cooling systems in low-temperature geothermal power plants to conserve water and boost power production during the summer peak period (Sohel et al., 2009; Ashwood and Bharathan, 2011). The chilled-water cooling system proposed here is closed-loop and could be operated even when the plant does not have a supply of water. However, the key difference between our system and other water-augmented cooling methods is that the chilled-water cooling system also serves as a thermal energy storage technology. Therefore, its use and economic feasibility depend on different factors from the traditional water augmented systems that have been studied in the literature.

The chilled-water cooling system requires electricity to produce chilled water. Therefore, the use of chilled water depends not just on the additional operating revenue from power gains during the summer peak period, but on the arbitrage value between the production and use periods. The additional operating revenue from using chilled water during the summer peak periods must outweigh the opportunity cost of foregoing the sale of power during the period of chilled-water production.

For the selected weeks in April and July, I showed that the relationship between electricity prices and the ambient air temperature changes day-to-day. This suggests that inter-day arbitrage opportunities are not always present despite the diurnal pattern in electricity prices. Arbitrage opportunities for a low-temperature geothermal power plant with a thermal energy storage system depend on a strong positive relationship between ambient air temperatures and prices for lowering the opportunity cost of chilling water on a per-unit basis and boosting the power production and operating revenues in time periods when the chilled water is used to cool the power plant. Figure 3-6 below shows that electricity prices and the ambient air temperature are out of phase. The phase difference is not constant.

Figure 3-6: Electricity Prices and Ambient Air Temperatures

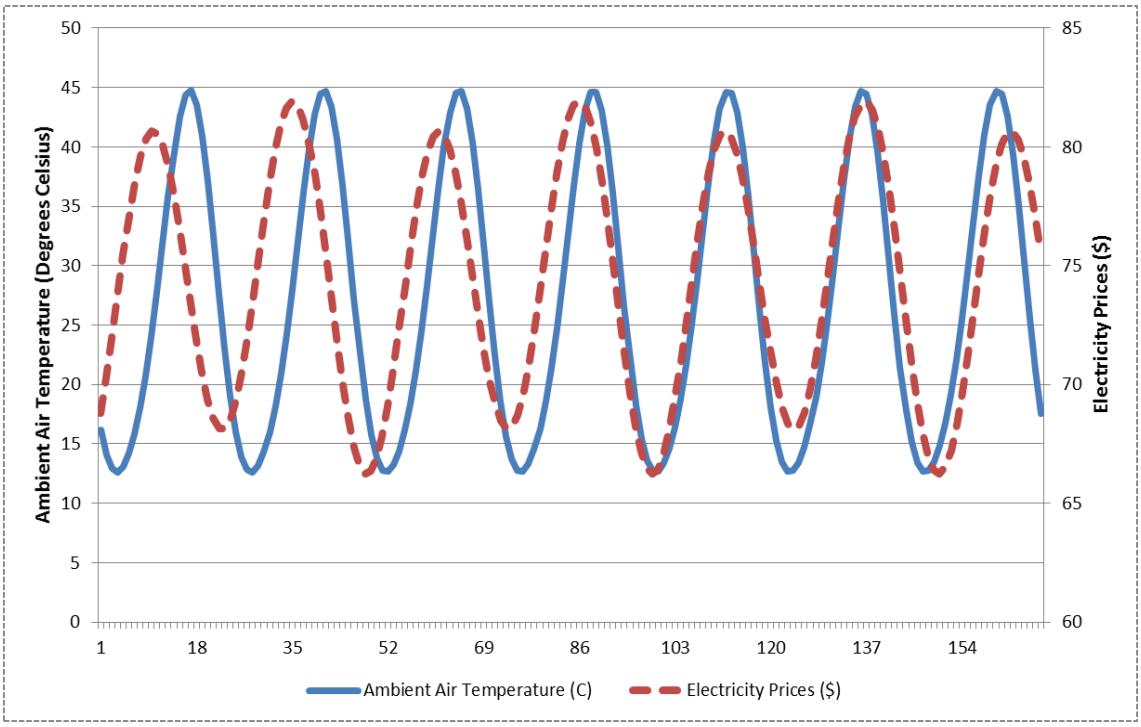

Notes: Fourier series models with two cosine and two sine terms were used to curve-fit one week of data from July 1, 2010 to July 7, 2010 at Mitchell, SD.

3.4.2 Comparison to other energy storage technologies

I define an energy storage technology broadly as any device that is capable of time-shifting electricity (allowing it to be produced at one time and consumed at another time). I noted previously that the low-temperature geothermal plant with a chilled-water cooling system is a type of thermal energy storage system – energy is used to chill water, which is stored in tanks for later use to boost power production during time periods with a high ambient air temperature. In comparison to other energy storage technologies on the supply-side, the round- trip efficiency of

our thermal energy storage system (defined as the boost in power production from cooling the power plant with chilled water divided by the energy consumed to produce the chilled-water) is also low. Estimating the round-trip efficiency of the chilled-water cooling system is difficult because the efficiency factor depends on the ambient air temperatures during the production and use periods. I estimate a range for the round-trip efficiency between 25 – 45 percent based on the simulated production of chilled water and use of chilled water in later periods. Other established grid-scale storage systems such as compressed-air energy storage (CAES) and pumped hydroelectric energy storage (PHES) achieve round-trip efficiencies of 70 percent and 78 percent respectively (Schoenung and Hassenzahl, 2003).

Energy storage devices with higher round-trip efficiencies are better able to take advantage of the arbitrage opportunities in the wholesale markets for electricity. The low round trip efficiencies achieved by our system means that a bigger price spread is needed between low-cost energy and high-cost energy to obtain positive economic returns.

3.5 Conclusion

The results presented in this paper suggest that adding a chilled-water cooling system to a low-temperature geothermal power plant would not be a cost-effective method for boosting overall efficiency when the ambient air temperature is high. The cooling system is essentially a thermal energy storage system and allows the plant operator to time-shift the supply of electricity. However, there is not always a positive relationship between prices and ambient air temperatures. I showed that the chilled-water cooling system does boost the overall efficiency of the power system when prices are high, but the arbitrage value is low primarily because of two factors: the inefficiency of the energy storage system and a mismatch between periods of high energy prices and high temperatures.

The thermal energy storage system is inefficient from a thermodynamic perspective. Therefore, large price and temperature changes are needed to yield positive economic returns. In all of the model runs, the chiller was never used. This brings into question the conditions under which our system would produce positive economic returns. I used a Fourier series model to curve fit electricity prices for a one-week period at Mitchell, SD with the goal of simply distinguishing between low-price and high price periods and artificially setting a price spread. Several model runs were performed for different cyclical amplitudes and for each model run I plotted the production and use of chilled water. Using this method, I was able to estimate that price spreads between low-price and high-price periods need to be increased significantly for the chiller to produce positive economic returns given the changes in ambient air temperatures.

Price spreads need to be increased by orders of magnitude in order for the arbitrage value to outweigh opportunity cost and to justify operating the chiller in real-time electricity markets on an economic basis. Future study could investigate whether similar price-temperature profiles to the conditions studied in this paper can be found and then explore whether operation of a low-temperature geothermal power plant with chiller is economically viable. Moreover, the increased volatility in real-time markets leads me to conclude that continuous discharge times would be shorter compared to day-ahead markets. Further study would need to be done to determine ramp rates and flexibility of the system described to be dispatched in real-time in the up and down directions. Shorter discharge times also reduce the amount of storage needed to exploit arbitrage opportunities, and this would reduce the annual revenue requirement of the system possibly making it economical to add on to an existing low-temperature geothermal power plant.

Second, and perhaps more important, there is a mismatch between the highest temperatures and the highest electricity prices. I showed that higher prices generally correlate with higher temperatures. However, the highest temperatures do not always occur when electricity prices are highest because the highest electricity prices depend strongly on the time of day (e.g., when people arrive home from their daily work). This mismatch significantly reduces the arbitrage opportunities for any thermal energy storage device such as the chilled-water cooling system proposed in this paper.

Although the chilled-water cooling system was not found to be cost effective, there may exist market conditions and institutions in the future that would make such a system economical. The nation is moving to a smart grid and dynamic pricing programs using real-time prices offer the opportunity to utilize a chilled-water cooling to increase the value of low-temperature geothermal. Perhaps more important, geothermal does not have to be thought of as just base load generation. Opportunities may exist, depending on the price-temperature profile, to utilize geothermal generation to match supply and demand by producing power during high demand periods and chilling water during periods with low demand.

4. Chapter 3 - Why Market Rules Matter: Optimizing Pumped Hydroelectric Storage When Compensation Rules Differ

4.1 Introduction

Energy storage could play an important role in the future United States electric system. Numerous federal and state policies have been implemented to stimulate development of low-carbon and renewable technologies. These policies include the wind production tax credit (PTC), a federal tax credit for solar as part of the Emergency Economic Stabilization Act of 2008, and many state Renewable Portfolio Standards (RPSs) (DSIRE 2014). With over 60,000 MW of installed wind power and 3,500 MW of PV solar, these policies have been successful, but managing the variability of wind and solar resources requires new approaches to operate the electric grid and makes storage a critical technology.

Natural variability of electricity flows from wind or solar plants can create grid instabilities that can negatively affect the electrical system's ability to reliably provide electricity when it is needed (Katzenstein and Apt, 2012). In addition, when conventional sources of electricity (e. g., coal or nuclear power plants) cannot be ramped up or down sufficiently to balance variability in wind or solar–generated electricity, wind turbines may have to be curtailed to prevent transmission line congestion and to maintain system balance. One solution to help with grid integration of renewable energy is to store electricity as it is generated (Hall, 2008). Energy storage technologies can help to integrate higher penetrations of low-carbon renewable energy into the electric system and a number of utility-scale energy storage technologies are being developed, including compressed air energy storage, electrochemical batteries and capacitors, and flywheel energy storage (Carnegie et al., 2013).

The need for utility-scale energy storage is also motivating new policy discussions to stimulate development of energy storage technologies—such as the procurement target of 1,325 MW of energy storage by 2020 set by the California Public Utilities Commission (CPUC press release, 2013)—and investigations of the reliable energy storage technologies with fast response times ("ramp rates") that can allow electrical grid operators to better accommodate large amounts of electricity generated from variable sources (CAISO Strategic Plan, 2013). Fast ramp rates allow electrical grid operators to accommodate large amounts of electricity generated from variable sources.

Among the bulk energy storage options, Pumped Hydroelectric Energy Storage (PHES) is the most widely deployed utility-scale energy storage technology (Foley et al., 2013), with over 127,000 MW of capacity installed globally and 40 projects totaling 22,000 MW in the United

States alone (EIA, 2012; Castelvecchi, 2012; The Economist, 2012). With PHES, water is stored in an upper water reservoir which is situated at a higher elevation than a lower water reservoir. Energy is stored by pumping water from the lower reservoir into the upper reservoir. The amount of energy that can be stored depends on the elevation difference between the reservoirs, or the "head height," and the total volume of water that can be moved between the reservoirs. When water flows from the upper to the lower reservoir, it flows through a pump-turbine that generates electricity. The ability to store energy and generate electricity when desired creates a number of opportunities for project developers.

In many parts of the United States, the value of PHES plants will be determined by the revenue the facility could earn in regional energy markets. ISOs manage about 70 percent of the wholesale electric power flows and operate energy markets (EIA, 2011). ISOs use a locational marginal pricing (LMP) approach to calculate electricity prices at different market nodes, so the value of a PHES would partially be determined by its location. Historically, prices have generally followed a diurnal pattern; prices are low during off-peak demand periods and higher during peak demand periods. These pricing dynamics create arbitrage opportunities for energy storage because a PHES operator can pump water from the lower reservoir and energy can be stored when prices are low and release water from the upper reservoir to generate electricity when prices are high.

In addition to calculating LMPs, ISOs have also established markets for grid stability services, such as frequency regulation or spinning reserves. Frequency regulation involves the commitment of capacity to ramp up or down according to a set of instruction from the RTO for the purpose of matching supply and demand on a second-by-second basis in order to maintain power quality. The substantial improvement in the pump-turbine technology used in PHES systems can also allow newer PHES turbine technologies to provide regulation services in both pumping and generating modes. So, for PHES facilities located in ISO electricity markets, PHES facility operators can generate revenues both by exploiting arbitrage opportunities and by selling regulation services.

The value of an energy storage project will thus depend on (1) how the electricity market functions; (2) how storage is valued for the sale of electricity; and (3) its ability to provide and earn money from regulation services. But while U.S. electricity markets follow standard market design, the value of an energy storage project depends on the very specific details of how each ISO's market rules compensate energy storage (Hogan, 2002). There are nine different ISOs in the United States—each of which determines its own rules for compensation in consultation with members and approvals by the Federal Energy Regulatory Commission (FERC).

PHES facility profits are partly determined by the stream of revenues, which depend on the future prices in electricity and regulation service markets, the ISO rules governing those markets, and the operational strategies used by the facility operator. Here, I examine and compare how the rules and markets of the Midcontinent ISO (MISO) and ISO New England (ISO-NE) would affect the optimal strategies employed by PHES operators and thus the total value of providing energy storage. These ISOs were chosen because, until 2011, they had different rules for compensation. In MISO, compensation for frequency regulation only included payments for capacity set aside and payments (charges) for net energy injected into (withdrawn from) the power system. ISO-NE makes capacity payments and "mileage" payments based on the absolute amount of energy injected and withdrawn. The mileage payment is intended to reward the quantity and accuracy of frequency regulation service provided by the participant and is explained in more detail below in Section 4.2.1.1.

In October 2011, FERC issued Order No. 755 mandating that all ISOs develop a compensation method that provides both a capacity payment and a mileage payment to reward resources with faster ramp rates. I estimate the net profits of a PHES facility under the MISO rules and ISO-New England market rules at the time Order No. 755 was issued to better assess how the rule affects strategy and compensation of storage projects. I estimate the difference in net profits and bidding activity under the different compensation formulas in place prior to the FERC mandate to gain insight into the level of impact that Order No. 755 has on the development and deployment of resources with faster-ramp speeds and to highlight the importance of ISO rules on operator value. In 2012 MISO changed is compensation formula to comply with Order No. 755 (FERC 2012).

The model and analysis focus on the perspective of a PHES facility operator, and not on the total system costs examined by other studies (Foley, 2013). Previous work has also investigated optimal bidding strategies for PHES facility operators, including approaches that fix the efficiency factor and power generation bid (Lu et al., 2004), model participation in the energy and spinning reserve markets (Kanakasabapathy and Swarup, 2010), and restrict pumping and generation modes to the traditional off-peak and peak periods, respectively, but do not model participation in ancillary services markets (Deb, 2000; Connolly et al., 2011). Kazempour et al. (2009) presents a detailed model that considers uncertainty in price forecasts and allows the PHES plant to participate in the energy, spinning reserve, and frequency regulation services markets, but this approach restricts the flexibility of PHES to set aside different amounts of frequency reserve and fixes the efficiency factor of the plant and of the power generation bid. Algorithms that have been employed require the PHES plant to pump before it generates

(Kanakasabapathy and Swarup, 2010), allow pumping to occur either before or after generation (Connolly et al., 2011), or are simple heuristics for dispatch that maximize potential revenues from energy and frequency regulation services for each hour (Deb, 2000).

The model determines the profit-maximizing behavior of a PHES facility and estimates revenue streams from selling both electricity and grid reliability services into different competitive wholesale electricity markets with different compensation mechanisms. The model also integrates detailed operational and physical specifications (BARR Engineering, 2009) that have previously received scant attention but are crucial for modeling system performance. Operationally, the PHES operator can choose to set aside capacity as frequency regulation reserve. Physically, the model accommodates how pump-turbine efficiencies vary according to head height and flow volume in both pumping and generating modes. Combined, upper and lower bounds are set to provide frequency regulation based on the relationships between head height, flow, and turbine efficiency. Our application determines optimal market bidding strategies for electricity and reliability services that operate under both the MISO and ISO-NE market rules. By comparing the value of PHES systems and the impacts of these different rules on revenue streams, a better understanding of the value of different policies and how they monetize the benefits provided by PHES can be achieved.

Section 2 presents a brief discussion of the day-ahead and real-time electricity markets and the market for frequency regulation. This section also presents the optimization model. In Section 3, I present the results of the model. Section 4 presents a discussion of the value of PHES in the MISO and ISO-NE.

4.2 Materials and Methods

The following section details the real time markets and reliability service markets and provides a description of the model.

4.2.1 Market Structure

4.2.1.1 Day-Ahead and Real-Time Markets

The wholesale market for electricity is co-optimized with ancillary services markets to solve for prices for electricity and ancillary services at LMP nodes. The electricity markets include a day-ahead market and a real-time market. The day-ahead market is a forward market, operated as an auction, where electric facilities submit hourly price-quantity electricity supply curves for the next operating day based on their estimates of demand. The ISO clears the day-ahead market while ensuring that the solution is physically feasible. This clearing process

determines which bids are accepted and settles the accepted offers. Hourly LMPs are calculated and a set of hourly schedules is produced for the next operating day.

The real-time market functions to match electricity generation with electricity demand because the quantity delivered may differ from the contracted quantity from the previous day in the day-ahead market. Hourly supply and demand for electricity can change for many reasons, including transmission and generation outages/failures and unexpected weather conditions.

Supply offers (Q_{DA}) are cleared in the day-ahead market and are paid the day-ahead price (P_{DA}). The difference between the physical production of electricity ($Q_{delivered}$) and the quantity cleared in the day-ahead market is compensated at the hourly real-time weighted price (P_{RT}). This real-time weighted price results from settling the market on a five-minute basis and bundling together twelve five-minute intervals. If a facility supplies less than the contracted quantity of electricity (Q_{DA}), it must purchase electricity on the real-time market to satisfy the contract. Net revenues are:

$$P_{DA}Q_{DA} - P_{RT}(Q_{DA-}Q_{delivered}). \quad (1)$$

The wholesale markets for electricity in the ISO determine P_{RT} and P_{DA} for each particular location or node or LMP, which is the price and value of producing electricity at that particular location and time. Prices at each location reflect the marginal cost of electricity generation at a commercial pricing node plus transmission line losses and costs of transmission congestion. The real-time market settles the difference between scheduled transactions and actual transactions. Real-time market prices are more volatile than day-ahead prices because mismatches between supply and demand, perhaps due to outages and intermittent generators, are not perfectly predictable and these shortfalls and oversupplies must be resolved in the real-time market. While the PHES operator may negotiate a bilateral contract to reduce price risk, the model does not incorporate them because the primarily interest is in finding the arbitrage value of energy storage and the value of reliability services under different market rules.

4.2.1.2 Reliability Service Markets

ISOs are responsible for maintaining the stability of the electricity transmission grid and must comply with National Electricity Reliability Council (NERC) requirements. ISOs have also created and administer electricity and ancillary services markets under FERC authority with the goal of increasing efficiency and reducing costs. For example, the MISO and ISO-NE both have markets for reliability service products, including a market for the highest valued reliability service: frequency regulation. Frequency regulation is used to balance supply and demand for electricity on a second-by-second basis. When supply exceeds (is less than) demand, the

frequency will be too high (low). Area Control Error (ACE) indicates how much supply and demand are out of balance and in which direction the system needs to be corrected. ISOs monitor the frequency of the power system in real time using the ACE and send control signals to generators in the frequency regulation market that instruct these generators to ramp up or down. These generators comprise the "frequency regulation reserve."

PHES is an ideal technology to provide frequency regulation because it can quickly ramp up or down in generating mode by adjusting the flow of water through the wicket gates. A typical PHES facility can ramp from shutdown to full power in less than two minutes (Black and Veatch, 2012); PHES also has a large load change capability in terms of it being a large-scale storage device. In comparison, new Combined-Cycle Gas Turbine (CCGT) power plants can be ramped about 10% of the rated capacity per minute (GE, 2011).

Resources participating in the ISO day-ahead frequency regulation market must be able to supply regulation services in either the up or down direction within the five minute maximum allowable frequency regulation response time. The resource must also be able to supply frequency regulation continuously for one hour. Furthermore, the resource must also be able to receive and respond to Automatic Generation Control (AGC) signals, sent by the system operator every four seconds increase or decrease power injections accordingly to balance supply and demand. The faster a resource can ramp up or down, the more accurately it can respond to AGC.

Prior to Order No. 755, compensation in MISO's frequency regulation market included payments for capacity set aside to provide frequency regulation, which included payments for the opportunity cost of providing frequency regulation. Payments were made for the net power the resource injects into the system. For example, suppose a generator sells 200 MW into the day-ahead electricity market and sets aside 20 MW for the regulation reserve market. Assume the average power output is 200 MW with regulation between 180 MW and 220 MW. If the generator is dispatched down, it must reduce output from 200 MW to 180 MW. Alternatively, if the generator is dispatched up, it must increase output to 220 MW. If the generator receives instructions to dispatch up and down for equal lengths of time in a given day, the average production will be 200 MW and it will receive the day-ahead locational LMP for the 200 MW sold into the day-ahead energy market (P_{DA}). The generator also receives the market-clearing price for frequency regulation for the 20 MW offered into the regulation services market. If the generator is dispatched up more than it is dispatched down, the average production will be higher than 200 MW and it will also receive the real-time LMP (P_{RT}) for the overage.

MISO rules for frequency compensation conformed to the ISO standard. These rules applied the same compensation formula—calculated on a per-MW basis for setting aside

capacity—to all resources that are cleared in the frequency regulation market. These rules did not compensate faster ramping resources, which are capable of providing more, and more accurate, ACE correction (see FERC, 2011). In contrast, ISO-NE designed its compensation formula to incorporate the additional value that faster ramping provides in terms of both the quantity and accuracy of ACE correction.

ISO-NE compensation has three components: (1) Regulation Capacity Payment, (2) Regulation Service Payment ("mileage" payment), and (3) Regulation Opportunity Costs. Like MISO, the ISO-NE capacity payment compensates power plants for setting aside regulation reserve capacity to provide regulation service. The mileage payment compensates power plants for movements in response to ACE instructions; this payment is based on the sum of the absolute values of the provision of regulation service in the up and down directions. The mileage payment incentivizes faster-ramping resources and accurate responses to ACE instructions. The opportunity cost payment rewards power plants for the loss in electricity revenues and is included in the payment for regulation capacity. The figure below illustrates how this payment is calculated in the ISO-NE territory.

Figure 4-1: Opportunity Cost for a Power Plant in ISO-NE Territory

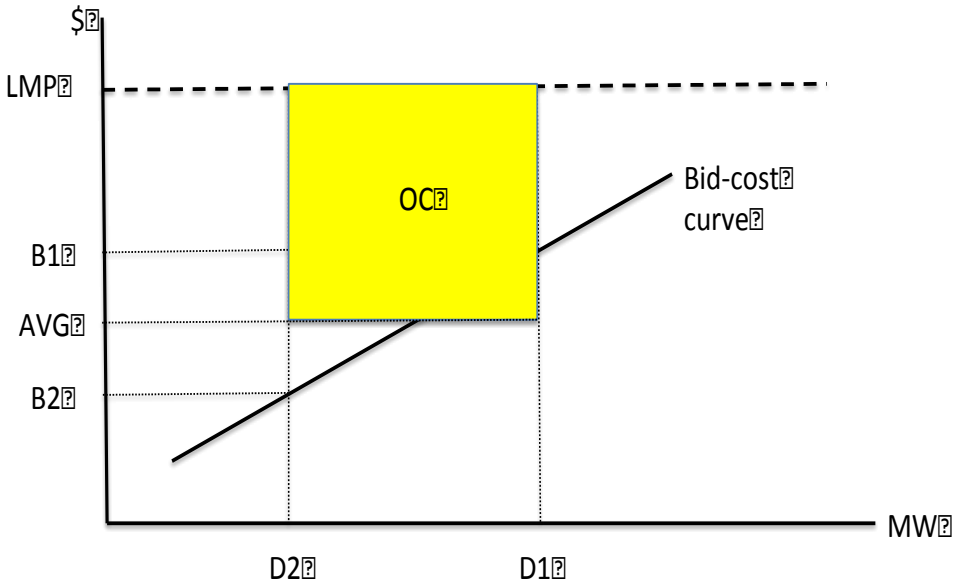

Notes: *D1* is the economic dispatch point, where the plant can provide maximum output at the prevailing LMP, and *D2* is the point where the power plant operates while providing regulation services. *AVG* is the average cost of a MW between the economic dispatch point (*B1*) and the point of operation while providing regulation services. The opportunity cost is $|LMP - AVG|*(D_1 - D_2)$.

4.2.2 Description of Models

I use a discrete state dynamic programming model to investigate the optimal dispatch of PHES in the markets from the perspective of an independent PHES operator. I assume that the PHES operator is a price-taker and sells electricity and frequency regulation services into the competitive markets. The day-ahead and real-time prices for electricity and the market clearing prices for frequency regulation are exogenous to the model and assumed to be known with certainty. The PHES operator chooses how to participate in the day-ahead electricity and frequency regulation markets with the objective of maximizing operating profit, and market rules for MISO and ISO-NE are imposed to assess their impact on the optimal dispatch decisions and financial returns to the PHES operator. I generate a vector of AGC instructions by simulating a random process for the ACE. For the purpose of our optimization model, I assume the future instructions from the ISO to ramp up or ramp down are known with certainty.

4.2.2.1 Discrete Time and Discrete State Dynamic Programming Model

The operator seeks to maximize the sum of current and expected future rewards. In this sequential decision problem, the transitions from one state to another state are governed by a state transition function and the set of actions and rewards depends on the current state and time period. With a one-week time horizon and sequential decisions made hourly, the Bellman equation is:

$$V_t(s_t) = max_{x \epsilon X}\{f(s_t, x_t) + V_{t+1}(s_{t+1}|x_t)\} \quad (2)$$

where $V_t(s_t)$ is the maximum sum of the current and future rewards when the system is in state *s* in time period *t*. The control variable is *x*, $f(s_t, x_t)$ is the current reward, and $V(s_{t+1}|x_t)$ is the maximized future reward given the state s_{t+1}.

The dynamic programming model has the following structure: in every period *t*, the operator observes an economic state s_t, takes an action x_t, and earns a reward $f(s_t, x_t)$ that depends on the current state and on the action. The state variables are: (1) head height (*h*), defined as the difference between the Upper Water Surface Elevation (UWSE) and the Lower Water Surface Elevation (LWSE); (2) prices in the competitive day-ahead (P_{DA}) and real-time (P_{RT}) electricity markets; and (3) prices in the day-ahead market for frequency regulation services (P_r). The head height reflects the amount of energy that is stored in the upper reservoir and thus the amount of power that can be generated from releasing water from the upper reservoir to the lower reservoir. For discrete head heights between upper and lower bounds (h_{min} and h_{max}), which are the constraints on the total volume of water that can be displaced, the set of possible states *s* at time *t* is:

$$s_t = \{h_{min}, \ldots, h_{max}; P_{DA,t}, P_{RT,t}, P_{r,t}\}. \quad (3)$$

If a PHES operator chooses to not participate in the market for regulation services, this operator completely controls the flow of water between the two reservoirs. In this case, the choice variable is the volume of water flowing through the wicket gates, with a positive flow corresponding to electricity generation and a negative flow corresponding to the energy required to pump water from the lower reservoir to the upper reservoir. The system is idle when the flow is zero. With this restricted set of controls, an operator could earn revenues by exploiting arbitrage opportunities that arise from diurnal variations in electricity prices. But if an operator chooses to participate in the market for regulation services, this operator relinquishes partial control to the ISO. The PHES operator's decision is thus how much regulation service to provide. I include this expanded set of control options in the model.

In the absence of pump-turbine efficiency considerations and mechanical limitations, a PHES facility could set aside half of its maximum output as frequency regulation reserve and be in compliance with the requirement that ramping must be possible in both the up and down directions within the five-minute maximum allowable response time. I add realism in the model by constructing a more restrictive operating envelope that takes into account pump-turbine efficiency and mechanical issues based on PHES facility specifications and turbine parameters in BARR Engineering Company's Giants Ridge project (BARR Engineering, 2009). The combination of head height and flow rate where the pump operates at its highest efficiency is the "best efficiency point" of the pump. The lower bound of the operating envelope is 90% of the head height at the best efficiency point and 90% of the flow rate at best efficiency point. The upper bound of the operating envelope is 110% of the head height at best efficiency point and 130% of the flow rate at the best efficiency point. The operating envelope puts a lower bound on efficiency at 87% based on the pump-turbine performance curves supplied by engineers at the St. Anthony Falls Laboratory (Lueker, personal communication, July 2011). Flow rates are discretized in 5% increments within this operating envelope, allowing the operator to choose between 21 different levels of participation in the frequency regulation market at both pumping and generating modes. These choices correspond to $r_{g,1}$ through $r_{g,21}$ in Equation 4, which specifies the set of mutually exclusive possible actions as

$$x \in \left(pump, g, i, \{r_{p,j}\}_{j=1}^{21}, \{r_{g,j}\}_{j=1}^{21}\right) \quad (4)$$

where *pump* denotes pumping mode, *g* denotes generating mode at best efficiency flow rate; *i* denotes idling, and *r* denotes the capacity level of regulation service with subscripts *p* and *g* to denote the provision of regulation service in pumping and generating modes. Each level of

regulation service corresponds to a regulation service capacity defined as the capacity to provide regulation in the up and down directions. The remaining capacity is used to serve the day ahead and real time energy markets.

I assume that the rotational speed of the pump can be varied $\pm 10\%$ of the nominal rotational speed. Because the pumping speed can be adjusted, the PHES facility can change the rate of energy use and can thus provide regulation services in pumping mode. Changing the rotational speed $\pm 10\%$ results in an approximate 60% change in power output. The ratio of actual power use ($E_{p1,t}$) to power use at the nominal pump speed ($E_{po,t}$) is the ratio of the rotational speed (γ_1) to the nominal pump speed (γ_0):

$$E_{p1,t}/E_{p0,t} = \gamma_1/\gamma_0. \quad (5)$$

The volumetric flow rate, *Vol*, depends on the choice of the control. If the PHES facility is in pumping mode, *Vol* is the best efficiency point flow rate. If the PHES facility is generating power without providing regulation service, *Vol* is the maximum flow rate. If the PHES facility is withholding capacity to provide regulation service, *Vol* is set based on amount of capacity offered into the regulation services market. In addition, when the operator offers capacity for regulation service, *Vol* is adjusted in response to AGC instructions from the system operator to ramp up or down. Power generation is computed using the following formula for approximating hydroelectric power (U.S. Army Corps of Engineers, 1981):

$$E_{g,t} = 9800 \cdot Vol_t \cdot h_t \cdot \theta_{Turbine}/(3600 * 10\text{^}6) \quad (6)$$

where $E_{g,t}$ is the electricity generated (MWh), Vol_t is the volumetric flow rate (m^3/h), h_t is the initial head height (m) for each time step, and $\theta_{Turbine}$ is the turbine efficiency, which is a function of the head height and the flow conditions. Electricity generation is computed for each of the discrete 5m head heights and volume. The change in the head height in one hour depends on the volume of flow and the size and shape of the upper and lower reservoirs. Electricity consumption for pumping is computed using the following equation (U. S. Army Corps of Engineers, 1979):

$$E_{p,t} = 9800 \cdot Vol_t \cdot h_t/(\theta_{Pump} \cdot 3600 \cdot 10\text{^}6)\ , \quad (7)$$

where $E_{p,t}$ represents power use as a function of head height and flow conditions and θ_{Pump} is the pump efficiency. I set $Q_{DA,t} = E_{p,t}$ when the PHES facility is in pumping mode and $Q_{DA,t} = E_{g,t}$ when the PHES facility is in generation mode. $E_{g,t}$ and $E_{p,t}$ also put an upper bound on regulation capacity because they indicate the maximum capacity given the head height and maximum achievable flow rate.

The current period reward function for MISO rules is:

$$R_M(s_t, x_t) = \begin{cases} 0, & \text{idle} \\ -p_{DA,t}Q_{DA,t}, & \text{pumping} \\ p_{DA,t}Q_{DA,t}, & \text{generating} \\ p_{DA,t}Q_{DA,t}+p_{r,t}Q_{r,t}+p_{RT,t}Q_{RT,t}, & \text{frequency regulation} \end{cases} \quad (8)$$

where $Q_{RT,t} = \sum_{i=1}^{120} AGC_i$ is the simulated vector of AGC instructions within an hour denoting the net frequency regulation provided in the up direction and $Q_{r,t}$ is the regulation service capacity. The ISO-NE compensation formula for frequency regulation has the three components described above (regulation capacity payment, the mileage payment, and regulation opportunity costs). These are reflected in the current period reward function for the ISO-NE rules. I set the economic dispatch point equal to zero based on the assumption that the marginal cost of producing power is zero for a PHES plant. The capacity-to-service ratio is set equal to 0.1 based on an historical analysis by ISO-NE which found that on average one MW of regulation capability produced 10 MW of regulation service (ISO-NE Market Manuals, 2013). The reward function with New England rules is, thus:

$$R_{NE}(s_t, x_t) = \begin{cases} 0, & \text{idle} \\ -p_{DA,t}Q_{DA,t}, & \text{pumping} \\ p_{DA,t}Q_{DA,t}, & \text{generating} \\ p_{DA,t}Q_{DA,t}+ p_{r,t}Q_{r,t}+0.1p_{r,t}\sum|\Delta MW|+LMP_t*GENOFF_t, & \text{frequency regulation} \end{cases} . \quad (9)$$

The mileage payment for frequency regulation is a major difference between the ISO-NE compensation (9) and the MISO compensation scheme before compliance with FERC rule 755 (8). This mileage payment rewards the total amount of up and down ramping that occurs in each time period; as with regulation capacity under ISO-NE rules, this mileage payment is compensated with the regulation clearing price, $p_{r,t}$. But this compensation differs from former MISO rules, which used the real-time price of electricity to compensate (charge) power injections (withdrawals).

I treat the change in head height in a stepwise fashion within the hour, and look up the efficiency factor for each step. The transition function for the head height is:

$$h_{t+1} = h_t + 8024m^3 * avg(Vol_t), \quad (10)$$

where $8024m^3$ is the volume of water that is displaced during each step change in head height and is calculated from the PHES facility parameters in the BARR Engineering Giants Ridge project. The variable $avg(Vol)$ is the average flow rate during the hourly period and is a function of the action, initial head height, and the simulated AGC instructions during the hour to

regulate up or regulate down if providing regulation service capacity. Prices for electricity and regulation service transition independently of the action taken by the operator.

4.2.2.2 Application: Minnesota's Iron Range

I applied the models above to a potential PHES plant in Minnesota's Iron Range. BARR Engineering identified a number of potential sites for PHES, one of which was Giants Ridge (BARR Engineering, 2009). I chose this site for its feasibility and its proximity to wind resources that could be used to generate electricity and are affecting the value of regional LMPs. Engineering specifications are taken from Barr Engineering (2009) and the parameters are listed in Table 1. BARR designed a preliminary PHES power plant for this site, where I assume that the upper and lower reservoirs are rectangular cube. The maximum and minimum head heights fix the total volume of water that can be displaced at 2,928,000 m^3. Turbine and pump efficiencies ($\theta_{Turbine}$ and θ_{Pump}) depend on flow and head conditions, and a wicket gate controls the flow of water from the upper reservoir to the lower reservoir. At full gate, the flow of water reaches its maximum attainable volume. I assume that the flow of water may be reduced to 90% of Q_{BEP} because this value puts a lower bound on η_t at approximately 0.88. Data relating turbine efficiency to various head height and flow conditions was obtained from BARR (2009) and conversations with engineers at the St. Anthony Falls Laboratory at the University of Minnesota. I interpolated these points with a second-degree polynomial and used this interpolation to generate data that relate the turbine efficiency to all of the possible discrete flow and head height conditions. This PHES plant can have a capacity as high as 111 MW and store up to 770 MWh.

Table 4-1: Parameters for Potential PHES Plant in Minnesota's Iron Range

Variable	Definition	Value
$LWSE_{min}$	Min Lower Water Surface Elevation	357 m
$LWSE_{max}$	Max Lower Water Surface Elevation	371 m
$UWSE_{min}$	Min Upper Water Surface Elevation	483 m
$UWSE_{max}$	Max Upper Water Surface Elevation	487 m
A_L	Surface Area for the Lower Reservoir	209,108 m^2
A_U	Surface Area for the Lower Reservoir (A_U)	714,027 m^2
h_{max}	Maximum Head Height	129.80 m
h_{min}	Minimum Head Height	111.60 m
h_{BEP}	Best Efficiency Pump Head Height	120.97 m

Q_{BEP}	Best Efficiency Pump Discharge	87.13 m^3/sec
P_{max}	Maximum Power Output	111 MW

I used electricity prices from 2010 near the potential Giants Ridge plant and the market clearing prices in the day-ahead market for frequency regulation reserve. The one-week arbitrage period begins Sunday at midnight and is selected because price forecasts are available for one-week periods, making the assumption of perfect foresight more realistic (Siohansi et al., 2009). The one-week period is also sufficient to allow for arbitrage opportunities that exist within and across days. LMPs in the day-ahead electricity market exhibit the typical diurnal pattern, with higher prices during the daytime and lower prices during the nighttime. LMPs are also typically lower during the weekend compared to weekdays, which suggests that inter-day arbitrage opportunities may exist.

Figure 4-2: PHES Regulation Service and Allowable Regulation Service

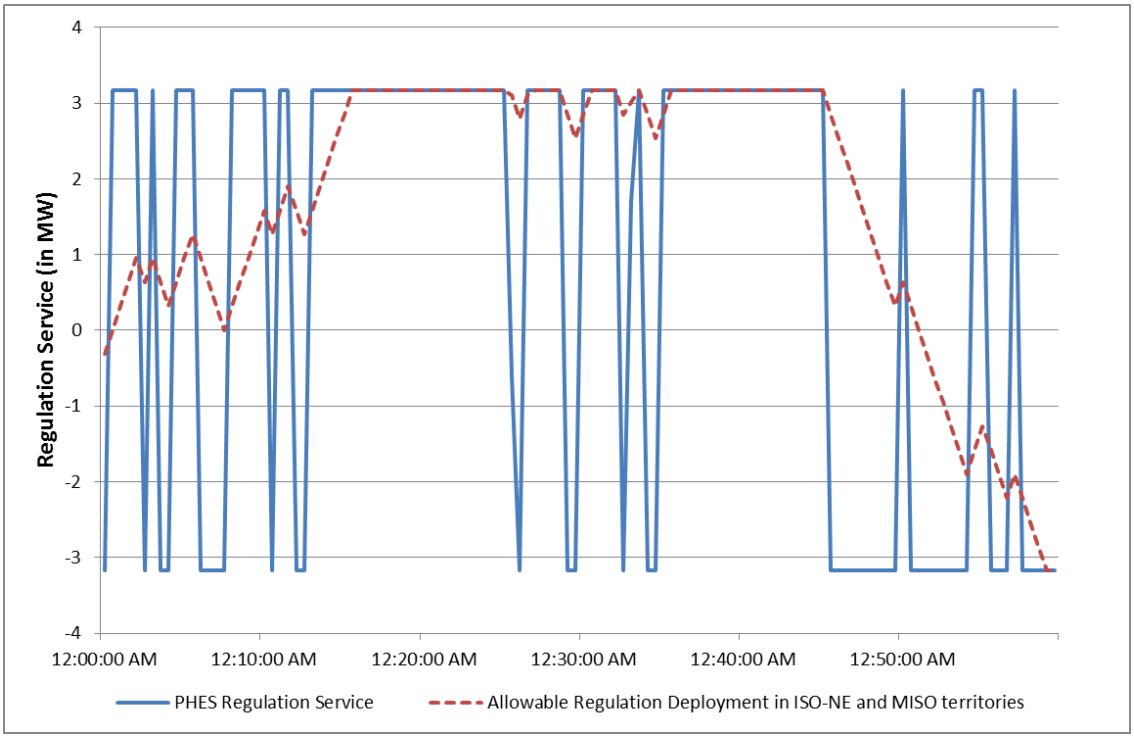

The figure above shows a simulated set of instructions (solid line) to provide regulation service in the up or down directions over a one-hour time period. In the simulation, the PHES plant offered 3.16 MW of regulation service capacity into the market. Since a PHES plant can ramp from shutdown to maximum capacity in less than two minutes, I assumed that the PHES facility could follow ACE without error. MISO and ISO-NE limit regulation capacity to the amount the resource can ramp in five minutes. The dotted line tracks this allowable regulation

deployment under the assumption that the resource needs five minutes to ramp 3.16 MW. The response time of PHES is on the order of a few seconds. Thus, PHES is capable of meeting its dispatch targets within the four-second-response time.

Our dynamic programming model is solved using backwards recursion for 52 one-week periods, starting with the last week in 2010 and ending with the first week in 2010. The optimal values for each state at $t=1$ for week $j+1$ are used as the carryover values for week j. The optimization assumes perfect foresight and assigns carry-over values to stored energy in the terminal period. The model produces a set of optimal actions for each time period and a series of revenues and costs that result from these optimal actions and resulting state variables. In addition, the value of the PHES facility in terms of operating profit for a time interval, including the entire year of the analysis, can be computed. I report on these results below.

4.3 Results

4.3.1 Results for a One-Week Period in January

The figure below shows the optimal dispatch schedule for a one-week period in January. Prices were acquired from the MISO's historical data archive, for a pricing node close to the Minnesota Iron Range (Midwest ISO Market Reports, 2012). The market-clearing price (MCP) for frequency regulation is for the MISO sub-region in which the Minnesota Iron Range is located. Increasing head heights indicate that the PHES facility is in pumping mode—the upper reservoir is recharging and stored energy is increasing—whereas decreasing head heights indicate that the upper reservoir is discharging (stored energy is decreasing).

During the winter within the MISO territory, demand peaks twice each weekday: late morning and evening, before and after the typical workday. The PHES facility is put into pumping mode (generating mode) during the off-peak (peak) periods when demand is low (high). Periods with low prices are long enough to allow the upper reservoir to completely recharge. In addition, the amount of storage capacity (six consecutive hours of storage at maximum capacity) is sufficient for the operator to bid into the day-ahead energy and frequency regulation markets for the entire period of high prices. The negative LMPs on Tuesday indicate a highly congested system at the node and are a disincentive for generating power at the node.

Figure 4-3: Upper Reservoir Discharge and Recharge, Electricity Prices, and Frequency Regulation

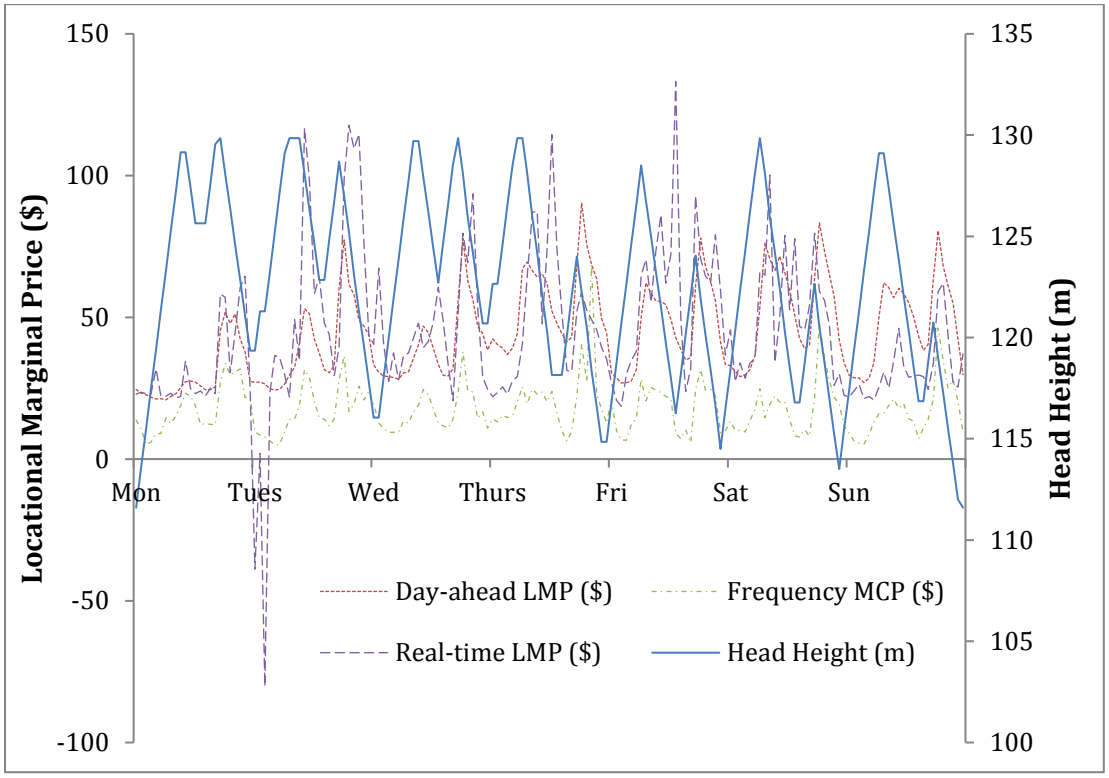

The daily operating pattern is similar but different across each day of the one-week period, suggesting the presence of both inter-day and intra-day arbitrage opportunities. I calculated the net operating revenues by summing the revenues from generating electricity and providing frequency regulation and subtracting payments for pumping and any net withdrawals during the provision of regulation service. Total operating revenue was $447,000, of which $54,000 came from providing regulation services. After subtracting the costs of pumping, the operating profit is $196,000 for the week.

Figure 4-4: One-Week Operating Profit and Storage Capacity under MISO Rules

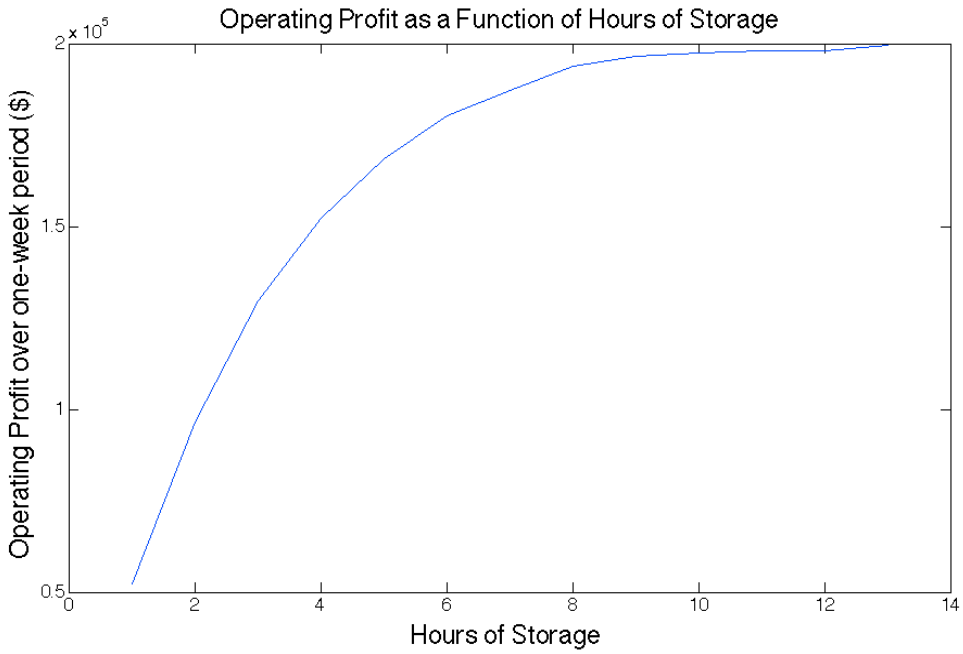

The figure above shows the relationship between the one-week operating profit and the number of hours of storage under MISO market rules. I defined "hours of storage" as the number of consecutive hours that the PHES facility can generate electricity at the maximum flow rate without recharging the upper reservoir. Hours of storage are a function of the maximum flow rate and the volume of water that can be displaced. The number of hours of pumping that are necessary to fully recharge the upper reservoir is calculated by dividing hours of storage by the PHES plant's pumping efficiency. Operating profits are computed by solving the model for different hours of storage. Therefore, we assumed that the operator makes optimal decisions in each one-hour time period.

Operating profit is the sum of the payments for providing regulation services and the profit from arbitraging the electricity market. I solved the model multiple times, using different levels of h_{min} and h_{max} to denote different storage capacities. The figure above shows diminishing returns as hours of storage increase and that these diminishing returns impose an upper limit on the one-week operating profit. Approximately 90% of the operating profit is captured in the first six hours of storage, which suggests that most of the arbitrage value of storage is derived from taking advantage of the diurnal price pattern rather than inter-day price variation.

I compared the optimal dispatch schedule for a PHES facility under the former MISO rules with one being compensated under ISO-NE rules, where the formula for providing

frequency regulation compensates generators with a mileage payment, based on the sum of up and down movements, in addition to a payment for capacity. Such a mileage payment encourages faster ramping resources—which provide more ACE correction and more accurate regulation services—to participate in the market for frequency regulation. As a consequence, the operator sets aside more capacity to provide frequency regulation reserve under ISO-NE rules.

Operating profit under ISO-NE rules is $464,000—2.4 times the operating profit under MISO rules for the same one-week period. Operating revenue is also much greater under ISO-NE rules, $733,000 (ISO-NE) compared to $447,000 (MISO). This additional operating revenue occurs because ISO-NE rules compensate for the total amount of ACE correction. Under the ISO-NE rules, $424,000 is attributable to regulation services, which is more than eight times the revenue from providing regulation services under MISO rules.

4.3.2 Profitability for One-Week Periods in Winter and Summer

I compared the operation of a PHES facility in the winter with its operation in the summer by using data for a one-week period in January and July, 2010. The major difference between the two one-week periods is the behavior of the day-ahead price series. The figure below shows the patterns for the electricity prices in the day-ahead markets in the two seasons. In contrast to the daily morning and evening peaks during the winter, the electricity prices in July have only one peak in the late afternoon.

Figure 4-5: Day-Ahead Electricity Prices

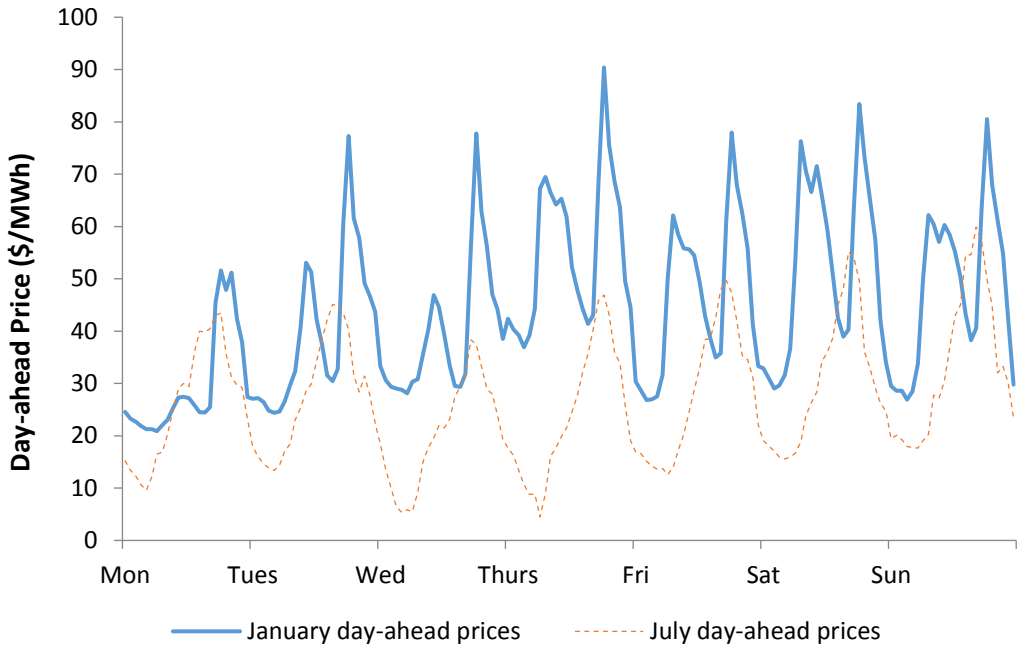

Notes: This figure presents day-ahead electricity prices for one-week periods in January 2010 (winter period) and July 2010 (summer period).

The table below presents summary statistics for one-week price series in January and July. The maximum and minimum price levels in the day-ahead market during the one-week period are $90.90 and $16.79 (January) and $60.81 and $4.71 (July). Note that electricity prices are both higher and more variable (higher standard deviation) for the one-week period in January than for the one-week period in July. The double-peak pattern in diurnal electricity prices increases the variability in electricity prices during the winter and creates additional opportunities for arbitrage.

Table 4-2: Summary Statistics for One-Week Time-Series of Prices

	Electricity Markets					
	Day-Ahead		**Real-Time**		**Regulation Services**	
	January	**July**	**January**	**July**	**January**	**July**
Mean	$45.00	$27.81	$43.87	$28.80	$17.75	$12.22
Std. dev.	$17.21	$12.81	$23.65	$18.76	$9.16	$5.98
Maximum	$90.90	$60.81	$119.46	$110.77	$68.55	$30.30

Minimum	$16.79	$4.71	-$17.95	-$28.24	$5.01	$4.60

Notes: This figure presents day-ahead electricity prices for one-week periods in January 2010 (winter period) and July 2010 (summer period).

Opportunities for arbitraging day-ahead electricity prices result from volatility in electricity prices, and revenues and profits should be lower in July as a result. The table below confirms this expectation; total operating profit under MISO market rules for the weeks in January and in July are $196,000 and $153,000, respectively, and operating revenues are $447,000 and $265,000, respectively. The same relationship with volatility exists when dispatch is optimized for the ISO-NE market rules. For the one-week period in July, total operating profit is $302,000 and total operating revenue is $450,000, compared to $464,000 and $763,000, respectively, for January. The table below also shows 57.8 percent and 60.4 percent of total operating revenue comes from frequency regulation under the ISO-NE market rules for one-week periods in January and July respectively. In contrast, frequency regulation under MISO market rules in January and July accounts for only 12.1 percent and 13.2 percent of total operating revenue respectively. Frequency regulation as a percentage of total operating revenue is slightly higher in January and July under either set of compensation rules, but varies significantly according to the rules under which the PHES facility operates. This result is consistent with expectations since load fluctuations of less than a minute exhibit random characteristics and do not depend directly on the amount of load.

Table 4-3: Profitability and Operations over One-Week

	January		**July**	
	MISO	**ISO-NE**	**MISO**	**ISO-NE**
A. Total Operating Profit	$196,000	$464,000	$153,000	$302,000
B. Total Operating Revenue	$447,000	$733,000	$265,000	$450,000
C. Frequency Regulation Revenue	$54,000	$424,000	$35,000	$272,000
D. C as a percentage of B	12.1%	57.8%	13.2%	60.4%

Notes: One-week periods were selected in January 2010 and July 2010 at same node used in the analysis in the above subsection.

4.3.3 Profitability over the Entire Year in 2010

The table below shows the operating profit, operating revenue, and the operating revenue attributable to frequency regulation over the entire year for under both MISO and ISO-NE rules for 2010. The table below underscores the importance of how market rules drive the value of

energy storage technologies like PHES; total operating profit and total operating revenue under ISO-NE market rules is approximately twice those under MISO market rules, and revenue from providing frequency regulation services are more approximately eight times more under ISO-NE rules than under MISO rules.

Table 4-4: Profitability and Operations over the Year 2010

	MISO	ISO-NE
A. Total Operating Profit	$6,386,000	$14,916,000
B. Total Operating Revenue	$13,786,000	$24,004,000
C. Frequency Regulation Revenue	$1,227,000	$10,166,000
C. as a percentage of B.	8.9%	42.4%

Notes: This analysis uses the same pricing node as in the above analysis.

A comparison between the two tables above indicates that there are seasonal differences in the profitability of energy storage technologies under the different market rules. The total profit under ISO-NE market rules was $0.464M and $0.302M for one week in January and in July, respectively (Table 4-3). It was more profitable to operate the PHES facility in January than in July, and more profitable in these months, on average, than during the remainder of the year. Calculating annual profit based on January and July profits yields $39.8M, which is substantially more than the actual annual profit of $14.9M (Table 4-4). Presumably, profitability peaks in the winter and the summer and decreases in the spring and the fall. This effect may be due to less demand for electricity in the temperate seasons of the year.

4.3.4 Capacity-to-Service Ratio Sensitivity Analysis

To explore the robustness of profits and how operating decisions depend on the mix of payments for regulation capacity and regulation services, I varied the capacity-to-service ratio from 0.01 to 0.4. The baseline capacity-to-service ratio used above is 0.1 which was chosen by ISO-NE to approximately equalize payments for regulation capacity and regulation service. Here, the endpoints of our sensitivity analysis achieve a 1:10 ratio of service payments to capacity payments (0.01 capacity-to-service ratio) and a 4:1 ratio, where payments for regulation service are four times payments for regulation capacity.

Figure 4-6: Total Operating Revenue for a One-Week Period in January 2010

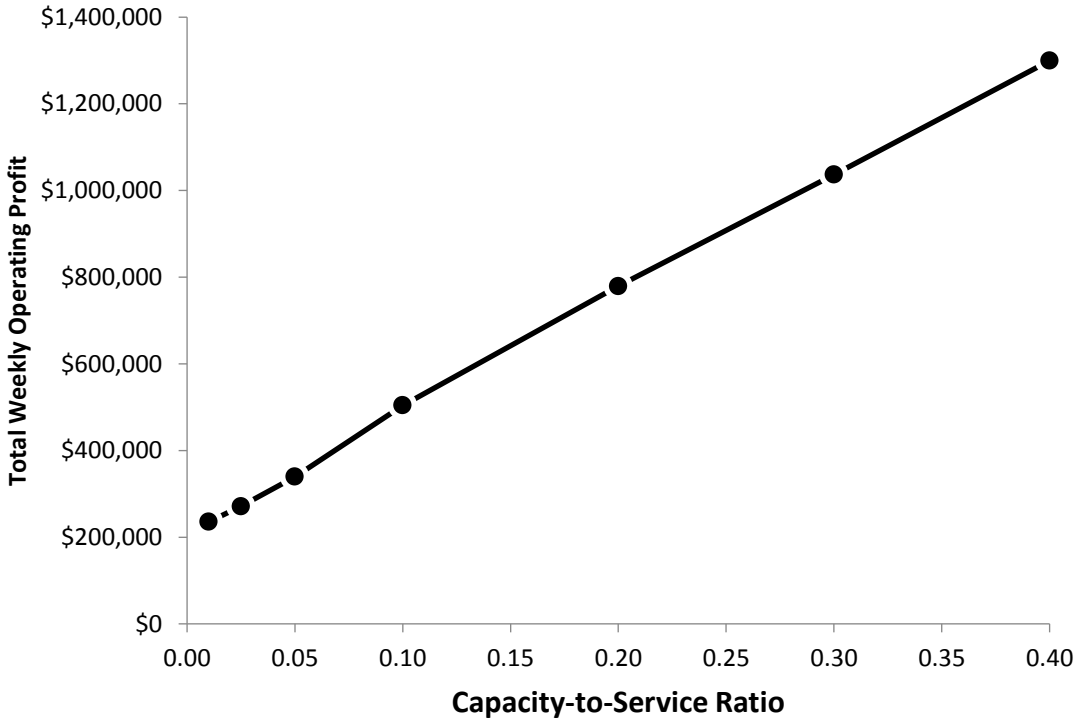

Table 4-5: Total Operating Revenue by Capacity-to-Service Ratio

Cap.-to-Serv. Ratio	Total Oper. Profit	Tot. Oper. Rev.	Freq. Oper. Revenue	# Hrs. Idling	# Hrs. Gen.	# Hrs. Pumping	# Hrs. Freq (intensity lvl=1)	# Hrs. Freq. (Intensity lvl=2)
0.01	$235,245	$478,086	$90,489	14	1	72	5	76
0.025	$271,167	$529,466	$146,470	8	1	74	56	29
0.05	$339,553	$611,962	$241,830	5	0	76	86	1
0.1	$504,309	$752,048	$421,626	3	0	78	87	0
0.2	$779,242	$1,025,526	$789,053	4	0	79	85	0
0.3	$1,036,597	$1,353,174	$1,165,520	2	0	78	88	0
0.4	$1,299,476	$1,603,293	$1,515,755	1	0	82	85	0

Figure 4-6 above shows total one-week operating profit increases in the capacity-to-service ratio. Total operating profit increases at an increasing rate up to a ratio of 0.2. This reflects changing operating strategies. For a ratio of 0.01, the PHES facility idles for fourteen hours, whereas the facility only idles for three hours when the ratio is 0.1 and one hour when the

ratio is 0.4. The PHES facility also allocates more capacity to providing regulation service at higher capital-to-service ratios. For a ratio of 0.01, the facility chooses to provide the maximum amount of frequency regulation (intensity level=1) for only 5 hours. This compares to 56 hours and 86 hours at a capacity-to-service ratios equal to 0.025 and 0.05 respectively. The positive impact on total operating revenues is an indication the PHES facility is capable of fast ramping and accurately following instructions to ramp up or down. The results show payments for regulation service are an important component of operating profit, suggesting that such payments are necessary for incentivizing the PHES installations. Revenues for providing frequency regulation account for 58% of total revenue in the baseline scenario and 95% of total revenue in the scenario with the ratio set equal to 0.4.

4.4 Discussion

Policies to promote renewable energy technologies and energy storage are well studied, but often in absence of electricity market rules. As energy storage technologies operate in markets and the rules of these markets can incentivize different operational decisions, profits, and the functioning, analysis within the context of the regional electricity system is critical. To study these issues, I developed a dynamic programming model to assess and evaluate the operational decisions of a PHES facility in competitive electricity markets. I parameterized this model with prices in the day-ahead markets for electricity and frequency regulation and the real-time market for electricity to investigate the arbitrage value of PHES, under two different sets of ISO rules: MISO and the ISO-NE. I used a one-week time horizon for the model to capture arbitrage opportunities that exist within and across days and to make the assumption of perfect foresight of prices realistic.

Our results show that arbitrage opportunities exist due to the well-known diurnal price pattern and inter-day variations, but that ISO rules are very important as they can provide a significant additional source of revenue. I calculated the value of market rules: in the MISO region, the weekly operating profit would be $196,000 in January and 2.4 times higher ($464,000) under ISO-NE rules. Profits under ISO-NE rules are consistently higher because the compensation mechanisms reward the responsiveness of PHES to instructions to ramp up or down. This difference presents an important, yet understudied, area for energy policy research.

The volatility of prices over a one-week period decreases significantly during the spring and fall seasons in most areas of the MISO footprint. I found that arbitrage opportunities over the one-week period in January are greater than in July and, in calculating the annual profits under both sets of market rules, I found the lower price volatility in the fall and spring also contributes

to lower average weekly profits.

The optimal size of a PHES facility is also a function of how the market operates. When I solved for the one-week operating profit as a function of storage capacity I found that approximately 90% of the weekly operating profit is captured in the first six hours of capacity, suggesting that the arbitrage opportunities within the day are more important than those across days. Payments for regulation capacity and the provision of regulation service are also important components of the operating profit. The model results show that, under both MISO and ISO-NE rules, an operator should set aside some capacity for providing frequency regulation. The incentives provided by the ISO-NE rules encourage a greater amount of capacity to be set aside.

The advantage of the model is its simplicity and its focus on PHES profitability. However, the purpose of the model is only to estimate revenue to a PHES facility from the sale of electricity and grid reliability services into the wholesale markets. I assume the PHES facility is a price-taker and examine the optimal bidding strategies from the perspective of an operator of a single PHES facility operator. The model does not provide insight into the self-scheduling problem confronting price-makers (e.g., de la Torre et al., 2002) nor do I focus on optimal grid market operations. Also, I do not address issues facing operators of a portfolio of resources (for example, electric utilities). In settings with large-scale penetration of wind or solar in the resource portfolio and regulatory obligations to provide electricity from these resources, energy storage may allow the reduction of wind curtailment which could drive the optimal dispatch of PHES and be another important source of profit.

One extension of this model would be to generalize the power producer's objective function and add risk constraints, which could include long-term bilateral agreements for the sale of peak power and the purchase of off-peak power. These agreements may be necessary for an Independent Power Producer to hedge risk, guarantee revenue streams, and secure financing for a PHES plant.

Large-scale deployment of PHES could increase off-peak prices, reduce peak prices, and reduce the arbitrage value of PHES making the price-taking assumption less realistic. But arbitraging electricity prices is one of several revenue streams; frequency regulation, for example, is the highest valued ancillary service. While PHES has the potential to serve numerous valuable market and transmission functions, only a few of these have been successfully monetized thus far. Private investors will likely under-invest in PHES if they are unable internalize the benefits of valuable market and transmission services. Consequently, the design of markets, as well as contract instruments and tariff structures, is extremely important and has significant policy implications.

The integration of large-scale wind energy or other variable renewables like solar into the electricity system and the increased need for significant expansion of the transmission system can create other important opportunities for storage technologies. Future research should seek to better understand the role that energy storage can play in reducing the cost of large-scale wind integration and deferment of transmission expansion. Better understanding of these sources of value is important for realizing other policy goals, as efforts to justify and promote development and investment in energy storage will fall short if the market mechanisms are not equally supportive.

4.5 Conclusions

Energy storage could become vital to ensuring the successful evolution of energy systems. PHES is an important and promising technology to bring supply and demand in to balance and to smooth the incorporation of electricity generated from variable resources into the electricity grid. But while the technologies are important, the rules governing them are critical for their deployment.

Market rules vary across regional ISOs and determine the optimal size of PHES facilities, influence optimal operational and bidding strategies for individual PHES operators, and affect the profits of these facilities. An important consequence of differences in these market rules is that they can lead to different profits in different areas of the country. In our study, it was more profitable to operate a PHES facility under ISO-NE rules than it was with MISO rules. Profit-maximizing developers may not choose to develop energy storage projects where they are most needed if market rules do not support them.

5. Conclusions

The objective of this dissertation is to analyze the operational strategies and economic viability of different power systems in the wholesale electricity markets from the perspective of an IPP. Additionally, the dissertation considers the ability of market participants to exercise market power in the wholesale electricity markets, which is the policy challenge that has received the most attention since the California energy crisis.

Chapter 1 investigated the potential for exercising market power in the PJM region. The results presented in this paper show some evidence that market power was exercised with and without the incorporation of start-up costs. Evidence that market power was exercised is strongest during months having unseasonably cold temperatures and fuel price spikes as well as during the winter peak season. The results also show the degree of market power increases during the peak hours of the day. These results are consistent with expectations because there are more opportunities to exercise market power during peak hours. Transmission congestion during peak hours will lead to the presence of more pivotal suppliers. Additionally, output during peak hours is on a steeper part of the aggregate marginal cost curve (output during peak hours is higher). This creates opportunities for power plants that anticipate a strategic advantage to manipulate market prices by withholding supply to boost prices. These results are also consistent with studies of market power in the California electricity market showing market power is typically exercised when temperatures increase during the warm summer months when demand for power is the highest. My results show there are generally more opportunities to exercise market power in the PJM region during the cold winter months when demand for power is high and fuel prices have potential to spike upward.

In Chapter 2, I investigated the conditions under which it would be profitable to operate a low temperature geothermal power plant with chilled-water cooling system. Although such as system was found to not be generally cost effective, there may exist market conditions and institutions in the future that would make such a system economical. I note that the Unted States is moving to a smart grid and dynamic pricing programs using real-time prices, which offers enhanced opportunities to utilize a chilled-water cooling to increase the value of low-temperature geothermal. Perhaps more importantly, Chapter 2 makes a contribution to the idea that geothermal does not have to be thought of as just base load generation. Opportunities exist to utilize the flexible geothermal generation to provide power during high demand periods and to provide other market and transmission services to the power system.

In Chapter 3, I showed that market rules vary across RTOs/ISOs and determine the optimal size of PHES facilities, influence optimal operational and bidding strategies for

individual PHES operators, and affect the profits of these facilities. An important consequence of differences in these market rules is that they can lead to different profits in different areas of the country. In our study, it was more profitable to operate a PHES facility under ISO-NE rules than it was with MISO rules. Thus, profit-maximizing developers may not choose to develop energy storage projects where they are most needed if market rules do not support them.

6. Bibliography

1. Ashwood A., Bharathan, D. (2011). Hybrid cooling systems for low-temperature geothermal power production. *National Renewable Energy Laboratory Technical Report NREL/TP-5500-48765*.

2. BARR Engineering Company. (2009). *Giants Ridge pumped storage project*. Memorandum to Great River Energy.

3. Black & Veatch. (2012). *Cost and performance data for power generation technologies*. Golden, CO: National Renewable Energy Laboratory. Retrieved August 8, 2014, http://bv.com/docs/reports-studies/nrel-cost-report.pdf.

4. Blumsack, S. (2002). Market Power in Deregulated Wholesale Electricity Markets: Issues in Measurement and the Cost of Mitigation. *The Electricity Journal*, 15(9), 11-24

5. Borenstein, S., (2000). Understanding Competitive Pricing and Market Power in Wholesale Electricity Markets. *The Electricity Journal*, 13(6), 40-57.

6. Borenstein, S. (2005). The long-run efficiency of real-time electricity pricing. The Energy Journal, 26(3), 93–116.

7. Borenstein, S., Bushnell, J. (2000). Electricity Restructuring, Deregulation or Re-regulation. *Working Paper No. CPC00-14, Competition Policy Center, Institute for Business and Economic Research, UC Berkeley*.

8. Borenstein, S., Bushnell, J. (2015). The US Electricity Industry After 20 Years of Restructuring. *Annual Review of Economics Annual Reviews*, 7(1), 437-463.

9. Borenstein, S., Bushnell, J., Knittel, C. (1999). Market power in electricity markets beyond concentration measures. *The Energy Journal*, 20(4), 65-88.

10. Borenstein, S., Bushnell, J., Stoft, S. (2000). The Competitive Effects of Transmission Capacity in a Deregulated Electricity Industry. *The RAND Journal of Economic*, 31(2), 294-325.

11. Borenstein, S., Bushnell, J., Wolak, F. (2002). Measuring market inefficiencies in California's Restructured Wholesale Electricity Market. *American Economic Review*, 92(5), 1376-1406.

12. Borenstein, S., Holland, S. (2005). On the efficiency of competitive electricity markets with time invariant retail prices. *RAND Journal of Economics*, 36(3), 469–493.

13. Boyd, A., Hanis, M. (2020). How Advanced Energy Companies can Navigate RTOs/ISOs to Business Success. *Advanced Energy Economy, Advanced Energy Perspectives*. Retrieved from https://blog.aee.net/how-advanced-energy-companies-can-navigate-rtos/isos-to-business-success.

14. Bushnell, J., Mansur, E., Saravia, C. (2008). Vertical arrangements, market structure and competition: An analysis of restructured U.S. electricity markets. *American Economic Review*, 98(1), 237-66.

15. California Independent System Operator, 2013. *Building a sustainable energy future: 2014-2016 strategic plan*. Retrieved from http://www.caiso.com/Documents/Decision-2014-2016StrategicPlan-Sep2013.pdf.

16. California Public Utilities Commission, 2013. *CPUC sets energy storage goals for utilities [Press release]*. Retrieved from http://docs.cpuc.ca.gov/PublishedDocs/Published/G000/M079/K171/79171502.PDF.

17. Carnegie, R., Gotham, D., Nderita, D., Preckel, P. (2013). *Utility scale energy storage systems: benefits, applications, and technologies*. State Utility Forecasting Group, Purdue University. Retrieved from http://www.purdue.edu/discoverypark/energy/assets/pdfs/SUFG/publications/SUFG%20Energy%20Storage%20Report.pdf.

18. Castelvecchi, D. (February 27, 2012). *How big a battery would it take to power all of the U.S.?* Scientific American. Retrieved from http://www.scientificamerican.com/article/castelvecchi-how-big-battery-would-it-take-power-usa/.

19. Connolly, D., Lund, H., Finn, P., Mathieson, B.V., Leahy, M. (2011). Practical operation strategies for pumped hydroelectric energy storage (PHES) utilising electricity price arbitrage. *Energy Policy*, 39(7), 4189-4196.

20. Cullen, J., Reynolds, S. (2017). Market dynamics and investment in the electricity sector. *Working Paper 17-05, University of Arizona*. Retrieved from http://www.josephcullen.com/resources/LR_v1.pdf.

21. Daikin McQuay, (2009). *Pathfinder™ Air-Cooled Chillers Catalog 600-2*. Retrieved July 13, 2021, https://oslo.dev.daikinapplied.com/api/sharepoint/GetDocument/Doc100/CAT_600-2_121109.pdf/.

22. de la Torre. S., Arroyo, J.M., Conejo, A.J., Contreras, J. (2002). Price maker self-scheduling in a pool-based electricity market: a mixed-integer LP approach. *IEEE Transactions on Power Systems*, 17(4), 1037-1042.

23. Deb, R. (2000). Operating hydroelectric plants and pumped storage units in a competitive environment, *The Electricity Journal*, 13(3), 24-32.

24. DSIRE, (2014). Database of state incentives for renewable energy and efficiency, NC State University. Retrieved August 10, 2014, http://www.dsireusa.org/summarytables/index.cfm?ee=1&RE=1.

25. The Economist. (March 3, 2012). *Packing Some Power*. Retrieved August 10, 2014, http://www.economist.com/node/21548495.

26. EIA. (n.d.). *RTO Backgrounders*. Energy Information Administration, Sustainable FERC Project. Retrieved May 14, 2021, https://sustainableferc.org/rto-backgrounders-2/

27. EIA. (Dec 2020). *Monthly Energy Review*. Energy Information Administration. Retrieved January 10, 2021, https://www.eia.gov/totalenergy/data/monthly/index.php

28. EIA. (2011). *About 60% of the U.S. electric power supply is managed by RTOs.* Energy Information Administration, U.S. Department of Energy. Washington DC. Retrieved August 10, 2014, http://www.eia.gov/todayinenergy/detail.cfm?id=790. Last accessed on.

29. EIA. (2012). *Annual energy outlook 2012*. Energy Information Administration, U.S. Department of Energy. Washington DC. Retrieved June 26, 2012, http://www.eia.gov/forecasts/aeo/pdf/0383(2012).pdf.

30. EIA. (2013). *Electricity: generating capacity*. Energy Information Administration, U.S. Department of Energy. Washington DC. Retrieved December 1, 2013, http://www.eia.gov/electricity/capacity/.

31. Ellis, B.E. (2012). TES for Medical Center. *ASHRAE Journal*, 54(11), 28-34.

32. Fischlein, M., Feldpausch-Parker, A.M., Peterson, T.R., Stephens, J.C., Wilson, E.J. (2014). Which way does the wind blow? Analyzing the state context for renewable energy deployment in the United States. *Environmental Policy & Governance*. 24(3), 169 – 187.

33. Fischlein, M., Larson, J., Hall, D.M., Chaudhry, R., Peterson, T.R., Stephens, J.C., Wilson, E.J. (2010). Policy stakeholders and deployment of wind power in the sub-national context: A comparison of four U.S. states. *Energy Policy*, 38(8), 4429-4439.

34. FERC Order No. 755, Final Rule. (2011). *Frequency regulation compensation in the organized wholesale power markets, Docket Nos. RM11-7-000, AD10-11-000*, United States Federal Energy Regulatory Commission. Retrieved August 2014, https://www.ferc.gov/sites/default/files/2020-06/OrderNo.755.pdf.

35. FERC Order on Compliance Filing. (2012). United States Federal Energy Regulatory Commission. Retrieved August 10, 2014, http://www.ferc.gov/whats-new/comm-meet/2012/092012/E-2.pdf.

36. Foley, A., Lobera, I.D. (2013). Impacts of compressed air energy storage plant on an electricity market with a large renewable energy portfolio. *Energy*, 57(1), 85-94.

37. Foley, A.M., Ó Gallachóir, B.P., McKeogh, E.J., Milborrow, D., Leahy, P.G. (2013). Addressing the technical and market challenges to high wind power integration in Ireland. *Renewable and Sustainable Energy Reviews*, 19(7), 692-703.

38. Gifford, R., Lunt, R., Larson, M., Wynne, H., Selmon, E. (2017). The Breakdown of the Merchant Generation Business Model: A Clear-eyed View of the Risks and Realities Facing Merchants. Power Research Group. Retrieved from https://www.powermag.com/what-is-the-future-of-independent-power/

39. Graeter, P., Schwartz, S. (2020). Recent Changes to U.S. Coal Plant Operations and Current Compensation Practices, *National Association of Regulatory Utility Commissioners*. Retrieved from https://pubs.naruc.org/pub/7B762FE1-A71B-E947-04FB-D2154DE77D45.

40. *GE FlexEfficiency™50 Combined Cycle Power Plant fact sheet*. (2011). Retrieved September 23, 2012, http://www.ge.com.

41. Harvey, S., Hogan, W. (2001). Identifying the exercise of market power in California. *Working Paper, JFK School of Government, Harvard University*.

42. Hogan, W. (2002). *Electricity standard market design: proposal A, analysis A-, Execution?* Harvard Electricity Policy Group, Cambridge MA. Presentation, 13 pages. Retrieved from https://scholar.harvard.edu/whogan/files/hogan_hepg_092602.pdf.

43. Hydrologic Engineering Center, Institute for Water Resources, U.S. Army Corps of Engineers. (1981). *Feasibility studies for small scale hydropower additions, a guide* manual, Volumes 1-6. Retrieved from https://www.hec.usace.army.mil/publications/ProjectReports/PR-3.pdf.

44. ISO-NE. (2012). *Market Manuals, M-11 Market Operations, Last revised on 10-26-2013*. Retrieved August 10, 2014, http://www.iso-ne.com/rules_proceds/isone_mnls.

45. Janke, B., Kuehn, T. (2011) Geothermal Power Cycle Analysis for Commercial Applicability using Sequestered Supercritical CO2 as a Heat Transfer or Working Fluid. *Paper ES2011-54397 in Proceedings of the ASME 2011 5th International Conference on Energy Sustainability, ES2011, Washington, D.C., August 7-10*.

46. Joskow, P., Kahn, E. (2002). A quantitative analysis of pricing behavior in California´s wholesale electricity market during summer. *Energy Journal*, 23(4), 392-394.

47. Kanakasabapathy, P., Swarup, K.S. (2010). Bidding strategy for pumped storage plant in pool-based electricity market. *Energy Conversion and Management*, 51(3), 572-579.

48. Kazempour, S.J., Moghaddam, M.P., Haghifam, M.R., Yousefi, G.R. (2009). Risk-constrained dynamic self-scheduling of a pumped-storage plant in the energy and ancillary service markets. *Energy Conversion and Management*, 50(5), 1368-1375.

49. Katzenstein, W., Apt, J. (2012). The Cost of Wind Power Variability, *Energy Policy*. 51, 233-243.

50. Kirby, B. (2007). *Ancillary services: technical and commercial insights*. Prepared for Wärtsilä North America Inc. Retrieved August 10, 2014, http://www.consultkirby.com/files/Ancillary_Services_-_Technical_And_Commercial_Insights_EXT_.pdf.

51. Kumar, A., Shivani, S., Deepika, A., Aman, S. (2013). Capacity Outage Probability Table Calculation (COPT) of Haryana Power Generation Corporation Using VBA, *International Journal of Technical Research (IJTR)*, 2(2), 6-11.

52. Lu, N., Chow, J.H., Desrochers, A.A. (2004). Pumped-storage hydro-turbine bidding strategies in a competitive electricity market. *IEEE Transactions on Power Systems*, 19(2), 834-841.

53. Mansur, E. (2008) Measuring welfare in restructured electricity markets. *Review of Economics and Statistics*, 90(2), 69–386.

54. Midwest ISO. (2012). *Market Reports*, Retrieved August 21, 2012, http://www.midwestiso.org.

55. Oldak, M. (2012). Working Together with the Smart Grid, Electric Utilities and the HVAC Industry, *ASHRAE Journal*, 54(11), 10-15.

56. PJM Interconnection. (n.d.). PJM Data Miner 2, Retrieved Dec, 2020 https://dataminer2.pjm.com/feed/da_hrl_lmps/definition.

57. PJM Interconnection. (n.d.). *PJM Zone Map*. Retrieved May 24, 2018, https://www.pjm.com/library/maps.aspx

58. *PJM Manual 22: Generator Power plant Performance indices, Revision 17* (April 1, 2017) Prepared by Power plant Adequacy Planning, PJM. Retrieved December 10, 2019, https://pjm.com/~/media/documents/manuals/m22.ashx.

59. *PJM Manual 11: Energy & Ancillary Services Market Operations, Revision: 105* (April 25, 2019) Prepared by Day-Ahead and Real-Time Market Operations, PJM. Retrieved from https://www.pjm.com/-/media/documents/manuals/m11.ashx.

60. Randolph, J.B., Martin, S.O. (2011). Combining geothermal energy capture with geologic carbon dioxide sequestration. *Geophysical Research Letters*, 38.

61. Reynolds, S. (2018). Measuring Market Power in Wholesale Electricity Markets: A Dynamic Competition Approach, *Working Paper*. Retrieved from https://sites.ualberta.ca/~ipe/IPE/PDF/StanleyReynolds.pdf.

62. Saar, M.O., Randolph, J. (2011). Impact of reservoir permeability on the choice of subsurface geothermal heat exchange fluid: CO 2 versus water and native brine. *Transactions – Geothermal Resources Council*. 35(1), 521-526.

63. Schoenung, S.M., Hassenzahl, W.V. (2003). Long- vs. Short-Term Energy Storage Technologies Analysis: A Life-Cycle Cost Study. *A Study for the DOE Energy Systems Program, Sandia National Laboratories, SAND2003-2783*.

64. Sioshansi, R., Denholm, P., Jenkin, T., Weiss, J. (2009). Estimating the value of electricity storage in PJM: Arbitrage and some welfare effects. *Energy Economics*, 31(2), 269-277.

65. Sherwood, L. (2013). U.S. solar market trends 2012. Interstate Renewable Energy Council: Latham, New York, July 2013.

66. Sohel, M.I., Seller, M., Brackney, L.J., Krumdieck, S. (2009). Efficiency improvement for geothermal power generation to meet summer peak demand. *Energy Policy*, 37(9), 3370-3376.

67. Staffell, I., Green, R. (2016). Is there still merit in the merit order stack? The impact of dynamic constraints on optimal plant mix. *IEEE Transactions on Power Systems*. 31(1), 43–53.

68. Stephens J.C., Rand, G.M., Melnick, L.L. (2009). Wind energy in the U.S. media: A comparative state-level analysis of a critical climate change mitigation technology. *Environmental Communication*. 3(2), 168-190.

69. Wald, M. (2013). *Catching rays in California, and storing them*. New York Times 23 Dec. 2013: B3. Retrieved from https://www.nytimes.com/2013/12/24/business/energy-environment/catching-some-rays-in-california-and-storing-them.html.

70. Williams, C.F., Reed, M.J., Mariner, R.H. (2008). A review of methods applied by the U.S. Geological Survey in the assessment of identified geothermal resources. *U.S. Geological Survey Open-File Report 2008-1296*. Retrieved from http://pubs.usgs.gov/of/2008/1296/.

71. Wolak, F. (2000). Market Design and Price Behavior in Restructured Electricity Markets: An International Comparison. In: Faruqui A., Eakin K. (eds) Pricing in Competitive Electricity Markets. *Topics in Regulatory Economics and Policy Series*, 36, Springer, Boston, MA.

72. Wolak, F. (2003). Measuring Unilateral Market Power in Wholesale Electricity Markets: The California Market, 1998-2000. *The American Economic Review*, 93(2), 425-430.

73. Wolak, F. (2010). Using restructured electricity supply industries to understand oligopoly industry outcomes. *Utilities Policy*, Vol 18(4), 227–246.

74. Wolak, F., Patrick R. (2001). The Impact of Market Rules and Market Structure on the Price Determination Process in the England and Wales Electricity Market. *NBER Working Papers 8248, National Bureau of Economic Research, Inc*.

75. U.S. Department of Energy. (2013). WINDExchange. Retrieved December 19, 2013, http://www.windpoweringamerica.gov/wind_installed_capacity.asp.

7. Appendix

7.1 Appendix A - Description of the PJM Interconnection

PJM administers the wholesale electricity market and transmission grid in all or parts of Illinois, Indiana, Ohio, Pennsylvania, Delaware, New Jersey, Maryland, Michigan, North Carolina, West Virginia, Virginia, the District of Columbia, and Tennessee. The following figure is a map of the transmission zones within the PJM balancing authority. There are 21 transmission zones within the PJM regional footprint.

Figure 7-1: PJM Transmission Zones

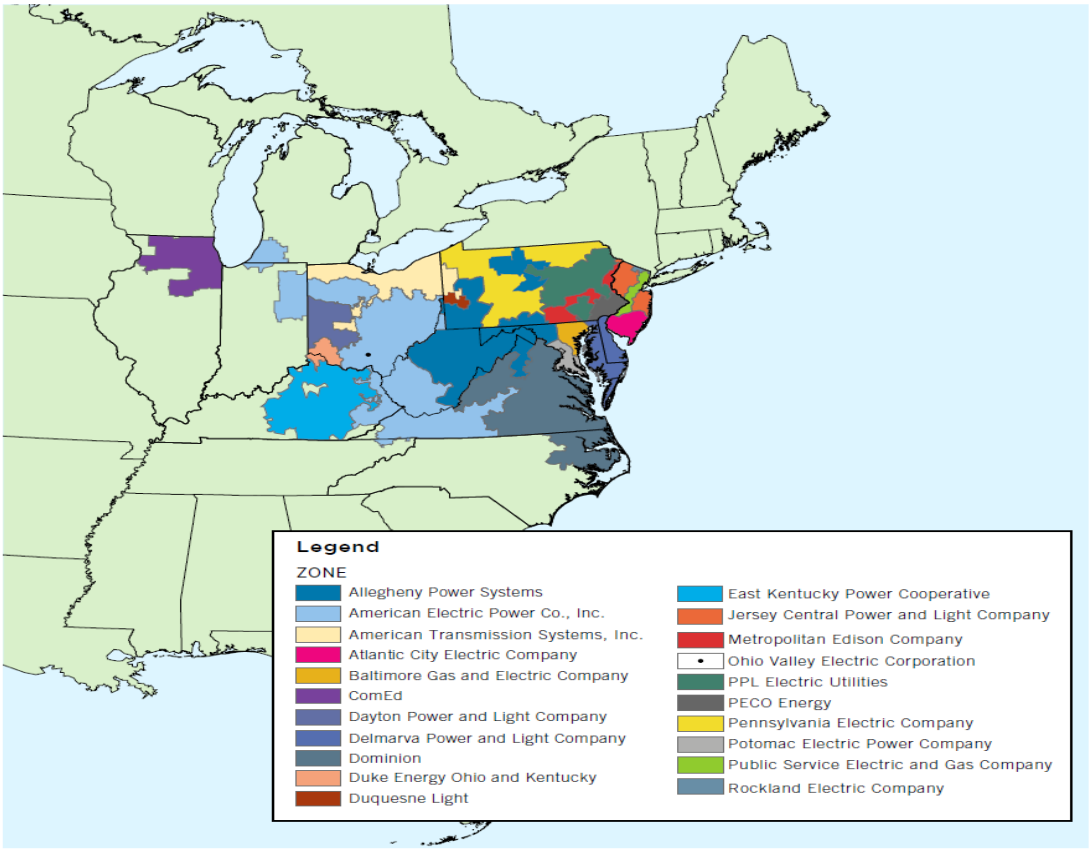

Notes: This figure was retrieved from PJM's map of transmission zones (PJM, n.d.).

7.2 Appendix B – Nameplate Capacity by Power Plant Type

Table 14 shows the nameplate capacity in MW for power plant types within the PJM region in 2016.[9] Most of the capacity in the PJM region is coal and natural gas generation. There is also a sizable amount of nuclear generation within the region.

Table 7-1: Nameplate Capacity and Power plant Type

Fuel Type	Nameplate Capacity (MW)
SOLAR	2,789
COAL	81,593
NATURAL GAS	113,013
NUCLEAR	35,991
WIND	10,992
HYDRO	8,435
OIL	14,216
OTHER	3,052
BIOMASS	2,515
Total	272,596

Notes: The data on nameplate capacity by fuel type are obtained from 2016 data on power plants located within the PJM region.

[9] The nameplate capacity is a term that represents the output level that could be maintained over a long period of time.

7.3 Appendix C - Data Sources used to Calculate Competitive Benchmark Price

The EPA eGRID 2016 was used to source data on power plants within the PJM region. I obtained data on the power plant fuel type, heat rate (the amount of energy required to generate one MWh of electricity), and capacity (in MW) for every power plant in the PJM region. Data on start-up costs was obtained from NREL in a study conducted by Kumar, Besuner, Lefton, Agan, and Hilleman (2012). Data on fuel prices were obtained from the U.S. Energy Information Administration (EIA). For coal, natural gas, and oil prices, I used a monthly dataset on the cost of coal, natural gas, and distillate fuel receipts at electric generating plants (dollars per million Btu, including taxes). Information on variable operations and maintenance costs was also sourced from the U.S. EIA.

Hourly data on total metered generation, system energy prices, price taking generation, regulation reserve capacity and net imports were obtained from PJM's public database. Monthly Equivalent Demand Forced Outage rates by generation type and nameplate capacity were also sourced from PJM's public database.

7.4 Appendix D - PJM Day-Ahead System-Wide Energy Prices

The following tables show the average day-ahead system energy prices by hour of the day and for dates by month and year.

Table 7-2: Day-ahead System Energy Price $/MW by Hour of the Day

Hour of the Day	Day-Ahead System Energy Price
12am	23.7
1am	22.6
2am	21.7
3am	21.3
4am	21.9
5am	24.2
6am	30.1
7am	32.1
8am	31.5
9am	32.3
10am	33.2
11am	33.4
12pm	33.6
1pm	34.3
2pm	35.0
3pm	36.2
4pm	38.8
5pm	41.1
6pm	38.8
7pm	37.6
8pm	36.4
9pm	32.4
10pm	27.4
11pm	24.7

Notes: These data were retrieved from https://www.pjm.com/markets-and-operations/etools/data-miner-2 with the PJM Data Miner. These are average hourly electricity prices for the year 2018.

Table 7-3: Day-ahead System-wide Market Price $/MW by Month

	System-wide market price		
Month	**Year 2016**	**Year 2017**	**Year 2018**
Jan	29.6	30.9	70.9
Feb	26.8	26.2	26.7
Mar	24	31.5	31.5
Apr	27.7	29	33.9
May	23.3	29.5	33.1
Jun	25.6	26.9	29.8
Jul	32.2	29.9	32.6
Aug	31.8	26.9	32.2
Sep	29	29.2	32.1
Oct	28.2	28.5	34
Nov	25.7	29	36.6
Dec	31.9	35.5	33

Source: PJM Data Miner (https://www.pjm.com/markets-and-operations/etools/data-miner-2)

7.5 Appendix E - Metered Loads

The following table shows the average daily metered load (in MW) for dates by month and year.

Table 7-4: Day-ahead System-wide Market Price $/MW by Month for the Year 2018

	Average Daily Metered load in MW		
Month	**Year 2016**	**Year 2017**	**Year 2018**
Jan	95,003	94,179	105,717
Feb	90,889	88,279	94,179
Mar	78,873	89,028	90,182
Apr	77,207	79,902	81,734
May	79,476	81,918	87,514
Jun	96,083	96,672	98,560
Jul	108,517	106,731	107,654
Aug	110,989	99,700	109,559
Sep	95,519	91,127	97,843
Oct	80,808	82,933	87,051
Nov	82,811	87,143	90,736
Dec	96,314	99,751	96,716

Source: PJM Data Miner (https://www.pjm.com/markets-and-operations/etools/data-miner-2)

7.6 Appendix F – Deviations from Competitive Benchmark without Start-up Costs

Table 7-5: Average Deviation from Competitive Benchmark by Month

	$100 \cdot \frac{1}{n} \sum_{i=1}^{n} \frac{P_i - MC_i}{MC_i}$		
Month	**Year 2016**	**Year 2017**	**Year 2018**
Jan	20.4%	17.7%	99.1%
Feb	13.1%	8.5%	2.8%
Mar	2.6%	25.9%	28.1%
Apr	18.7%	22.3%	39.6%
May	0.7%	18.8%	36.1%
Jun	5.9%	4.8%	14.4%
Jul	12.2%	11.8%	16.1%
Aug	16.8%	6.4%	17.8%
Sep	14.0%	18.1%	26.9%
Oct	17.7%	20.5%	39.9%
Nov	8.5%	20.3%	45.9%
Dec	20.0%	35.8%	22.0%

Table 7-6: Average deviation from Competitive Benchmark by Hour of Day

Hour of the Day	$100 \cdot \frac{1}{n} \sum_{i=1}^{n} \frac{P_i - MC_i}{MC_i}$
12am	-3.4%
1am	-6.9%
2am	-10.2%
3am	-11.8%
4am	-9.7%
5am	-1.0%
6am	20.6%
7am	25.9%
8am	23.5%
9am	26.4%
10am	30.0%
11am	30.2%
12pm	30.2%
1pm	31.8%
2pm	33.5%
3pm	37.0%
4pm	45.3%
5pm	52.8%
6pm	44.8%
7pm	41.8%
8pm	38.9%
9pm	24.9%
10pm	8.0%
11pm	-0.4%

7.7 Appendix G – PHES Model Solution

Model Solution:

To obtain the MW h from generation, the procedure is as follows:

- LOOKUP the initial head height
- LOOKUP efficiency factor corresponding to the INITIAL HEAD HEIGHT and maximum flow rate
- CALCULATE the time it takes to reach NEXT HEAD HEIGHT
- CALCULATE generation (in MW h) for INITIAL STEP
- Proceed through the head heights in discrete space in a stepwise fashion
- Repeat process above for each step until the end of the hourly period
- Sum generation (in MW h) at step to get the total MW h produced for the hourly period

A similar procedure is used to find the MWh required to store energy.

- Part-flow efficiency considerations put an upper bound on the amount regulation capacity that can be offered into the market. The partial flow is defined as Vol/Vol_{max} where Vol_{max} is the maximum flow rate. I set a lower bound for the partial flow at $Vol/Vol_{max} = 0.75$ and discretize the partial flow rates. The discrete space contains 21 different points corresponding to the 21 different regulation capacities that can be offered. The action space contains 24 different actions – the 21 different regulation capacities, pumping, generating, and idling.
- The head height h is a controlled Markov process so that h_{t+1} depends on h_t and the action x_t. In the model, the prices for electricity and frequency capacity transition independently of the action x_t taken by the operator. The equation of motion for h is a function of the flow rate, which depends in turn on the action taken in time period t. The discrete time state transition lookup table is a 366×366 array where the number of rows and columns correspond to the number of points in the discrete head height space. I constructed a state transition lookup table for each action. The state transition array is a matrix of 0s and 1s. The 1s indicate the next state given the current state and the action taken in current time.
- Backward recursion is used to solve the optimization problem. The terminal point is free, so I use a backward recursive process to solve beginning at the terminal point plus one additional time period. The following algorithm is used to solve the model recursively backward.
    - START process in time period T

- EVALUATE the current plus expected future rewards for each point in the Cartesian product H $\times$ X where H is set the points in the discrete head height space and X is the set of actions
- SET $\boldsymbol{V_{T+1}} = \mathbf{0}$ where $\boldsymbol{V_{T+1}}$ is a 366×1 vector of expected future values of reaching the next state in time period $T + 1$
- RETRIEVE a point in the set $Y = \text{H} \times \text{X}$
- COMPUTE the current reward
- LOOKUP the next state in the state transition array
- LOOKUP the expected future value of reaching the next state in time period $T + 1$ from $\boldsymbol{V_{T+1}}$
- SUM the current and expected future rewards
- REPEAT this process for all the points in the set Y
- FIND the action that maximizes then sum of current and expected future rewards for each point in the discrete space of head heights– this is the optimal action for time period *T* given the current head height
- SET each element of V_T equal to the maximized sum of the current and expected future rewards for the corresponding head height
- REPEAT the process for time periods $T - 1 \ldots 1$

The following algorithm describes the simulation process used to compute operating revenues and profits:

- Set the initial state in time period 1
- LOOKUP the current reward for each action
- LOOKUP the state transitions for each action
- LOOKUP the expected future reward of reaching the next state in time period 2
- SUM the current and expected future rewards for each action
- Select the maximum sum – this corresponds to the optimal action given the initial state in time period 1
- LOOKUP the state transition corresponding to the optimal action – this gives the state in time period 2
- Repeat the process for time periods $t = 1 \ldots T$
- Output a vector of states and a vector of optimal actions for each time period periods $t = 1 \ldots T$